Characterization of lymphoid compartments and hematopoiesis in a TSLP transgenic mouse model

Inauguraldissertation

zur

Erlangung der Würde eines Doktors der Philosophie

vorgelegt der

Philosophisch-Naturwissenschaftlichen Fakultät

der Universität Basel

von

Simone Neu

aus Rheinfelden, Deutschland

Basel, 2017

Genehmigt von der Philosophisch-Naturwissenschaftlichen Fakultät
auf Antrag von

Prof. Dr. Daniela Finke (Fakultätsverantwortliche und Dissertationsleiterin)

Prof. Dr. Georg Holländer (Korreferent)

Basel, 15.09.2015

Prof. Dr. Jörg Schibler
Dekan der Philosophisch-Naturwissenschaftlichen Fakultät

The most exciting phrase to hear in science, the one that heralds the most discoveries, is not "Eureka!" (I found it!) but "That's funny..."

- Isaac Asimov -

Acknowledgements

First of all, I would like to give a huge thank you to Daniela Finke for supervising my thesis. Your door was always open for questions and discussions and you found the right encouraging words when needed. Thanks Daniela for supporting me during my PhD.

Moreover, I want to thank my PhD committee: Georg Holländer and Cornelia Halin – Winter for their ideas and discussions.

Another thank you goes to Thomas, Karin and Carlos from the Holländer group for sharing experimental skills, having scientific discussions in the middle of the staircase or next to the printer and for several hours of sorting. I would like to thank also Simona Rossi for sharing her experimental skills and ideas.

I want to thank all members of the Finke group. Thanks Anne, Edit, Nicole, Annick, Frank, Gleb, Madeleine, Julia and Urs for creating such a stimulating and enjoyable work environment. Thanks, for all the good laughs, for crazy Fridays (and other week days), for the best cakes in town and for all the fruitful discussions and support in the last 4 years. I could always count on all of you when I needed a hand during my experiments. I also owe you a lot for tolerating me during my hyper active phases after the coffee breaks.

I would like to thank the people from the animal facility especially Angelika, Lothar and Emilia for their patience and for their continuous hard work with the mice.

My thank goes also to my family who always believed in me and gave me the strength to go on and especially to my parents who taught me to keep going also during difficult times.

A special huge thanks goes to Stefan. You always believed in me, supported and helped me with constant encouragement. Thanks for your patience, for your comforting “everything will be fine” and for providing me with nerve nutrition in form of chocolate. I love you.

Table of Contents

1 Summary

Immunodeficiencies are severe diseases, which are inherited or acquired after cytotoxic treatment or radiotherapy. Hematopoietic stem cell transplantation (HSCT) has become a common treatment for patients suffering from immunodeficiency, but especially the re-establishment of a functional T cell pool is often delayed and patients suffer from infections and relapse of malignancies. The generation of an adequate T cell pool can be achieved by *de novo* generation and peripheral expansion of donor T cells. However, T cell development after pretransplantational treatment is often impaired due to damage of the thymic environment. To improve thymic engraftment and preserve the thymic microenvironment, current treatments involve application of cytokines, which have often severe side effects. Therefore it is important to find alternative ways to improve T cell reconstitution after HSCT.

LTi cells are members of the family of innate lymphoid cells group 3 (ILC3s), which promote lymphoid tissue generation and are involved in tissue remodelling in primary and secondary lymphoid organs. In my study, I wanted to investigate the impact of ILC3s and secondary lymphoid organs on T cell reconstitution after HSCT. Therefore immunodeficient $Rag2^{-/-}\gamma c^{-/-}$ mice, which have reduced numbers of ILC3s and severe defects in LN development and K14 $TSLP^{+/-}$ $Rag2^{-/-}$ $\gamma c^{-/-}$ mice with increased numbers of ILC3s were compared before and after transplantation with hematopoietic stem cells or mature T cells.

Characterization of the recipient mice showed that TSLP overexpression in $Rag2^{-/-}\gamma c^{-/-}$ mice increases the number of double negative thymocytes DN2 and DN3s, and improves the thymic architecture with the development of mTECs and Aire expression. Reconstitution of the hematopoietic system with fetal liver (FL) HSCs from $TSLPR^{-/-}$ mice showed that TSLP overexpression results in an accelerated T cell reconstitution in the thymus and peripheral organs. The reconstitution of B cells did not differ between $Rag2^{-/-}\gamma c^{-/-}$ and K14 $TSLP^{+/-}$ $Rag2^{-/-}\gamma c^{-/-}$ mice, suggesting that the reconstitution itself was equally efficient.

T cells depend on IL-7, as this cytokine promotes T cell proliferation and survival. I could show that the IL-7 expression was significantly higher in the spleen of K14 $TSLP^{+/-}$ $Rag2^{-/-}\gamma c^{-/-}$ compared to $Rag2^{-/-}\gamma c^{-/-}$ mice most likely as a result of higher numbers of dendritic cells (DCs) expressing IL-7. Finally, I could demonstrate that TSLP overexpression increases T cell proliferation in secondary lymphoid organs.

Taken together, these data suggest, that TSLP overexpression accelerates T cell reconstitution by improving *de novo* T cell development in the thymus and T cell expansion in secondary lymphoid organs.

2. Introduction

2.1 The Immune System

The human body is constantly exposed to a variety of potentially harmful microorganisms such as bacteria, fungi and viruses and has to discriminate between self and non-self cells. To protect the organism, the immune system with an innate and adaptive branch has developed, whereas the latter is only found in vertebrates. The innate immune system is the first line of defence in all animals and is able to react within minutes or hours to pathogen- and danger- associated molecular patterns (PAMPs and DAMPs), typical components of microorganisms. Cells of the innate immune system include professional (e.g. dendritic cells) as well as non-professional antigen presenting cells (APC) (endothelial and epithelial cells) and phagocytic cells like macrophages (MΦ). The release of cytokines and chemokines by innate immune cells and endothelial or epithelial cells is important to recruit and activate the second branche, the adaptive immune system. Contrary to innate immune cells, cells of the adaptive immune system, namely T and B lymphocytes are able to recognize antigens (Ags) due to the expression of highly specific Ag receptors, which are generated by random recombination of gene segments. The number of B and T cells that recognize a given foreign Ag is small, on the order of 1 cell per million. The high diversification of the T and B cell repertoire through recombination, however, ensures clonal and highly specific immune responses towards a broad spectrum of different Ags.

T and B cells develop in primary lymphoid organs such as thymus and bone marrow (BM), respectively. T cells contribute to cell - mediated immune response. $CD8^+$ cytotoxic T cells can eliminate intracellular pathogens, whereas $CD4^+$ T helper cells help other immune cells through the secretion of cytokines. There are two major subsets, T helper (Th) 1 and Th2. While Th1 cells mediate cellular immunity by stimulating MΦ and stimulating proliferation of $CD8^+$ cytotoxic T cells, Th2 cells support B cell proliferation and antibody (Ab) class switch[1]. Continuing studies identified also new subsets of $CD4^+$ T cells, which include Th9, Th17 and Th22 named after their key effector cytokine secretion[2].

The recognition of Ags by $CD4^+$ and $CD8^+$ T cells are different. $CD4^+$ T cells recognize extracellular Ags presented by MHC class II, whereas $CD8^+$ cytotoxic T cells recognize intracellular Ags complexed with MHC class I. $CD4^+$ T cell activation

leads to the production of cytokines, which in turn activate other cells of the immune system[1]. B cells on the other hand recognize native Ags and secrete immunoglobulins (Ig) Abs with two functional parts: the Fab part of Igs recognizes extracellular pathogens, whereas the Fc part activates other host cells Fc receptors (humoral immune response). B cell activation and maturation is possible via two different pathways: The thymus - dependent (TD) and thymus - independend (TI) B cell activation. During TD B cell activation, Th2 cells primed for a specific Ag by APCs activate B cells by cytokine secretion, if the B cell presents the same Ag. This results in B cell division and maturation into an Ab producing plasma blast.

A hallmark of the adaptive immune system is the formation of immunological memory. Following reactivation with the same Ag peptide, lymphocytes mount a faster and more efficient immune response. Important places for lymphocytes are secondary lymphoid organs including spleen and lymph nodes (LNs) because they provide special niches for mounting an immune response but also for maintenance of immune homeostasis. Exposure to most pathogens elicit both innate and adaptive immune responses, which help to clear the infection and prevent chronic inflammation[1,3].

2.2. Reconstitution of the adaptive immune system

2.2.1 Immunodeficiencies and hematopoietic stem cell transplantation

Immunodeficiency diseases are either inherited or acquired diseases, in which the immune system is compromised and fails to fight infections. Inherited or primary immunodeficiencies are caused by mutations that control the differentiation and activities of immune cells. These mutations can occur on different levels during cell development. Mutations in the Ikaros gene, for instance, affect already lymphocyte progenitors[4], whereas recombination activating gene (Rag) deficiency results in the arrest of T and B cell development because of a failure to rearrange the Ag receptor genes. Moreover, defects in surface molecules like CD40L or common γ chain or in cytokine production can prevent their essential interaction with other immune cells to mount an immune response[5]. Acquired or secondary immunodeficiencies include HIV infection and chemotherapy. Hematopoietic stem cell transplantation (HSCT) has become a common therapeutic treatment for patients suffering from immunodeficiency like severe combined Immunodeficiency or after radiation – and

chemotherapy of hematologic malignancies such as different types of leukemia[6]. It involves the transplantation of autologous hematopoietic stem cells (HSC's from the patients themselves) or allogenic stem cells (HSC's from another donor), which can be harvested from BM or umbilical cord blood (UCB). HSCs can also be obtained by the mobilization of these cells from the BM into the peripheral blood by treatment with granulocyte colony-stimulating factor (G-CSF).

In 2012, more than 33 000 patients in Europe were reported to receive HSCT, of which 42% were performed allogeneic and 58% autologous. The main indications for HSCT were lymphoid neoplasias (57%) followed by leukemia (32%), solid tumors (5%) and nonmalignant disorders (6%) (Fig. 1)[7].

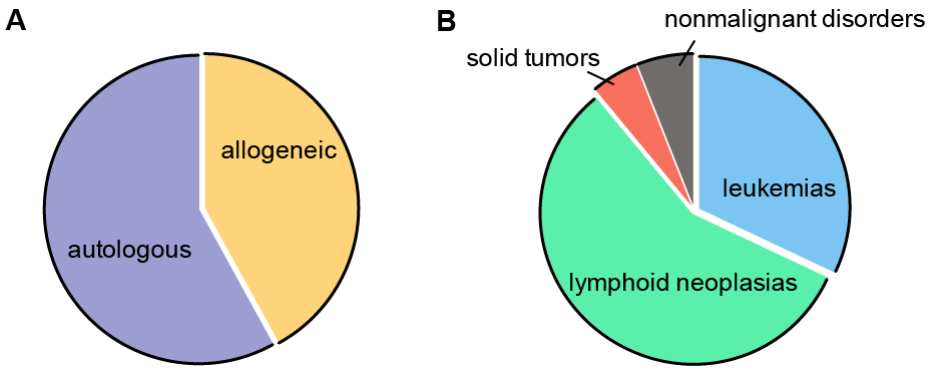

Figure 1: Proportions of HSCT in Europe in 2012

(A) Proportion of HSC transplant type in Europe in 2012. **(B)** Proportions of disease indication for HSCT in Europe in 2012. Adapted from *Passweg et al., Bone marrow transplantation (2014)*[7]

The successful outcome of HSCT depends on several parameters like stage and progress of the underlying disease, pretransplantational conditions like chemo- or radiation therapy, age of the patient and genetic disparity of donor and recipient[7-9]. The re-establishment of the functional immune system in the patient after HSCT is a major clinical issue, and improving the adaptive immune system is crucial for a successful outcome of HSCT.

While the innate immune system including monocytes, granulocytes and natural killer (NK) cells recovers quickly after HSCT, the restoration of the adaptive immune system is a long - lasting and often insufficient process[10-12]. Delayed reconstitution of adaptive immunity bears, especially in the first two years after HSCT[13,14], a high risk for opportunistic fungal (aspergillus spp) as well as bacterial and viral infections (Cytomegalovirus (CMV), Epstein-Barr virus (EBV), Varizella zoster virus (VZV),

influenza) and even relapse of malignancies[15]. Another high risk for HSCT patients are late bacterial infections caused by defective Ab production and defective class switch due to failure in B cell development[16]. The generation of an adequate T cell pool can be achieved by either peripheral expansion of donor T cells, which bears a higher risk for graft versus host disease (GVHD) or *de novo* T cell generation. However, the development from a hematopoietic precursor into a T cell is insufficient after HSCT because treatments like chemo- or radiotherapy damages the thymic environment and perturbs normal T cell development. Current immunomodulary treatments try to improve thymic engraftment or to preserve the thymic microenvironment with cytokines, such as keratinocyte growth factor (KGF)[17-19], IL-2[20], IL-7[21], growth hormones[22] or blockade of sex hormones[23]. Other therapies involve the transplantation of ex-vivo isolated cells such as T cells [24] or co-transplantation of mesenchymal stem cells (MSC)[25].

Although there are a number of treatments available to accelerate immune reconstitution and to improve the outcome of HSCT, regaining fast and efficient immune competence is still a matter of ongoing research. It is therefore essential to gain further insights into immunological processes involved in the reconstitution of the adaptive immune system after HSCT.

2.2.2 Models for reconstitution of the adaptive immune system

As described, there are several difficulties to efficiently reconstitute the adaptive immune system after HSCT in humans. However, ethical issues prevent extensive research on these obstacles. Therefore, mouse models are needed to provide insight into molecular and cellular mechanisms during HSC engraftment. Since adult BM and fetal liver (FL) are rich in HSCs, common assays to study murine HSC activity and their engraftment is the transplantation of BM or embryonic FL cells via intravenous (i.v.) injection into either lethally irradiated wild type (WT) mice or immunodeficient mice such as $Rag^{-/-}$ or $Rag^{-/-}\gamma c^{-/-}$[26]. However, such immunodeficient mutant mice have an abnormal development of thymus and LNs[27], which leads to less efficient engraftment and function of donor cells. Therefore, new and better animal models would be beneficial to study HSC engraftment and to improve HSCT.

2.3 Development and differentiation of adaptive immune cells

2.3.1 B cell development in the bone marrow

B cells originate from hematopoietic precursors, which can give rise to lymphoid progenitors (CLP) in the BM of adult mice. B cell development requires several recombination steps of the gene segments on the immunoglobuline locus V (variable), D (diversity) and J (joining) thus leading to randomly arranged B cell receptors (BCR). This process is initiated by the expression of Rag1 and Rag2. In addition to Rag1 and Rag2, B cell development is coordinated by transcription factors such as Pax - 5[28] and cytokines such as stem cell factor (SCF), fms-related tyrosine kinase 3 Ligand (Flt3L) and IL-7[29-34]. Further B cell developmental stages are discriminated by the expression of surface molecules shown in Fig. 2. After rearranging a functional BCR, B cells undergo selection processes within the BM to remove potential auto-reactive B cells. B cells, which recognize self-antigens in the BM are clonally deleted[35], become anergic[36] or start to rearrange their light chain locus (receptor editing)[37]. B cells with a functional and non-auto-reactive BCR leave the BM and acquire further maturation in the periphery.

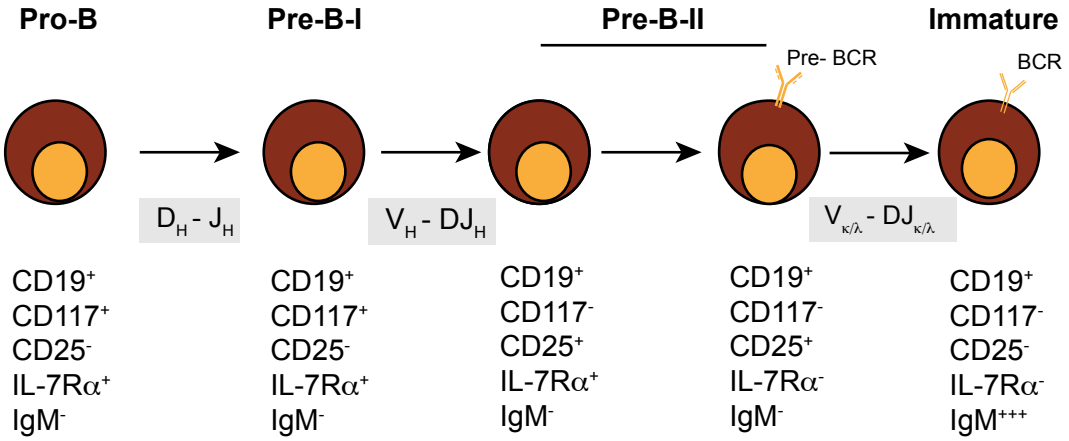

Figure 2: B cell development in the Bone marrow. *Adapted from Ceredig and Rolink, Nature reviews Immunology, (2002)*[38]

2.3.2 Peripheral B cells

Immature B cells, which leave the BM, enter the blood stream and recirculate through peripheral lymphoid tissues. During their migration, B cells undergo further maturation processes with the upregulation of IgD and downregulation of IgM. B cells in the spleen can be separated into $CD21^{high}$ $CD23^{-}$ marginal zone (MZ) B cells and $CD21^{+}$ $CD23^{+}$ follicular B (fol B) cells. MZ B cells are located in the marginal zone of the white pulp in the spleen. They express polyreactive and therefore less specific BCRs and high levels of Toll like receptors (TLR), comparable to DCs[39]. This allows them to react fast to a broad range of blood borne Ags and hence contribute to early immune responses. After Ag encounter MZ B cells become activated in a TD or TI pathway[40]. Whereas MZ B cells are exclusively detectable in the murine spleen, Fol B cells can also be found in the B cell areas of the LNs and Peyer's patches (PP), the lymphoid follicles in the intestine. Fol B cells mediate TD high-affinity immune responses to protein Ags. Thereby, Ags recognized by IgM on the surface of naïve B cells are internalized, processed and presented via MHC II to T cells. T cells, which were primed by the same Ag produce cytokines which lead to B cell differentiation and maturation into Ab-secreting cells. Crosslinking CD40 on B cells with CD40L on T cells induces point mutations of the rearranged V region (somatic hypermutation), which creates additional diversity within the highly Ag specific B cell clone and isotype switch to either IgG, IgA or IgE. Afterwards, fol B cells can further differentiate either into short-lived plasma blasts or into plasma cells, which migrate to the BM and persist as long-lived plasma cells[41].

B-1 cells are another subtyp of peripheral B cells, which are mainly found in the peritoneal and pleural cavities. During their migration through the blood and lymphoid organs, they contribute to TI immune responses e.g. against bacterial Ags such as phosphorylcholine[41].

2.3.3 T cell development in the thymus

The thymus is the primary lymphoid organ that is specialized for T cell development and generation of a highly diverse T cell repertoire that recognizes foreign Ags[42]. It is organized into a subcapsular region, cortex, cortico-medullary junction (CMJ) and medulla, and gives major contribution to cell-mediated immunity in the periphery. The thymus needs to be continuously seeded by lymphoid progenitors from the blood. These newly immigrating thymocytes migrate through

the different thymic regions where they undergo several maturation steps until they develop into mature T cells (Fig. 3).

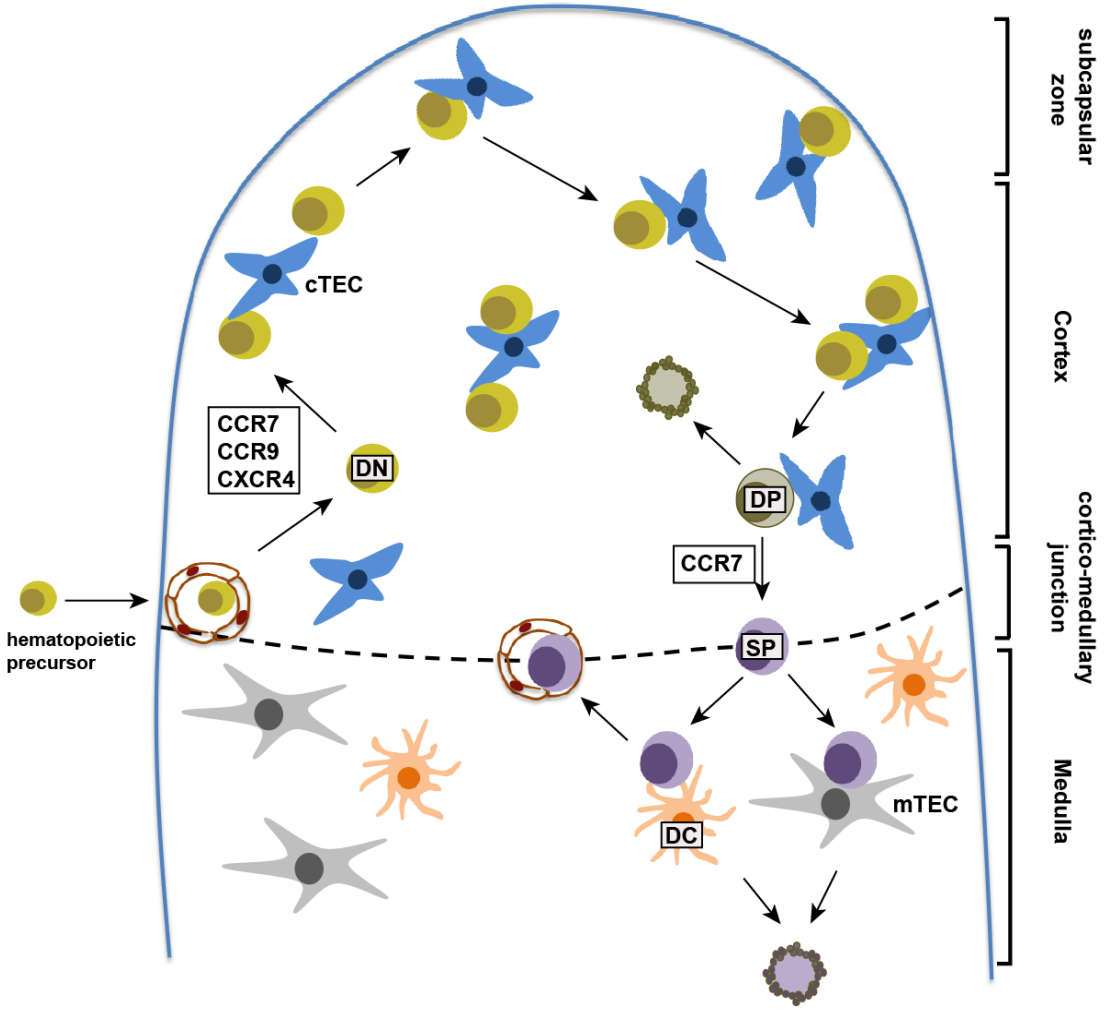

Figure 3: Thymocyte development and trafficking in the thymus. Hematopoietic precursors enter the thymus at the cortico-medullary junction. Chemotactic migration guides the double negative thymocytes through the cortex. Positive T cell selection in the cortex followed by negative selection in the medulla establishes a self-tolerant T cell pool with broad antigen specificity, which finally emigrate from the thymus into the periphery (DN: double negative; DP: double positive; SP: Single positive; cTEC: cortical thymic epithelial cell; mTEC: medullary thymic epithelial cell). *Adapted from Takahama, Nature reviews Immunology, (2006)*[43]

Thymic stromal compartment

The stromal compartment of the thymus is a 3-dimensial network structured into a cortical and medullary region, whose stromal cells are phenotypically and also functionally different. Thymic epithelial cells (TECs) are the major component of the thymic stromal compartment, but it includes also mesenchymal cells and cells of hematopoietic origin like DCs and macrophages. This network builds a microenvironment essential to promote and support survival, differentiation, maturation and selection of thymocytes[44,45]. Various extra- as well as intracellular markers help to discriminate cortical epithelial cells (cTECs) from medullary thymic epithelial cells (mTECs). Major markers to characterize the TEC subsets of the murine thymus are cytokeratins (CK) such as CK8 and CK18 expressed by cTECs and CK5 and CK14 expressed by mTECs. Both cTECs and mTECs share expression of epithelial cell adhesion molecule (EpCAM, CD326), MHC II molecules and lack CD45, a transmembrane protein expressed by hematopoietic cells. Characteristic for cTECs is the surface molecule Ly51 whereas the reactivity with Ulex europaeus agglutinin I (UEA-1) is a typical feature of mTECs[**46,47**]. In addition, mature mTECs express the intracellular transcription factor Autoimmune Regulator (Aire). Aire is responsible for the transcription of a broad spectrum of self-Ags, which are usually only present in the periphery like e.g. insulin[48,49]. These so-called tissue restricted Ags (TRA) are produced by mTECs and presented to developing thymocytes by either mTECs or by thymic DCs via cross-presentation[50]. This mechanism is crucial for central tolerance[51], as T cells, which recognize self-Ags are potentially auto-reactive and undergo therefore negative selection.

Thymocyte development

After lymphoid progenitors enter at the CMJ, thymocytes pass through the cortex, where they progress through intermediate developmental stages. The first stage is a $CD3^-$ $CD4^-$ $CD8^-$ triple negative phenotype, which is followed by different expression levels of c-kit, CD25 and CD44, characterizing the phenotype of double negative states one to four (DN1-DN4). DN1: c-kit^{high} $CD25^-$ $CD44^+$, DN2: c-kit^{high} $CD25^+$ $CD44^+$, DN3: c-kit^{low} $CD25^+$ $CD44^-$, DN4: c-kit^{low} $CD25^-$ $CD44^-$ [38,52]. At the DN3 state, Rag 1 and 2 are expressed, which catalyse the rearrangement of the β, γ and δ loci. Successful rearrangement of the T*crb* locus and later the assembling of the T cell receptor β (TCRβ) and pre-TCRα chains result in the expression of the pre-TCR

complex on the cell surface and drives the cell further into a $CD4^+$ $CD8^+$ double positive (DP) stage. Rearrangement of the α-chain locus leads to a complete randomly created, unique Ag-specific TCR$\alpha\beta$ receptor. At the DP stage, the TCR is tested for its recognition of self-peptide/self-MHC present on cTECs and DCs. Current models propose that self-Ag induced positive or negative selection is defined by an apparent affinity threshold of the interaction of TCR and co-receptor with a self peptide-MHC complex. Thereby cells with a TCR below the threshold undergo apoptosis (death by neglect), whereas cells above the threshold, hence having a high affinity towards self-MHC become negatively selected[53].

After the first round of selection, only 3-5% of the DP thymocytes have a low-affinity interaction, and therefore receive survival and further differentiation signals to progress to the single positive (SP) stage and to migrate further into the medulla.
Additional rounds of negative selection to eliminate potential auto-reactive T cells from the system accompany the final maturation process. Thereby, TCR with a too high affinity for self-Ags, which are presented by mTECs and DCs, are eliminated. The medulla is also the site for development of regulatory T cells (Tregs)[54]. This T cell subset is able to suppress an immune response by inhibiting proliferation of effector T cells and promotes tolerance to self-antigens.

T cell development is also associated with distinct transcription factor and cytokine ensembles. Transcription factors, such as Ikaros, GATA3 and T-cell-factor (TCF) -1 control the expression of important genes and guide the developing thymocytes from one stage to the next[55]. Notch1 signals are required to differentiate hematopoietic cells into T cells[56] and support Vβ-DJβ recombination[57]. Important cytokines during T cell development are Stem cell factor (SCF) and IL-7 by promoting proliferation, differentiation and survival of DNs[33,58,59].

Thymocyte - TEC interaction

The crosstalk between stromal cells and hematopoietic cells is crucial for the development and differentiation of thymocytes. Specifically the CC-chemokine ligand 21 (CCL21) and 25 (CCL25) were reported to play significant roles in thymus colonialization[60-62]. The presence of CXC-chemokine ligand 12 (CXCL12) or its receptor CXC-chemokine receptor 4 (CXCR4) is also involved in thymic seeding but to a lesser extend than CCL21 and CCL25 and is rather related to T cell expansion during embryogenesis[63,64]. The migration of thymocytes through the cortex, follows defined rules in such a way, that the thymocytes make their developmental changes

in distinct cortical regions[65]. Cortical DP cells show an increase in CCR7 expression, whereby mTECs are the major source of its ligands CCL19 and CCL21. Therefore, DP thymocytes are attracted by chemotaxis to the medulla, whereas deficiency for CCR7 leads to the accumulation of positively selected thymocytes in the cortex. Negatively selected DP thymocytes undergo apoptosis irrespectively of chemotactic attraction[66]. Another role of the CCL19-CCR7 axis was discovered by Ueno et al., in which CCL19 promotes the egress of mature T cells out of the thymus[67], emphasizing again the importance of thymocyte - TEC crosstalk for T cell development. Beside the requirement of lymphocyte - TEC interaction for thymocyte development, TEC development relies also on interaction with thymocytes. It was reported that arrest in thymocyte development at stage DN1 leads to a failure of normal cortical as well as medulllary compartment[68]. Furthermore, it was demonstrated that mTEC development, differentiation and maturation is strongly dependent on signals provided by hematopoietic cells in the thymus[69,70]. The interaction of mTECs with thymocytes is mediated by nuclear factor kappa-light-chain-enhancer of activated B-cells (NF-κB) signaling[71,72]. Signals through various TNF superfamily members, which are expressed by mTECs, play key roles in the maturation and differentiation of mTECs[73,74]. Rossi and colleagues identified receptor activator for NF-κB (Rank) *in situ* during embryogenesis as an important mediator for mTEC development. By the engagement with the ligand (RankL), which is present on $CD3^-$ $CD4^+$ cells, namely lymphoid tissue inducer (LTi) cells, mTECs develop into a mature state concomitant with the expression of CD80 and Aire[75]. However, *Rorc*$^{-/-}$ mice, which lack LTi cells, also have $Aire^+$ mTECS. This indicated the involvement of another cell type in regulating mTEC development during embryogenesis. Indeed, γδ T cell progenitors ($V\gamma5^+$ dendritic epidermal T cells; DETC) express RankL thereby contributing to mTEC growth and maturation[76]. In adults, LTi cells as well as γδ T cell progenitors are severely reduced in their frequency, as αβ T cells outnumber them. As soon as αβ T cells develop, they take over the function as mTEC inducer with expression of several other molecules e.g. CD40L and lymphotoxin, which were revealed to also regulate the development and differentiation of mature mTECs[77-81] (Fig. 4).

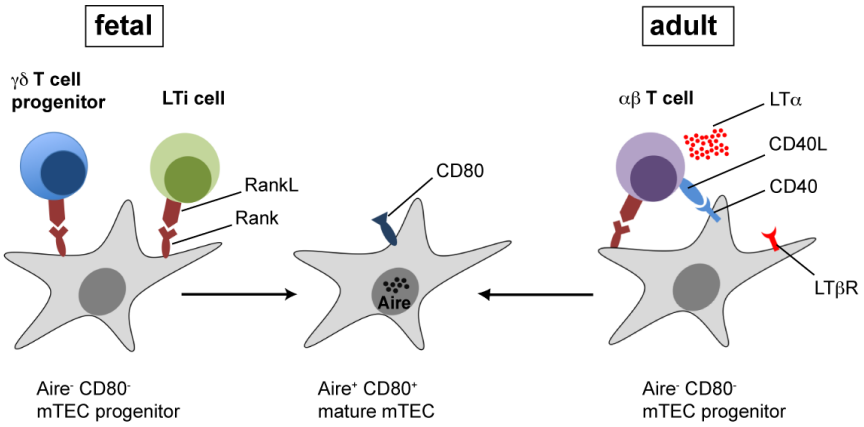

Figure 4: mTEC development and Aire induction/maintenance in fetal and adult mice. In fetal mice, receptor activator of NK-kB ligand (RankL) interaction provided by $V\gamma5^+$ γδ T cell progenitors and LTi cells, induces the development of mature mTECS with expression of Aire and CD80. Under steady state conditions in adults, signals like LTα, CD40L and RankL are provided by αβ T cells which engage the respective receptor resulting in a mature $CD80^+$ $Aire^+$ mTEC.

2.3.4 Peripheral T cells

The majority of peripheral T cells are positive for αβ TCR and express either CD4 or CD8. While the effector function of $CD8^+$ T cells is characterized by their cytotoxicity against target cells, $CD4^+$ T cells have divers functions as helper T cells and are characterized by their production of cytokines. The major Th subsets are Th1, Th2, Th17 and Tregs. T helper (Th) 1 cells develop in response to IL-12 and IFN[82,83] and are described to produce IFN-γ in a positive feedback loop as well as IL-2 and tumor necrosis-factor (TNF) - β. They are important in protection against intracellular pathogens[83], but are also involved in unwanted inflammatory diseases like rheumatoid arthritis or intestinal inflammation[84,85]. Th2 differentiation is driven mainly by IL-4[86] and TSLP[87,88]. Th2 cells produce IL-4, IL-5, IL-9, IL-10 and IL-13 and are often associated with humoral immune response. Therefore, Th2 immunity is important to resist extracellular pathogens such as helminthes or nematodes[89]. However, elevated Th2 responses are also associated with chronic inflammatory diseases such as allergy and asthma[90].

Th17 cells produce IL-17 and IL-22 and are associated with autoimmune diseases but also with the clearance of bacterial and fungal infections[82]. Tregs are a subset of

$CD4^+$ T cells, which either develop in the thymus (naturally occurring Tregs: nTregs) or are generated in the periphery (pTregs) from naïve T cells after TCR stimulation in the presence of TGF-β and IL-2. Tregs express forkhead box P3 (FoxP3), are immuno-suppressive, and maintain self-tolerance as well as immune homeostasis[91]. To distinguish nTregs from pTregs, the Ikaros family member Helios and Neuropilin-1 (Nrp1) were suggested as potential markers[92-94].

Peripheral T cells either have a naïve or memory phenotype. Naïve T cells are $CD44^{low}$ and express CCR7 and L-selectin (CD62L), an adhesion molecule, which enables them to enter LNs via high endothelial venules (HEV). Indeed, the majority of naïve T cells are found within secondary lymphoid organs, where they encounter foreign Ags followed by differentiation into effector T cells[95]. Effector T cells migrate to peripheral sites where they encounter Ags and mount Ag-specific immune responses. The majority of effector T cells undergo apoptosis to maintain immune homeostasis. Only a minor subset differentiates into long-lived memory cells, which home to lymphoid as well as non-lymphoid tissue where they can be reactivated upon recurrent Ag encounter[96]. Memory T cells have an activated phenotype and are identified by $CD44^{high}$ expression[97]. Survival, proliferation as well as homeostasis of naïve T cells are dependent on the interaction of TCR with self-peptide / MHC and several cytokines, whereas current studies indicate that maintenance of memory T cells does not require TCR / self-peptide interaction.

Common cytokine receptor γ - chain (γ_c)-dependent cytokines like IL-2, IL-7 and IL-15 support proliferation and survival of naïve as well as memory T cells. While both IL-7 and IL-15 control the survival of $CD8^+$ T cells, with IL-7 playing the major role[98,99], IL-15 is redundant for the proliferation and survival of $CD4^+$ T cells[100]. IL-7 is an important factor to induce slow homeostatic proliferation in $CD4^+$ and $CD8^+$, whereas IL-2 and IL-15 lead to rather rapid proliferaton[101]. In addition to IL-7 and IL-15, IL-2 is an important cytokine produced by activated T cells for T cell growth and proliferation. Especially Treg expansion is heavily depended on IL-2 and mice deficient in IL-2 signaling suffer from autoimmune diseases[102].

2.4 The lymph node

LNs are encapsulated secondary lymphoid organs, which are important to initiate immune responses. They are organized into two compartments, the cortex and the medulla. The cortex can be further separated into an outer cortical area with B cell follicles and the paracortical area with mainly T cells and DCs.

The medulla contains macrophages, Ab secreting plasma cells and the efferent lymphatics through which lymphocytes leave the LNs (Fig. 5)[103,104]. A dense network of reticular fibres and the secretion of their chemokines maintain the compartmentalization into B and T cell areas. Follicular dendritic cells (FDC) in the B cell zone, which are also present in the spleen, are the major source of B cell survival factors such as BAFF and APRIL and secrete CXCL13 to attract and preserve B cells[105,106]. T cells on the other hand are associated with T zone reticular cells (TRC), which produce CCL19 and CCL21. These cytokines are recognized by CCR7 expressed on naïve T cells and DCs and are important for motility[107], survival as well as antigen uptake by DCs[108]. Beside its crucial role in initiating immune responses, LNs provide also an environment for lymphocyte homeostasis by producing growth and survival factors[109], which will be further described in 2.4.1.

Ags from peripheral tissues and Ag-loaded DCs enter the LN via afferent lymphatic vessels. Naïve lymphocytes can enter the LN directly via HEVs and encounter Ags expressed by APCs in the respective compartments of the LN. After Ag exposure B cells undergo intense proliferation and form germinal centers, in which B cells undergo important modifications such as somatic hypermutation, affinity maturation and isotype switching. These steps result in the generation of mature high affinity B cells.

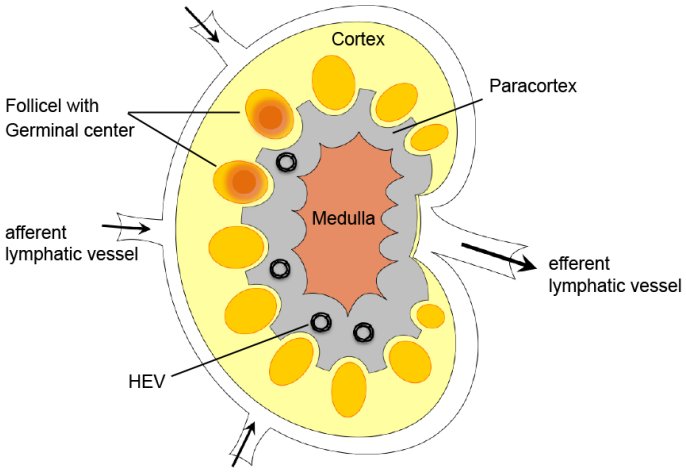

Figure 5: Lymph node architecture: Lymph enters through afferent lymphatic vessels, whereas naïve lymphocytes enter the LN via HEVs. Lymph fluid is drained through cortex and medulla, where cells of the immune system are activated to mount an immune response against foreign antigens. The lymph and lymphocytes leave the LN through efferent lymphatic vessels.

2.4.1 Lymph node stromal cells

Lymph node stromal cells (LNSC) are cells of mesenchymal origin, which provide the network within the LN to sustain immune homeostasis. Four different cell types can be identified by the expression of CD31 and the glycoprotein podoplanin (gp38): T zone reticular cells (TRC) (also known as follicular reticular cells), which are $CD31^-$ $gp38^+$, lymphatic endothelial cells (LEC), which are $CD31^+$ $gp38^+$, blood endothelial cells (BEC), which are $CD31^+$ $gp38^-$, and finally a subset of double negative stromal cells (DNSC)[109]. BECs and LECs surround blood vessels and lymphatic vessels, respectively. They are important for lymphocyte migration from the blood into the LN by the expression of chemokines and adhesion molecules. TRC and LECs were identified as a main source of IL-7, which promotes survival of naïve T cells[109,110]. Furthermore, IL-7 producing TRCs and LECs were reported to be essential for virus-induced LN remodelling and LN regeneration after avascular transplantation[111]. Beside IL-7, TRCs produce CCL19 and CCL21, which are recognized by CCR7 expressed on the surface of naïve T cells. These cytokines are chemoattractants for T cells and DCs promoting leukocyte traffic and T cell - DC interactions[112]. Just recently, it was found that IL-15, which is critical for proliferation and maintenance of $CD8^+$ T cells as well as NK cells and NKT cells, is expressed not only by BECs but

also by TRCs and DNSCs. This suggests a role for IL-15 in T cell homeostasis[113]. The idea that TRC support immune homeostasis is further supported by some evidence that they can express and present peripheral Ags to naïve T cells and hence may contribute to peripheral tolerance[114,115]. The function of the forth subset of LN stromal cells, the DNSC is not revealed yet[116] but their global gene expression closely resembles the one of TRCs[117].

2.4.2 Lymph node development

The first LN anlagen emerge early during embryogenesis. It was shown that signaling through lymphotoxin β receptor (LTβR) mediated by LTα1β2 is crucial for the development of lymphoid tissues, as mice deficient for either LTα or its receptor have neither LN nor PP. Similarly, LTβ -deficient mice also lack PP and peripheral LN except cervical and mesenteric LNs (mLNs). This suggested that another ligand than LTα1β2 is involved in their formation. Indeed, it was found that mice double deficient for LTβ and another LTβR ligand LIGHT had even lower numbers of mLN[118-120]. LTα1β2 and LTβR is the main pathway involved in peripheral LN generation. Studies from other genetic mouse models revealed further important receptor ligand interactions for LN development. Mice with deficiency for either Rank or RankL completely lack LNs, whereas deficiency for CXCR5 or its ligand CXCL13 just leads to a reduction of LNs. Additionally, intracellular molecules like inhibitor of DNA binding 2 (Id2), Ikaros and the transcription factor retinoid related orphan receptor γ (RORγt) play essential roles in the formation of LNs. Both factors are crucial for LTi cell development and the deficiency of Id2 or RORγt results in complete lack of LNs and PPs[121-124].

Lymphoid tissue inducer cells

LTi cells are cells of the hematopoietic system and first identified as $CD4^+$, $CD3^-$ and IL-$7R\alpha^+$ in fetal and newborn blood, LN and spleen[125]. As they were also found as one of the first cells colonizing lymphoid tissues, they were discussed as initiators of lymphoid organogenesis. The proof came from two independent transfer experiments in mice lacking lymphoid tissue. Adoptive transfer of LTi cells isolated from fetal spleen into $CXCR5^{-/-}$ induced PP development[126], whereas LTi cells form

fetal intestine transferred into Id2 deficient mice resulted in the generation of nasal-associated lymphoid tissue. These experiments demonstrated that LTi cells are in fact capable to rescue lymphoid organogenesis[121]. However, the mechanism of development for the different lymphoid tissues like LNs or PP might differ and involves other cellular interactions.

LN organogenesis relies on the interaction of LTi cells with organizer stromal cells[127,128]. LTα1β2, which is induced on LTi cells by triggering IL-7Rα and Rank[129], interacts with LTβR on organizer cells and activates NFκB pathways. NFκB activation results in the expression of adhesion molecules Vcam, Icam and MadCam on stromal cells and the production of CXCL13, CCL19 and CCL21[130,131]. As LTi cells express the respective chemokine receptors, this leads to attraction and retention of further LTi cells and amplification of their interaction with stromal cells. IL-7 and RankL expression, which are provided by stromal cells induce the expression of LTα1β2 on freshly migrated LTi cells, resulting in enhanced LTβR triggering on stromal cells, which closes the positive feedback loop[132]. Recruitment and colonialization of other hematopoietic cells to the initial cell cluster leads finally to the formation of lymphoid tissue (Fig. 6).

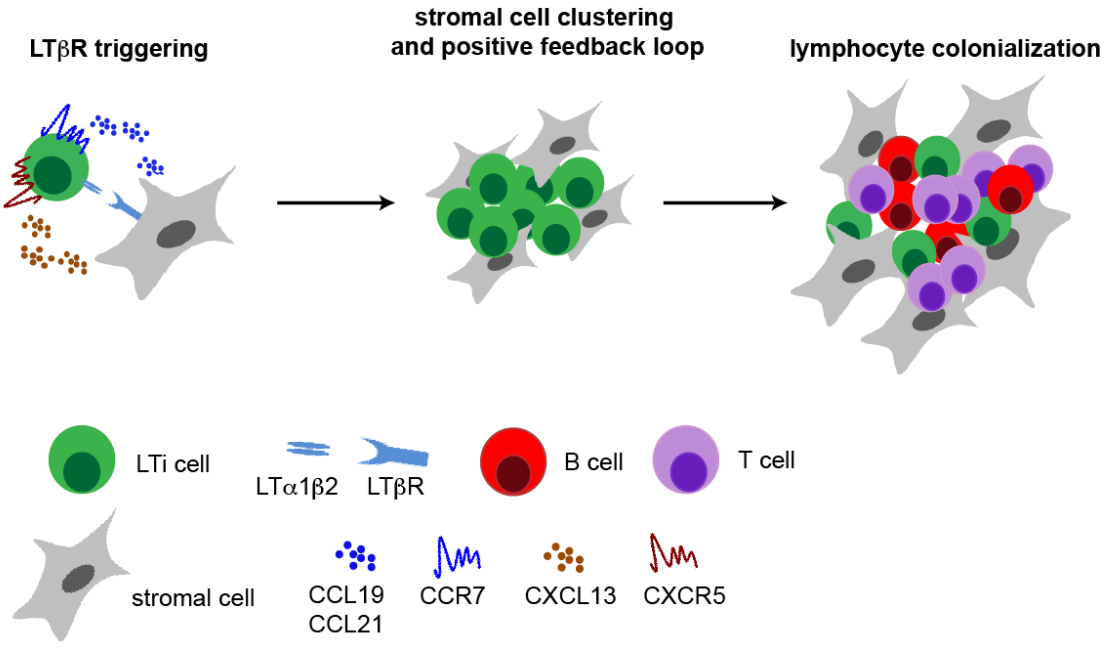

Figure 6: Model for LN development: LTi cells interact with stromal organizer cells via LTα1β2 - LTβR. Activated NFκB pathways lead to chemokine secretion and further recruitment of LTi cells. Final lymphocyte colonialization leads to the generation of a functional LN. *Adapted from Mebius, Nature reviews Immunology, (2003)*[133]

2.5 The family of innate lymphoid cells

2.5.1 ILC subsets

Innate lymphoid cells (ILC) are a heterogeneous family of immune cells, which recently came into research focus of numerous research groups. ILCs are thought to be integrators of the innate and adaptive immune system, orchestrating homeostasis, immunity and inflammation[134,135]. All members of the ILC family share a classic lymphoid morphology and lack the characteristical surface-molecule expression of other immune cells and are therefore referred to as lineage marker negative (Lin^-). In contrast to T and B cells, ILCs also lack the expression of Rag and cannot acquire Ag specificity[136]. They express the common cytokine receptor γ chain (γ_c) and depend on cytokines that signal via this receptor. All ILC family members are dependent on the transcriptional repressor Id2[137] and require different transcription factors and cytokines for the development. The function of ILCs is very diverse. They play crucial roles in the development of lymphoid tissue, tissue repair, maintenance of organ homeostasis and contribute to immunity against pathogens. On the other hand, ILCs are also reported to have a role in the promotion of inflammation and cancer progression[134,135]. As ILC subgroups are regulated by transcriptional factors and exert effector functions similar to Th subsets, the nomenclature of ILCs is based on their Th counterpart. Therefore, ILCs are grouped into i) Group 1 ILC, ii) Group 2 ILC and iii) Group 3 ILC.

Group ILC1 consist of the conventional natural killer (cNK) cells and the ILC1s. Both cell types are dependent on the T-box transcription factor (T-bet) and are capable to secrete IFN-γ. ILC2s are characterized by their developmental dependence on IL-7, GATA3, RORα and TCF1 and their production of Th2 cytokines IL-4, IL-5 and IL-13 upon stimulation. Several studies identified ILC2s as a critical mediator of allergic diseases and protective immune cells in helminth infections. Group 3 ILCs are dependent on the transcription factors RORγt and cytokines such as IL-7, SCF and TSLP[138,139135] for their development. ILC3s are further subdivided into three different cell types: LTi cells in fetal and neonatal tissue and the natural cytotoxicity receptor (NCR) $NKp46^+$ and $NKp46^-$ cells, which were discovered in adults. While $NKp46^+$ ILC3s are $CD4^-$, $CD4^+$ and $CD4^-$ subpopulations exist in the $NKp46^-$ ILC3 compartment. All ILC3 subtypes can secrete IL-17 and IL-22 with $NKp46^-$ also being able to secrete IFN-γ under certain conditions[135] (Fig. 7).

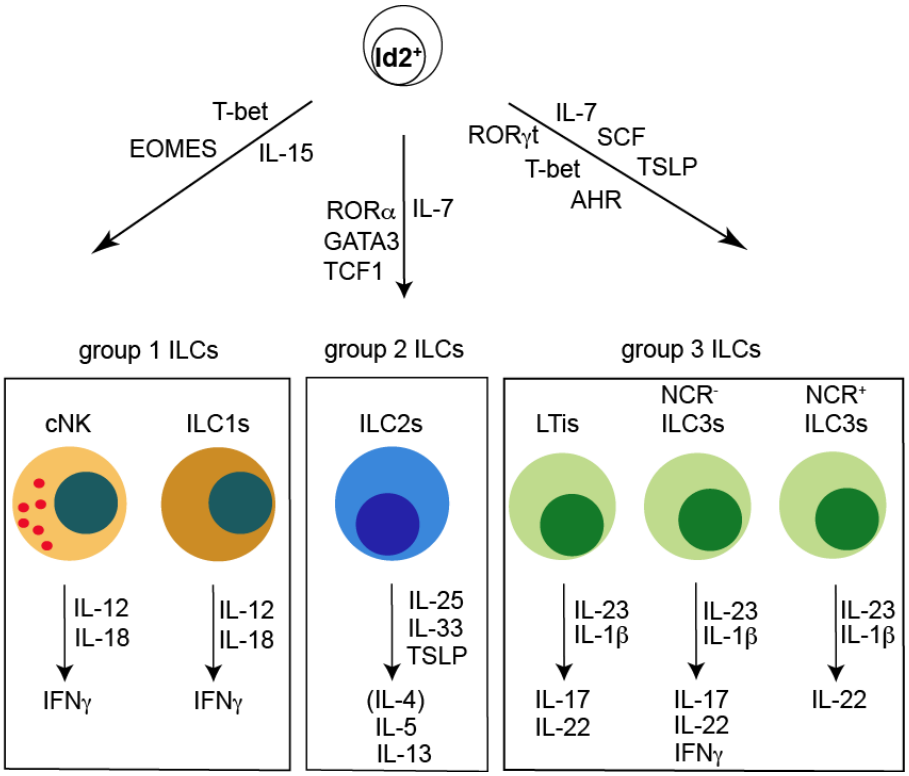

Figure 7: Family of innate lymphoid cells: Illustration of the developmental requirements and cytokine production of the different ILC subsets. *Adapted from Spits et al., Nature reviews Immunology, (2013)*[135] *and Artis and Spits, Nature (2015)*[136]

2.5.2 Immune functions of ILC3s in adults

LTi cells were originally named after their function to induce lymphoid tissues during embryogenesis. Several studies described cells with a similar phenotype also in the adult system[140], named as LTi - like cell[141]. However, a new nomenclature introduced the terminus NCR$^-$ ILC3s for adult RORγt$^+$ ILC3s, which lack NKp46 expression and resemble very likely the LTi - like cells[135]. Adult ILC3s exert a broad spectrum of functions, which range from tissue remodeling[142,143] and maintenance of immune homeostasis to pathological properties[144-147].

IL-17 and IL-22 are cytokines not only produced by T cells but also by ILC3s. Studies in mice showed an attribution of IL-17 and IL-22 in psoriasisform plaque formation, an inflammatory skin disease. Indeed, analysis of Rag2$^{-/-}$γc$^{-/-}$, RORγt$^{-/-}$ and Rag$^{-/-}$ mice suggest that ILC3s play a substantial role in psoriasisform plaque

formation, since $Rag^{-/-}$ mice had more sever inflammatory symptoms than $Rag2^{-/-}$ $\gamma c^{-/-}$ and $ROR\gamma t^{-/-}$ mice[146]. Further roles for ILC3s in inflammation were shown in the intestine of mice[145,147]. Here, ILC3s were reported to induce colitis through production of pro - inflammatory cytokines IL-17 and IFN-γ, driven by TNF-α and IL-23 producing DCs. This could be confirmed by Thy1 depletion or IL7R-α blocking respectively, since reducing ILC3 numbers abrogated colitis[145,147]. The role of ILC3s in promoting immune homeostasis and tissue repair is often mediated by the secretion of IL-22[134,144,148]. In the intestine IL-22 secretion upregulates anti-microbial peptide expression by intestinal epithelial cells[149] and improves epithelial barrier function, which is involved in immune defence against pathogenic bacterial colonialization[150,151]. Mice deficient for IL-22 show higher susceptibility to intestinal pathogens and intestinal inflammation[152]. In addition, ILC3s were found to interact with intestinal $CD11c^+$ DCs via membrane bound $\alpha 1\beta 2$, which is known to be crucial for IgA production[153]. Promoting an immunologically tolerogenic state in the intestine is important to prevent unwanted inflammation and ILC3s seem to play a substantial role in maintaining tolerance. ILC3s process and present antigens via MHC II to T cells[154,155]. Hepwoth et al. observed that ILC3 depletion resulted in dysregulated immune responses against commensal bacteria leading to low - grade inflammation. This effect occurred independently of IL-17 or IL-22 and was due to missing MHC - T cell interaction between ILC3s and $CD4^+$ T cells[154]. In contrast, other groups could not detect spontaneous inflammation in mice lacking MHC II on ILC3[155,156], which argues for additional factors such as microbiota for triggering inflammation in these mice. A recent study described another mechanism of ILC3s to promote tolerance in the intestine by production of GM-CSF, which increases the function of intestinal DCs and Tregs[157]. However, the host protective effects of ILC3s are not limited to the intestinal environment, since ILC3s were also an important source of IL-17 in the lung to mount an immune response against fungal infections[158]. Tissue remodelling functions like wound healing and repair of damaged tissue is also ascribed to ILC3s. In an infection model with lymphocytic choriomeningitis virus (LCMV), infected TRCs of the LN were targeted by virus-specific $CD8^+$ T cells. This resulted in the destruction of the secondary organ integrity. Restoration of the TRC network was due to proliferation of LTi cells and their interaction through LTβR with lymphoid stromal cells[142]. Furthermore, it was reported that IL-22 from ILC3s protects the intestinal stem cell niche after pretransplantational conditioning and is critical for reducing tissue damage during GVHD[159]. In line with this, Dudakov et al. observed a similar effect in the thymus. After total body irradiation, IL-22 production and

upregulation of RankL from radio resistant ILC3s resulted in regeneration of the thymic environment in an IL-23 dependent manner[160].

2.6 TSLP

Thymic stromal lymphopoietin (TSLP) is a member of the Interleukin (IL) -2 like cytokine family, which was first discovered in the supernatant of the murine thymic stromal cell line Z210R.1. It was shown to promote the differentiation of FL cells into B cell lineage and also the growth of pre - B cells *in vitro*[161]. Murine TSLP is a protein of 140 amino acids (aa) harbouring a four-helix bundle with three potential sides for N-linked glycosylation[162]. Purification of TSLP upon expression in mammalian cells resolved a 23-kD major isoform (140aa) and an 18-kD minor species[162].

Human TSLP gene encodes a protein of 159 amino acids and has poor homology with murine TSLP (43% amino acid residues)[163,164]. However, a set of disulfide bonds between 6 cysteines is conserved between human and mouse[163]. TSLP exerts similar biological functions in both species. It is predominantly produced by cells of non - hematopoietic origin like epithelial cells in lung, skin and gastrointestinal tract[165-167] and it was shown that multiple cell types of the adaptive and innate immune system are capable to respond to TSLP.

2.6.1 TSLP receptor and signaling

The TSLP receptor (TSLPR) also known as cytokine receptor - like factor 2 (CRLF2), is a heterodimer and consists of the TSLP - receptor chain, which binds TSLP with low affinity and IL-7-Receptor α chain. It has a N-terminal region outside the plasma membrane, a single hydrophobic transmembrane domain and an extracellular domain, which is also the ligand - binding domain[168-170]. It is likely that alternative splicing results in the two observed murine TSLP - receptor forms of 359 and 370 amino acids[169,171,172].

TSLPR stimulation activates multiple signal transduction pathways via kinases[180] such as Janus and Src kinases. These kinases regulate the activity of signal transducers and activators of transduction (STAT) e.g. STAT5, promoting activation and cell proliferation[173-175]. Similar to TSLP, also mouse and human TSLPR share only low amino acid identity (39%). The TSLPR is expressed in mouse and man by

various cells of the hematopoietic system, like T and B cells, natural killer (NK) cells, monocytes, mast cells, basophils, eosinophils and DCs. The various target cells for TSLP reflect the potential role of this cytokine in a wide range of diseases, including allergy, cancer and intestinal inflammation[176].

2.6.2 Role of TSLP in lymphopoiesis

TSLP was initially described to support murine B cell development[161]. Further studies revealed an effect of TSLP on pre B cells and the support of differentiation from uncommitted fetal liver and BM precursor into B cell lineage[162,177] as well as their further differentiation into mature $B220^+$ IgM^+ B cells[178]. The effect of TSLP on B cell maturation was also observed in human and can even substitute the effect of IL-7 deficiency[177,179]. In addition to its role in B cell development, TSLP was also described to affect T cell development. TSLP can drive thymopoiesis independently of IL-7 and favours especially the proliferation of DN1 and DN2 thymocytes *in vitro*[180] and *in situ*. *In vivo*, daily injections of recombinant TSLP in WT and $\gamma_c^{-/-}$ mice resulted in an increase in T cell populations in thymus and periphery[181]. However, in adult $TSLPR^{-/-}$ mice, there is no reduction in DN, double positive or single positive T cells. Furthermore, $TSLPR^{-/-}$ mice have neither a deficiency in B cell precursor in the bone marrow (BM) nor in the peripheral B cell compartment. Therefore, TSLP seems to be redundant in T and B cell development and maintenance under steady state coditions[181,182], but is essential for their development in the absence of IL-7 [180].

2.6.3 Activity of TSLP on dendritic cells

DCs were identified to be a potent source of TSLP after Toll like receptor (TLR) stimulation[183,184]. On the other hand, several studies in human and mice identified myeloid DCs as a major responder to TSLP. Treating DCs with TSLP improved their survival and maturation such as upregulation of MHC II and co-stimulatory molecules CD40, CD80 and CD86. These TSLP - conditioned DCs can polarize $CD4^+$ T cells towards the Th2 subset and can induce homeostatic proliferation of naïve $CD4^+$ T cells, which acquire characteristics of a central memory phenotype[185]. Through interaction of TSLP primed DCs, also $CD8^+$ T cells become activated and undergo expansion. After co - culture with DCs, stimulated with TSLP and CD40L, $CD8^+$ T cells increase IFN-γ production and gain cytolytic potential[186].

2.6.4 Regulation of TSLP

Numerous studies using primary human epithelial cells were designed to understand the regulation of TSLP. It was shown that TSLP expression is induced upon stimulation with IL-1β, TNF, different TLR like polyI:C and LPS as well as bacterial peptidoglycans. It appeared that the activation of the TSLP promoter after IL-1β and TNF-α treatment is mediated by an upstream NFκB site[187,188], but could also be activated via the MAPK pathway[189]. TSLP conditioned DCs were shown to induce the differentiation of naïve $CD4^+$ T cells into Th2 cells, which produce IL-4, IL-13 and TNF-α [87,190]. TSLP expression can be further induced by the Th2 cytokines IL-4 and IL-13 as well as dsRNA. This indicates a positive feedback loop to amplify Th2 inflammation e.g. during viral infections [191,192]. The nuclear receptor subtypes Retinoic X receptors α and β (RXRα/β) seem to be negative regulators of TSLP, since mice deficient for RXR α and RXR β in epidermal keratinocytes expressed higher amounts of TSLP and developed cutaneous inflammation[193]. RXR can form a heterodimer with vitamin D receptor (VDR). Application of vitamin D3 results in increased TSLP expression in keratinocytes, whereas application of vitamin D3 on the skin of $RXR^{-/-}$ mice or mice deficient for VDR does not increase TSLP expression[194,195]. There is evidence that RXR mediates TSLP repression via the inhibition of NFκB, rather than direct binding of RXR to the TSLP promoter[196]. Aberrant Notch signaling in the skin results in a loss of barrier function. As a result TSLP is systemically released in large amounts leading to atopic dermatitis - like symptoms[197,198]. Taken together, these results suggest, that inflammation, epithelial damage and skin barrier dysfunction positively regulate TSLP expression.

3 Aim of the study

Reconstitution of the adaptive immune system after HSCT is a major clinical issue, as the re - establishment of a functional T cell pool is delayed and even years after transplantation, patients suffer from infections and relapse of malignancies. Pretransplantational treatments with cytotoxic drugs and radiotherapy destroy the thymic microenvironment, which leads to impaired T lymphocyte development. Studies in fetal mice demonstrated that ILC3s as well as γδ T cell progenitors exhibit a supportive function in the maturation process of mTECs before birth, which assures adequate T cell development[75,76]. It remains unclear whether ILC3s also indirectly play a beneficial role in *de novo* T cell development in immunodeficient settings.

$Rag2^{-/-}\gamma c^{-/-}$ mice are devoid of T, B and NK cells and therefore represent a mouse model for combined immunodeficiency in humans. In addition, these mice are devoid of LNs, PPs and ILCs. In $Rag2^{-/-}\gamma c^{-/-}$ mice overexpressing TSLP (referred to as K14 $TSLP^{+/-}$ $Rag2^{-/-}$ $\gamma c^{-/-}$mice) ILC3 numbers are increased and almost all LNs are present. In my project, I wanted to investigate the role of increased ILC3 numbers and LNs on the reconstitution of the adaptive immune system after HSCT in immunodeficient mice. In order to address this question, $Rag2^{-/-}$ $\gamma c^{-/-}$ and K14 $TSLP^{+/-}$ $Rag2^{-/-}$ $\gamma c^{-/-}$ mice were transplanted with FL cells or mature T cells from $TSLPR^{-/-}$ mice and analysed for the efficiency of reconstitution in primary and secondary lymphoid organs.

4 Materials and methods

4.1 Materials

4.1.1 Reagents and chemicals

Acetone	Sigma-Aldrich
Agarose	Sigma-Aldrich
Amphotericin B	Sigma-Aldrich
2'-Deoxyguanosine monohydrate	Sigma-Aldrich
2-Mercaptoethanol	Gibco
2-Propanol ($CH_3CH(OH)CH_3$)	Merck KgaA
2x SensiMix SYBR Hi-ROX	Bioline
Albumin from bovine serum (BSA)	Sigma-Aldrich
Alum (Aluminium potassium sulphate, $AlK(SO_4)_2$)	Sigma-Aldrich
Ammonium chloride (NH_4Cl)	Sigma-Aldrich
Anti-CD4 microbeads	Miltenyi Biotec
Anti-PE microbeads	Miltenyi Biotec
4-Bromo-2-chlorophenol	Sigma-Aldrich
Brefeldin A (BFA)	Sigma Aldrich
Calciumchloride	Merck KgaA
Carboxyfluorescein succinimidyl ester (CFSE)	Molecular Probes
Ciproxine	Bayer (0.2%)
Collagenase D	Roche
4', 6-Diamidino-2-pheylindole (DAPI)	AppliChem
Deoxyadenosine triphosphate (dATP)	Sigma-Aldrich
Deoxycytidine triphosphate (dCTP)	Sigma-Aldrich
Deoxyguanosine triphosphate (dGTP)	Sigma-Aldrich
Deoxythymidine triphosphate (dTTP)	Sigma-Aldrich
Di-ethanolamine ($C_4H_{11}NO_2$)	Sigma-Aldrich
Di-nitrophenyl phosphate (dNPP)	Sigma-Aldrich
Di-potassium hydrogen phosphatate (K_2HPO_4)	Merck KgaA
Di-sodium hydrogen phosphatate (Na_2HPO_4 x 2 H_2O)	Merck KgaA
Di-thiothreitol (DTT)	AppliChem
DMEM (1x) GlutaMax^{TM}-I	Gibco
DNase I	Roche

EDTA disodium salt dihydrate	AppliChem
Fluoromount-G™	eBioscience
Ethanol (C_2H_5OH)	Merck KgA
Fetal calf serum (FCS, heat-inactivated)	Gibco
D (+) – Glucose monohydrate	Merck
Gentamycin	Life technologies
GlycoBlue™	Life technologies
Hydrochloric acid (HCl)	Sigma-Aldrich
Insulin Transferrin Selenium	Gibco
Ionomycin	AxonLab
Iscove`s modified Dulbecco`s medium (IMDM)	Sigma-Aldrich
Kanamycin	Sigma-Aldrich
Liberase	Roche
Methanol	Merck KgA
Magnesium chloride hexahydrate ($MgCl_2$ x 6 H2O)	AppliChem
Nonessential amino acids (NEAA)	Gibco (100 x)
Nuclease free H_2O	life technologies
O.C.T™	Tissue-Tek®
Oligo dT	Promega
Phosphate buffered saline (PBS)	Biochrom AG
Penicillin Streptomycin (Pen/Step)	Gibco
Percoll	GE Healthcare
Paraformaldehyde (PFA)	AppliChem
Phorbol-12-myristat-13-acetat (PMA, $C_{36}H_{56}O_8$)	Sigma-Aldrich
Potassium bicarbonate ($KHCO_3$)	Sigma-Aldrich
Potassium chloride (KCL)	AppliChem
Primatone	Sigma-Aldrich
Proteinase K	Roche
Saponin	Sigma-Aldrich
Sodium acide (NaN_3)	Merck KgaA
Sodium chloride (NaCL)	AppliChem
Sodium dodecyl sulfate (SDS)	BioRad
Sodium hydrogen carbonate ($NaHCO_3$)	Merck KgaA
Sodium hydroxide (NaOH)	Merck KgaA
SuperScript™ III Reverse Transcriptase	Invitrogen
Taq Polymerase	Sigma-Aldrich
Tris ($C_4H_{11}NO_3$)	Carl Roth GmbH

TRI-Reagent®	Sigma-Aldrich
Tween-20	AppliChem

4.1.2 Buffers, solutions and media

1x PBS	137 mM NaCl 2.7 mM KCl 10 mM Na_2HPO_4 x 2 H_2O 2 mM KH_2PO_4 in dH_2O
1x TE buffer	10 mM Tris 1 mM EDTA in dH_2O
DMEM (1x) GlutaMax^{TM}-I	(+) 4.5 g/L D-Glucose (-) Pyruvate
dNTP mix	10 mM sATP 10 mM sCTP 10 mM sGTP 10 mM sTTP in nuclease free H_2O
ELISA buffer (NP-OVA ELISA)	1 % BSA 0.2 % Tween-20 in 1x PBS
ELISA wash buffer (NP-OVA ELISA)	0.1 % Tween-20 in H_2O
Erythrolysis buffer	0.15 M NH_4Cl 10 mM $KHCO_3$ 0.1 mM EDTA in dH_2O (pH 7.2 – 7.4)

Fixation buffer	1x PBS 4 % PFA
FACS buffer	1x PBS 3 % FCS
IMDM	(SF) IMDM (powder) 3.02 g $NaHCO_3$ 1 % Pen/Step 1 % Ciproxine 0.1 % Kanamycin 1 % Insulin Transferrin Selenium 0.3 % Primatone 1 % NEAA 0.1 % 2-mercaptoethanol
IMDM 5 % FCS	IMDM (SF) 5 % FCS
IMDM 10 % FCS	IMDM (SF) 10 % FCS
Lysis buffer (for DNA isolation from mouse biopsies)	100 mM Tris (pH 8.0) 200 mM NaCl 5 mM EDTA (pH 8.0) 0.2 % SDS in dH_2O
Permebabilization buffer for intracellular staining	0.5 % Saponin 10 mM NaN_3 in FACS buffer
Stromal cell isolation buffer	DMEM (1x) GlutaMax^{TM}-I 2 % FCS 1.2 mM $CaCl_2$ 1 % Pen/Step

Substrate buffer (NP-OVA ELISA)	0.1 g $MgCl_2$ x 6 H_2O 10 mM NaN_3 10 % $C_4H_{11}NO_2$ in dH_2O (pH 9.8)
Thymus organ culture (TOC) medium	IMDM 10% FCS 10^{-5} nM β-mercaptoethanol 1 % Kanamycin

4.1.3 Cytokines, TLR ligands, peptides, proteins

IL-7, recombinant	Peprotech
IL-23, recombinant	eBioscience
SCF, recombinant	Peprotech
TSLP, recombinant	R&D
RankL	home made
4-Hydroxy-3-nitrophenylacetyl NP- (18)-OVA	Biosearch Technologies Inc.

4.1.4 Antibodies (Abs)

Abs for flow cytometry analyses (directed against murine proteins)

Specificity	**Clone**
Aire	5H12
CD3ε	17A2, 145-2C11
CD4	RM4-4, RM4-5 and GK1.5
CD8α	53-6.7
CD11b	M1/70
CD11c	N418
CD19	6D5
CD21	7G6
CD23	B3B4

CD24	M1/59
CD25 (IL-2Rα)	PC61
CD31	390
CD35	8C12
CD40	1C10
CD44	IM7
CD45	30-F11
CD45R (B220)	RA3-6B2
CD54 (ICAM-1)	3E2
CD62L	MEL-14
CD69	H1.2F3
CD80	16-10A1
CD86	GL1
CD90.2 (Thy1.2)	30-H12
CD103	2E7
CD106 (VCAM-1)	429
CD117 (ckit)	2B8
CD127 (IL-7Rα)	A7R34
CD196 (CCR6)	140706
CD278 (ICOS)	C398.4A
CD326 (EpCAM)	G8.8
Foxp3	FJK-16s
GATA-3	TWAJ
GmCSF	MP1-22E9
Gp38 (Podoplanin)	8.1.1
Gr-1	RB6-8C5
Helios	22F6
IFNγ	XMG1.2
IgM	II/41
IL-5	TRFK5
IL-13	eBio13A
IL-17	TC11-18H10
IL-22	1H8PWSR
Ly51	6C3
MHC II	M5/114.15.2,
NKp46	29A1.4

NK1.1	PK136
RORγt	AFKJS-9, B2D
STAT5	47
TCRβ	H57-597
TCRγδ	GL3, UC7-13D5
TER-119	TER-119
UEA-1	

All reagents were purchased from BD Bioscience, eBioscience, Biolegend, R&D systems or Vector Laboratories. Primary monoclonal Abs (mAbs) were conjugated to either fluorescein isothycyanate (FITC), phycoerythrin (PE), allophycocyanin (APC), Alexa Fluor® 700, brilliant violet 421, 510, or 605 (BV421™, BV510™ BV605™,), phycoerythrin cyanine 7 (PECy7), peridinin chlorophyll (PerCP)-eFluor 710, Percp-Cy5.5, allophycocyanin cyanine 7 (APC-Cy7), or Texas Red®.
Biotin-conjugated primary mAbs were detected using secondary anti-rat polyclonal Abs conjugated to Streptavidin/APC-Cy7, Streptavidin/BV421™, Streptavidin/BV510™ or Streptavidin Percp-Cy5.5. Blocking of Fc receptors was performed using anti-mouse FcγRII/III mAb (clone 2.4G2, purified supernatant, home made).

Abs used for ELISA (NP-OVA)

For coating of plates:

Purified anti-mouse IgM (unlabeled)	M41 (A. Rolink, University of Basel)
Purified anti-mouse IgG (unlabeled)	15H6 (SouthernBiotech)

For detection:

Biotin-conjugated goat anti-mouse IgG	Caltag Laboratories
Alkaline phosphatase (AKP) – Streptavidin	Roche

Abs used for Immunofluorescence

Aire	5H12
CK5 Rabbit	PRB-160B (Covalence, Princeton, NJ)
CK8-Cy5	TROMA-1 (Developmental Studies Hybridoma Bank, University of Iowa)
goat-αRabbit-Alexa 555	Molecular Probes

4.1.5 Primers for quantitative real time PCR (qRT PCR)

Primer	**Sequence**
Aire forward	5'TGTGCCACGACGGAGGTGAG3'
Aire reverse	5'GGTTCTGTTGGACTCTGCCCTG3'
β -actin forward	5'CAATAGTGATGACCTGGCCGT3'
β -actin reverse	5'AGAGGGAAATCGTGCGTGAC3'
CCL19 forward	5'CCTGGGTGGATCGCATCATCCG3'
CCL19 reverse	5'AGAGCATCAGGAGGCCTGGTCCT3'
CCL21 forward	5'AGCTATGTGCAAACCCTGAGGA3'
CCL21 reverse	5'TTCCAGACTTAGAGGTTCCCCG3'
CCL25 forward	5'GTTACCAGCACAGGATCAAAT3'
CCL25 reverse	5'GGAAGTAGAATCTCACAGCA3'
CD80 forward	5'CCTGGGAAAAACCCCCAGAA3'
CD80 reverse	5'ACAACGATGACGACGACTGT3'
CxCL12 forward	5'AAATCCTCAACACTCCAAAC3'
CxCL12 reverse	5'GCTTTCTCCAGGTACTCTTG3'
EpCAM forward	5'TGAGGACCTACTGGATCATC3'
EpCAM reverse	5'TATCGAGATGTGAACGCCTC3'
FGF 10 forward	5'AGGGGAAACTCTATGGCTCAAAAG3'

Primer	Sequence
FGF 10 reverse	5'GCCACATACATTTGCCTGCC3'
IL-7 forward	5'GATAGTAATTGCCCGAATAATGAACCA3'
IL-7 reverse	5'GTTTGTGTGCCTTGTGATACTGTTAG3'
IL-15 forward	5'GACGGGATCCTGCTGTGTTT3'
IL-15 reverse	5'AGGTGGATTCTTTCCTGACCTC3'
IL-22 forward	5'GAGTCAGTGCTAAGGATCAG3'
IL-22 reverse	5'TCAGAGACATAAACAGCAGG3'
KGF forward	5'CATGCTTCCACCTCGTCTGT3'
KGF reverse	5'CAGTTCACACTCGTAGCCGT3'
PDGFRα forward	5'AAGACCTGGGCAAGAGGAAC3'
PDGFRα reverse	5'GAACCTGTCTCGATGGCACT3'
RankL forward	5'CCTGTACTTTCGAGCGCAGA3'
RankL reverse	5'CCAGAGTCGAGTCCTGCAAA3'
SCF forward	5'AAGGAGATCTGCGGGAATCC3'
SCF reverse	5'CGGCGACATAGTTGAGGGTTA3'
TBP forward	5'GGCACCACCCCCTTGTACCCT3'
TBP reverse	5'ACGCAGTTGTCCGTGGCTCT3'
XCL1 forward	5'ATGGGTTGTGGAAGGTGTGG3'
XCL1 reverse	5'AGCCGCTGGGTTTGTAAGTT3'

4.1.6 Kits

Foxp3 staining buffer set	eBioscience
LIVE/DEAD® Fixable Aqua Dead Cell Stain Kit	Molecular Probes
RNeasy Micro Kit	Qiagen
RNeasy Mini kit	Qiagen
RT^2 HT first strand kit	Qiagen
RT^2 PCR Arrays	Qiagen
SensiMix SYBR Hi-ROX Kit	Bioline
SuperScript™ III Reverse Transcriptase	Invitrogen
Zombie Aqua™ Fixable Viability Kit	BioLegend

4.1.7 Tools and instruments

Asys Expert Plus Microplate Reader	Biochrom
AutoMACS Pro	Miltenyi Biotec
Cell strainer (70 µm / 100 µm)	Falcon
Cell counter CASY INNOVATIS	Roche
Eppendorf centrifuge 5810 R, 5415 R, 5417 R	Eppendorf
Eppendorf Mastercycler Gradient	Eppendorf
ELISA plate reader	ASYS Expert Plus
Flow cytometer BD FACSAria IIu	BD Bioscience
Flow cytometer BD FACSCanto II	BD Bioscience
BD LSR Fortessa	BD Biosciences
gentleMACS™ Octo Dissociator	Miltenyi Biotec
MAXI sorb 96 well plates for ELISA	Nunc
Microscope DMI 4000	Leica
Micro tube 1.3 mL K3E	Sarstedt
Nanodrop 2000c	Thermo Scientific
Nucleopore Track-Etch Membrane (poresize: 0.8 µm)	Millipore
Rotorgene RT PCR machine (RG-3000A)	Corbett Research
Zirconia beads	BioSpec Products

4.1.8 Software

FlowJo 9.7.6
GraphPad Prism 6
ImageJ
Microsoft Office for Mac 14.4.3

4.1.9 Mice

C57BL/6 were purchased from Janvier (Saint Berthevin Cedex, France). TSLPR$^{-/-}$[181], K14 TSLP$^{+/-}$ Rag2$^{-/-}\gamma c^{-/-}$[180], ROR$\gamma^{-/-}$[199], Rag2$^{-/-}$[200](Jackson), were previously described. Rag2$^{-/-}\gamma c^{-/-}$ on C57BL/6 background were provided by Jörg Kirberg,MPI Freiburg, Germany. All mice were kept under specific-pathogen free (SPF) conditions. The

animal experiments received the approval of the Cantonal Veterinary Office of the city of Basel, Switzerland.

4.2 Methods

4.2.1 Genotyping

Isolation of DNA

For isolation of genomic DNA, biopsies were digested in 500 µL lysis buffer containing 100 µg/mL Proteinase K (at least 3 h at 55 °C while shaking at 700 rpm on a heat block). 500 µL H_2O was added for further dilution and stored at 4 ºC.

TSLP PCR

Primer TSLP Fwd: 5' GGAGCCTCTTCATCCTGCAA 3'
Primer TSLP Rev: 5' TCCGGGCAAATGTTTTGTCG 3'

PCR reaction mix:

2.5 µl	10x buffer
0.5 µl	TSLP fwd primer (10 µM)
0.5 µl	TSLP rev primer (10 µM)
0.5 µl	dNTPs (10 mM)
0.1 µl	Taq Polymerase (Sigma)
20 µl	dH_2O
1 µl	genomic DNA

PCR program for amplification:

step 1	94 ºC	5'	
step 2	94 ºC	30"	
step 3	63 ºC	30"	
step 4	72 ºC	30"	**step 2 - 4 31 x**
step 5	72 ºC	10'	
step 6	20 ºC	hold	

product length:

TSLP: ~252 base pairs (bp)

4.2.2 Cell isolation

Lamina propria lymphocytes (LPL) from **colon** and **small intestine** (SI) were isolated by enzymatic digestion. Briefly, **SI** was opened longitudinally, feces were removed, and SI was cut into 2 cm pieces. After incubation in 25 mL of 30 mM EDTA solution in Ca2+- and Mg2+- free PBS for 30' on ice, the tube was shaken vigourously and washed with PBS several times until PBS was clear without debris. Tissue was cut in smaller pieces and incubated in pre – warmed DMEM plus 0.025 mg/mL DNaseI (Roche) and1 mg/mL Collagenase D (Roche) at 37 ºC. After 15 min, tissue pieces were pipetted up and down and supernatant was filtered through a 100 µm filter into a collection tube containing 15 mL DMEM, 5% FCS, 2mM EDTA. Incubation steps were repeated 3 times with fresh Collagenase D. After the last digestion step, cell suspension was pelleted, resuspended in 5 mL 40 % Percoll, underlaid with 3 mL 80 % Percoll and centrifuged for 30' at 20 ºC (1800 rpm, acceleration 4, brake 1). Cells of the interphase were collected and washed once with PBS.

Colon (w/o cecum) was opened longitudinally, feces were removed, and colon was cut into 1 cm pieces. Tissue pieces were incubated in 25 mL of 5 mM EDTA plus 10 mM HEPES solution in $Ca2^{+}$- and $Mg2^{+}$- free PBS for 20 min at 200 rpm shaking at 37 ºC. Incubation steps were repeated 3 times in fresh EDTA/HEPES solution followed by a washing step with DMEM. Tissue was transferred to gentle MACS tube with 5 mL pre-warmed DMEM, 0.025 mg/mL DNaseI, 1 mg/mL Collagenase D, 0.25 mg/mL Collagenase VIII and incubated for 2x 30' at 37 ºC interrupted by 2 cycles of tissue dissociation with gentleMACS™ Octo Dissociator (Miltenyi Biotech). Cell suspension was filtered through a 100 µm filter into a collection tube containing 15 mL DMEM, 5% FCS, 2mM EDTA, peletted, resuspended in 2 mL 40 % Percoll underlaid with 1.2 mL 80 % Percoll and centrifuged for 30' at 20 ºC (1800 rpm, acceleration 4, brake 1). Cells of the interphase were collected (total LP lymphocytes).

Thymocytes and **splenocytes** were either gained by mashing the tissue through a metal grid (Ø 0.8 mm) in FACS buffer or by cutting the tissue and digesting it enzymatically by 4 rounds with DMEM, 0.025 mg/mL DNaseI, 1 mg/mL Collagenase D at 37 ºC as described earlier. Erythrocytes were lysed with erythrolysis buffer (2' at RT).

Thymic ILC3s were isolated by enzymatic digestion as described. For WT and RORγt$^{-/-}$ mice, thymocytes were depleted with a Lin cocktail (CD3ε, CD8α, CD11c, B220, CD19 TCRαβ, TCRγδ, GR-1, NK1.1) by MACS before staining for ILC3 marker, whereas total thymi were analysed in case of Rag2$^{-/-}$γc$^{-/-}$ and K14 TSLP$^{+/-}$ Rag2$^{-/-}$γc$^{-/-}$ mice.

Bone marrow (BM) was recovered by crushing the bones of femurs and tibias in FACS buffer. Erythrocytes were lysed with erythrolysis buffer (2' at RT).

Thymic epithelial cell isolation of K14 TSLP$^{+/-}$ Rag2$^{-/-}$γc$^{-/-}$ and Rag2$^{-/-}$γc$^{-/-}$ was performed by enzymatic digestion in PBS with 1 Wünsch unit/mL Liberase (Roche), 0,025 mg/mL DNaseI at 37 ºC. Total cells were used for antibody staining.
For WT, thymi were isolated and enzymatically digested with 1 Wünsch unit/mL Liberase (Roche), 0,025 mg/mL DNaseI at 37 ºC. The enzymatic digests were incubated with biotin-conjugated EpCAM (G8.8) followed by anti-biotin magnetic microbeads (Miltenyi Biotec, Bergisch Gladbach, Germany) and enrichment of EpCAM^{+} stromal cells by positive selection on an AutoMACS Pro (Miltenyi).

Isolation of stromal cells from spleen and lymph nodes
Stromal cell populations were isolated according to the protocol adapted from Link et al.[109]. Briefly, spleen and lymph nodes were opened with needles and digested in DMEM (1.2 mM CaCl2, 2% FCS, Pen/Strep) plus Collagenase IV (1mg/mL) and DNaseI (0.04 mg/mL) to isolate lymphocytes. In a second digestion step with DMEM, Collagenase D (1mg/mL) and DNaseI (0.04 mg/mL), stromal cells were isolated and analysed by flow cytometry or further sorted to isolate subpopulations.

4.2.3 Flow cytometry and cell sorting

Cell suspensions were stained with biotinylated or fluorochrome-conjugated Abs (30', 4 ºC) in FACS buffer. Fc receptors were blocked by incubation with anti-mouse FcγRII/III mAb (clone 2.4G2). Fluorochrome-conjugated streptavidin was added as a second incubation step (30', 4 ºC) for stainings, which included biotinylated Abs.
Intracellular RORγt staining was performed using Foxp3 staining buffer set (eBioscience) after surface molecule staining according to manufacturer's protocol. For intracellular cytokine staining, cells were stimulated for 4h with PMA (50 ng/mL) and Ionomycin (2.5 µg/mL) or IL-23 (20 ng/mL) and incubated with BFA (10 µg/mL)

for the last 2h at 37ºC. Cells were washed with FACS buffer and fixed with 4 % PFA in PBS for 10min on ice, washed twice with FACS buffer and stained for the respective Abs in 0.5 % Saponin in FACS buffer. Intracellular Aire staining was also performed in 0.5 % Saponin in FACS buffer after fixation with 4 % PFA in PBS.
Dead cells were identified using LIVE/DEAD® Fixable Aqua Dead Cell Stain Kit or in case of non-fixed cells with DAPI.

Data were acquired with either FACS Canto II or LSR Fortessa and analysed with FlowJo software (Tree Star). Cell sorting was performed with FACS Aria Ilu (BD Bioscience, >98 % purity). Absolute cell numbers derived from various organs were determined by counting cells with the cell counter CASY INNOVATIS (Roche).

4.2.4 Fetal and re-aggregated thymus organ culture (FTOC and RTOC)

For **FTOCs**, fetal thymic lobes were isolated from embryonic day 14.5 (E14.5) WT embryos and cultured for 5 days on membranes (Millipore) in the presence of 1.35 mM 2``- Deoxyguanosine in TOC medium (IMDM, 10% FCS, 10^{-5} nM β-mercaptoethanol, 1 % Kanamycin) to deplete hematopoietic cells. Membranes were transferred to fresh medium for one day followed by application of RankL (home made): 10 µg/mL; TSLP (R&D): 25, 50 or 100 ng/mL) for 5 days. Lobes were harvested and disaggregated in FACS buffer, 0,025 mg/mL DNaseI, 1 mg/mL Collagenase D for 15'at 37 ºC followed by surface molecular staining.

For **RTOCs**, fetal thymic lobes were isolated from WT E14.5, disaggregated in TOC medium with 0,025 mg/mL DNaseI, 1 mg/mL Collagenase D for 15'at 37 ºC and sorted for $CD45^-$ $TER119^-$. Sorted cells were re-aggregated in TOC medium (supplemented with 0.25 mg/mL Gentamicin, 10µg/mL Amphoterizin, 4000U Pen/Strep, 25 ng/mL IL-7 and 20 ng/mL SCF) in a 1 : 2 ratio with DN3s (sorted for $CD25^+$ $CD44^-$) or LPL ILC3s (*Lin^-, $CD90.2^+$, $CD117^+$) from $Rag2^{-/-}$ mice for 4 days and analysed by flow cytometry. (*CD3ε, CD8α, CD11c, CD19, B220, GR-1, NK1.1)

4.2.5 Phosphoflow

WT tymic epithelial cells were isolated and stained for surface molecules according to manufactured protocol; BM cells were recovered as described. Cells were resuspendet in appropriate amount of SF-IMDM 5% FCS and allowed to rest for 2h at 37ºC in 1.5 mL Eppendorf tubes. Cells were then stimulated for 10min at 37ºC with either recombinant TSLP (R&D): 25, 50 or 100 ng/mL or IL-7: 20ng/mL (Peprotech) or left unstimulated. Cells were fixed for 15 minutes with 2% PFA (AppliChem) at 37ºC.

Permeabilization was done with 100% methanol on ice for 30 min and phospho - STAT5 staining was performed at room temperature (RT) for 30 min.

4.2.6 Reconstitution with FL cells and immunization

Fetal liver (FL) cells from E14.5 TSLPR$^{-/-}$ were isolated. Erythrocytes were lysed with erythrolysis buffer (2' at RT) and 5x10^6 cells/mouse were injected i.v. into Rag2$^{-/-}\gamma c^{-/-}$ or K14 TSLP$^{+/-}$ Rag2$^{-/-}\gamma c^{-/-}$ mice.

Mice were immunized intraperitoneally (i.p.) with 100 μg alum-precipitated NP-Ovalbumin (NP (18)-OVA) 6 weeks after FL transfer (day 42) and boosted with 100 μg alum-precipitated NP-OVA 12 days after the first immunization. Sera were collected before immunization (day 42) and 7 days after the second immunization (day 61) with NP-OVA.

4.2.7 Antibody detection by ELISA

To detect NP-OVA-specific Abs in the serum of immunized mice, NUNC immunoplate Maxisorb F96 plates were coated with 5 μg/mL NP-OVA (Biosearch Technologies Inc.) in 1x PBS at 4ºC o/n. Plates were washed (H_2O 0.1% Tween-20) and incubated with sera for 1 h at RT. After washing, biotin-conjugated goat anti-mouse IgG (Caltag Laboratories, 1 h, RT) was added and detected by alkaline-phosphatase (AKP)-conjugated Streptavidin (Roche, 45', RT). Plates were developed with dinitrophenyl phosphate (dNPP, 1 mg/mL, Sigma) in substrate buffer. The reaction was stopped with 1 M NaOH (Fluka). The optical density (OD) was determined at 405 nm with an ELISA reader (ASYS Expert plus).

To detect total IgM and total IgG levels in the serum of reconstituted mice, NUNC immunoplate Maxisorb F96 plates were coated with either 5 μg/mL purified anti-mouse-IgM (unlabeled, clone M41) or purified anti-mouse IgG (clone 15H6) in 1x PBS at 4ºC o/n, followed by described protocol.

4.2.8 T cell proliferation assay in vivo

T cells from spleen and lymph nodes of TSLPR$^{-/-}$ mice were magnetically purified with αCD4 - beads (LTR4, Miltenyi Biotec) or stained for αCD8 – PE followed by an incubation step with αPE - beads. CD4$^+$ and CD8$^+$ T cells were pooled (ratio 1:2) and labeled with 45 μM carboxyfluorescein succinimidyl ester (CFSE) for 8' at RT in the dark. The reaction was stopped with 80% FCS in Ca2$^+$- and Mg2$^+$- free PBS.

Cells were washed, resuspended in PBS and $1x10^7$ cells/mouse were injected i.v. . For naïve T cell transfer, a magnetic depletion (Miltenyi Biotech) with B220, CD19, CD11c, NK1.1 was performed and naïve T cells were sorted for $CD4^+$ respective $CD8^+$, $CD62L^+$ and $CD44^{low/-}$ expression (>98 % purity). Sorted naïve $CD4^+$ and $CD8^+$ cells were pooled (ratio 1:2), labeled with 45 µM CFSE as described and $2x10^6$ cells/mouse (ratio 1:2) were injected i.v.

4.2.9 Immunfluorescence

Organs were frozen in O.C.T™ (Tissue-Tek®) in liquid N_2. Sections were cut on a cryostat (8 µm), fixed in acetone and rehydrated in PBS. After blocking with 1 % BSA in PBS (30' at RT) in a wet chamber, sections were incubated with fluorochrome-conjugated or purified Abs (1 h at RT). Secondary Abs were applied (1h at RT or o/n at 4ºC) for stainings including purified Abs after washing twice in PBS (5' at RT). After one wash in PBS, sections were embedded in Fluoromount-G™.

4.2.10 RNA isolation, cDNA synthesis and qRT PCR

For RNA isolation from tissue, tissue pieces were frozen in liquid nitrogen ($LiqN_2$) in 1.5 mL Micro tubes PP (Sarstedt) containing Zirconia beads (BioSpec Products). Tissue was homogenized in 1mL TRI-Reagent® with a FastPrep-24 instrument (MP Biomedicals) for 1' at 6.5 m/s and RNA was isolated according to manufacturer's protocol. For sorted cells or small tissue quantities, homogenization was performed through a 25G needle. RNA was isolated according to manufacturer's protocol with the help of GlycoBlue as a co - precipitant. In case of sorted stromal cells, RNA was isolated using the RNeasy Micro Kit (Qiagen) according to manufacturer's protocol. RNA quantification and quality assessment were performed on a Nanodrop 2000c (Thermo Scientific Inc.). First strand cDNA was synthesized by using SuperScript™ III Reverse Transcriptase (Invitrogen) according to manufacturer's instructions. Quantitative Real –time (qRT) PCR was performed on a Rotor-Gene RG-3000A (Corbett research) using SensiMix SYBR Hi-Rox Kit (Bioline, London, UK). Results were normalized to the housekeeping gene TATA box binding protein (TBP) or β-actin, using the comparative threshold cycle method (ΔC_T) for relative quantification.

Data of mRNA levels in the small intestine were obtained by RNA isolation of 3x1 cm tissue combined from duodenum, jejunum and ileum of the small intestine. RNA was isolated with RNeasy Mini Kit (Qiagen) according to manufacturer's instructions followed by first strand cDNA synthesis with RT^2 HT First Strand Kit (Qiagen).

Custom arranged RT^2 PCR Arrays (Qiagen) were performed by T. Dolowschiak, Microbiology ETH Zürich. Results were normalized to the housekeeping gene β-actin, using the comparative threshold cycle method (ΔC_T) for relative quantification.

4.2.11 Statistical analyses

Statistical analyses were performed using Mann Whitney U test or unpaired Students t-test with Prism software (GraphPad Software, Inc.). P values < 0.05 are considered to be statistically different.

5 Results

5.1 Characterization of Rag2$^{-/-}$ γc$^{-/-}$ and K14 TSLP$^{+/-}$ Rag2$^{-/-}$ γc$^{-/-}$ mice

Primary and secondary lymphoid organs were characterized in Rag2$^{-/-}$ γc$^{-/-}$ and K14 TSLP$^{+/-}$ Rag2$^{-/-}$ γc$^{-/-}$ mice with a particular emphasis on the architecture and maturation of the thymus stroma as well as LN stromal cells.

5.1.1 TSLPtg increases thymus size and thymic cellularity

Macroscopic analysis of 6 - 8 weeks old Rag2$^{-/-}$ γc$^{-/-}$ mice revealed that these mice had very small thymi containing cysts compared to K14 TSLP$^{+/-}$ Rag2$^{-/-}$ γc$^{-/-}$ mice and WT mice (Fig 8A). Contrary to Rag2$^{-/-}$ γc$^{-/-}$ mice, in which thymocytes accumulate at the CD25^{-} CD44^{+} double negative (DN) 1 stage, K14 TSLP$^{+/-}$ Rag2$^{-/-}$ γc$^{-/-}$ mice showed higher thymocyte frequencies in the DN2 and DN3 stage (Fig. 8B). This was also reflected by the higher total thymus cellularity (Fig. 8C) as well as the significant higher numbers of DN2s and DN3s in K14 TSLP$^{+/-}$ Rag2$^{-/-}$ γc$^{-/-}$ mice (Fig. 8D). These results are in line with previous studies demonstrating a role for TSLP on thymocyte precursor development[180]. However, mice with TSLP overexpression do not reach DN frequencies of WT controls beyond DN1 (Fig. 8B).

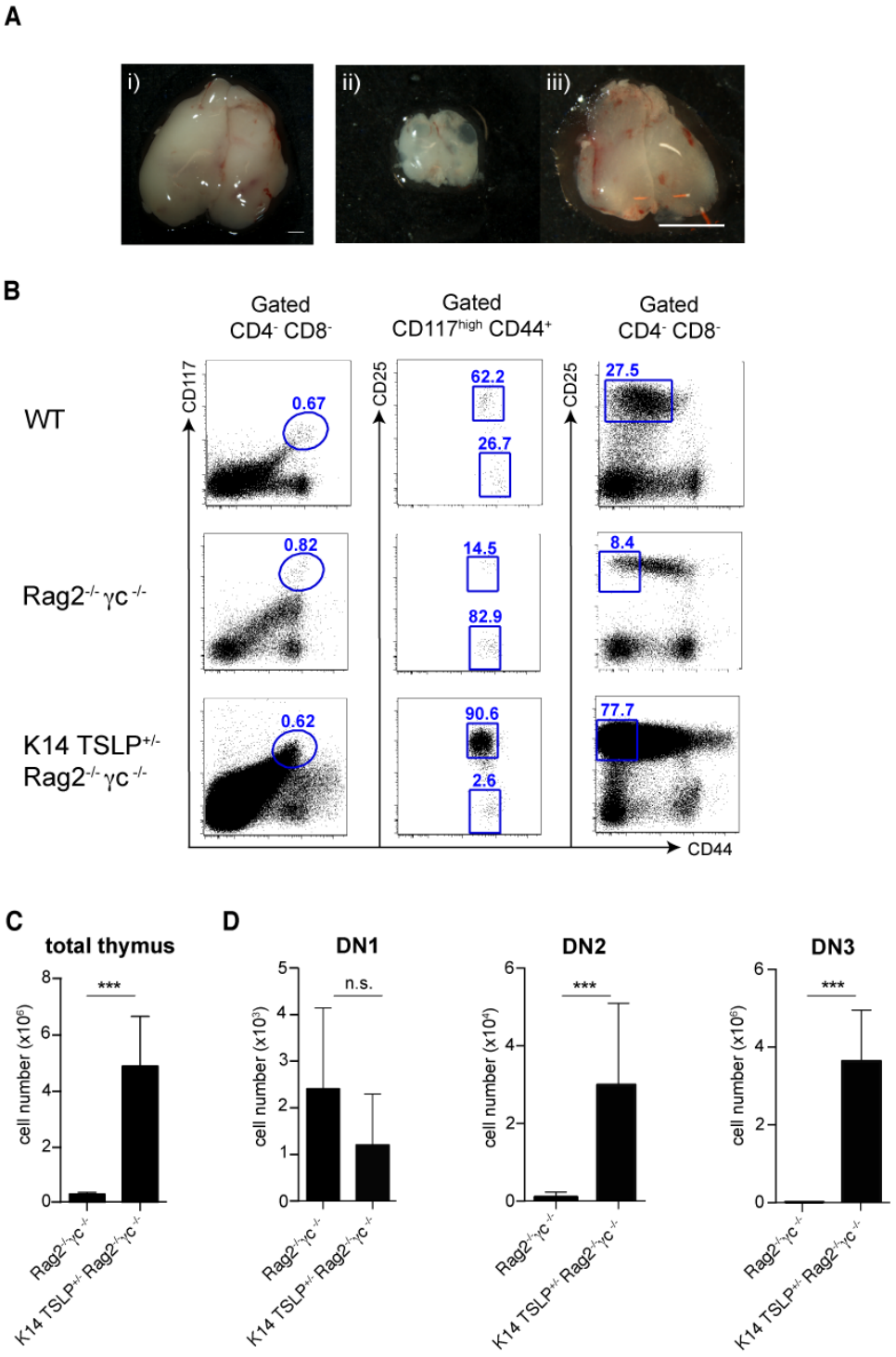

Figure 8: TSLPtg increases thymus size and number of DN thymocytes in Rag2$^{-/-}$γc$^{-/-}$ mice. A) Representative photographic picture of thymi from WT (i) Rag2$^{-/-}$ γc$^{-/-}$ (ii) and K14 TSLP$^{+/-}$ Rag2$^{-/-}$ γc$^{-/-}$ mice (iii). Scale bar represents 1mm. **B)** Flow cytometry analysis of DN1 (CD117^{high} CD25^{-} CD44^{+}), DN2 (CD117^{high} CD25^{+} CD44^{+}) and DN3 (CD25^{+} CD44^{-}). Numbers in dot plots represent frequencies of a representative experiment **C)** Absolute cell numbers of total thymus. **D)** Absolute cell numbers for DN1, DN2 and DN3; **C - D**) n = 7 from 2 independent experiments; median values + interquartile range; n.s. = not significant, ***P<0.001.

5.1.2 TSLPtg expression improves thymic stromal compartment

To investigate whether TSLPtg expression does not only increase the absolute number of DN thymocytes but has also an effect on the thymic epithelial compartment, WT, Rag2$^{-/-}$ γc$^{-/-}$ and K14 TSLP$^{+/-}$ Rag2$^{-/-}$ γc$^{-/-}$ thymi were stained with αCK5 (medulla marker) and αCK8 (cortical marker). Immunofluorescence analysis of WT thymic sections showed a compartimentalization into cortex and medulla (Fig. 9A, i and ii), whereas Rag2$^{-/-}$ γc$^{-/-}$ mice showed preferentially CK5 CK8, double positive cells and no segregation into compartments (Fig. 9A iii and iv). K14 TSLP$^{+/-}$ Rag2$^{-/-}$ γc$^{-/-}$ thymi showed partial segregation of the epithelial cells in CK5 as well as CK8 single positive cells, beside double positive cells for CK5 and CK8 (Fig. 9A v and vi). A feature of medullary thymic epithelial cells (mTECs) is the expression of the transcription factor autoimmune regulator (Aire), which is crucial for the establishment of central tolerance[51]. In WT mice, Aire^{+} cells were confirmed to localize in the thymus medulla. No Aire^{+} cells were detected in Rag2$^{-/-}$γc$^{-/-}$ mice, and a very small number of Aire^{+} cells were found in the thymi of K14 TSLP$^{+/-}$ Rag2$^{-/-}$γc$^{-/-}$ mice (Fig. 9B). The presence of Aire and the Aire dependent marker xCL1 was confirmed by qRT PCR in K14 TSLP$^{+/-}$ Rag2$^{-/-}$γc$^{-/-}$ mice, whereas these factors were undetectable in Rag2$^{-/-}$γc$^{-/-}$ mice (Fig. 9B). Another marker of mature mTECs is CD80, which showed a ~7 times higher expression in K14 TSLP$^{+/-}$ Rag2$^{-/-}$γc$^{-/-}$ compared to Rag2$^{-/-}$γc$^{-/-}$ mice (Fig. 9B). In summary, the results obtained from histology indicate the presence of mTECs in K14 TSLP$^{+/-}$ Rag2$^{-/-}$γc$^{-/-}$ mice. This observation was confirmed by FACS analysis of the thymic epithelial compartment in Rag2$^{-/-}$γc$^{-/-}$ and K14 TSLP$^{+/-}$ Rag2$^{-/-}$γc$^{-/-}$ mice (Fig. 10).

In K14 TSLP$^{+/-}$ Rag2$^{-/-}$γc$^{-/-}$ mice total mTEC numbers were significantly increased (~ 200 cells/thymus compared to ~20 cells/thymus in Rag2$^{-/-}$γc$^{-/-}$ mice). MHC II levels were lower in Rag2$^{-/-}$γc$^{-/-}$ mice compared to WT mice (Fig 10A), indicating an immature TEC phenotype. Nevertheless, 38% of mTECs in K14 TSLP$^{+/-}$ Rag2$^{-/-}$γc$^{-/-}$ mice expressed Aire, which argues for mature mTECs. Aire protein expression was undetectable in Rag2$^{-/-}$γc$^{-/-}$ mice (Fig. 10A), which is in line with histology (Fig. 9A iii and iv) and qRT PCR data (Fig. 9B). cTEC and fibroblast numbers did not differ between Rag2$^{-/-}$γc$^{-/-}$ and K14 TSLP$^{+/-}$ Rag2$^{-/-}$γc$^{-/-}$ mice (Fig. 10B), indicating that TSLP overexpression had no significant effect on these cellular subsets of the thymic stromal compartment.

A

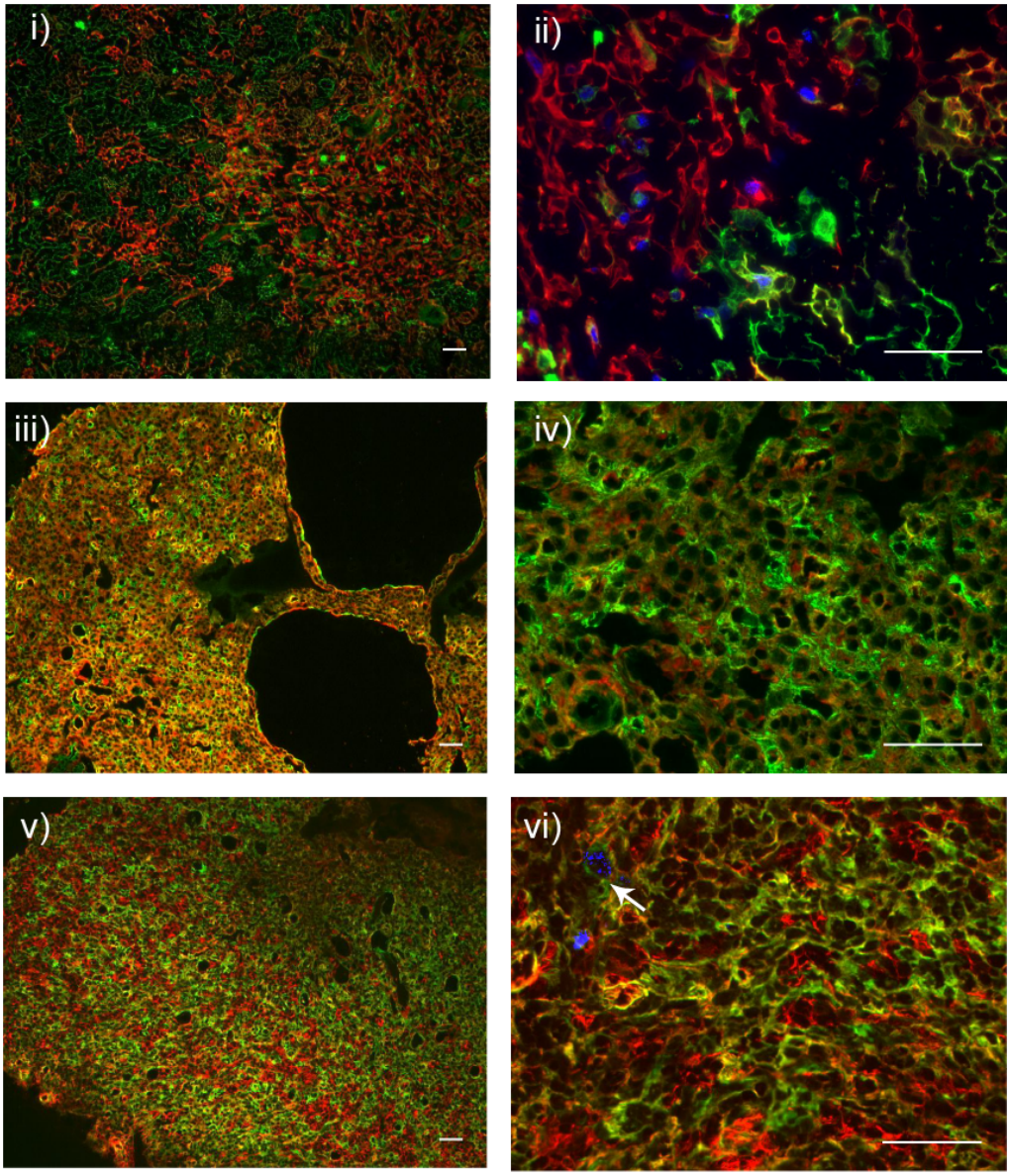
i)
ii)
iii)
iv)
v)
vi)

B

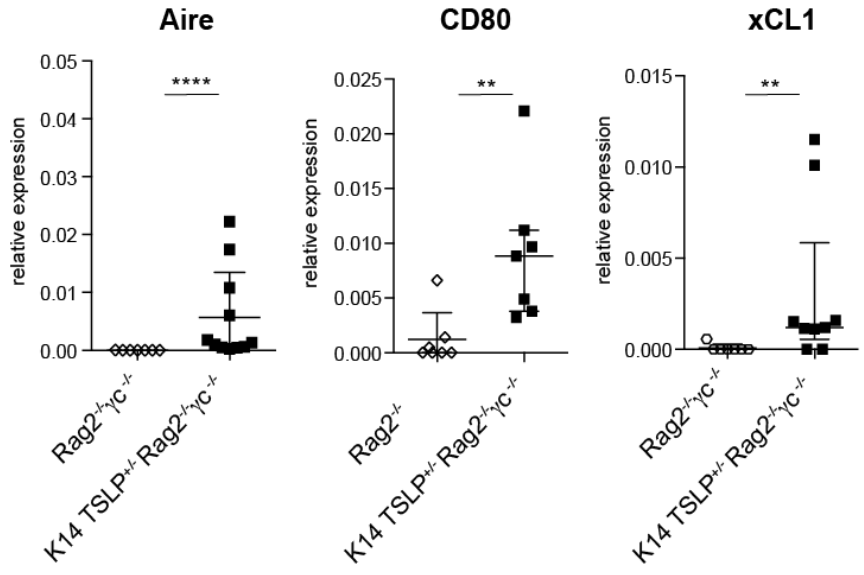
Aire
CD80
xCL1
relative expression
0.05
0.04
0.03
0.02
0.01
0.00
0.025
0.020
0.015
0.010
0.005
0.000
0.015
0.010
0.005
0.000
****
**
**
Rag2-/-γc-/-
K14 TSLP+/- Rag2-/-γc-/-
Rag2-/-
K14 TSLP+/- Rag2-/-γc-/-
Rag2-/-γc-/-
K14 TSLP+/- Rag2-/-γc-/-

Figure 9: TSLPtg improves thymic stromal compartment in Rag2$^{-/-}$γc$^{-/-}$ mice. A) Immunohistochemistry was performed on O.C.T™ embedded frozen sections of thymi from WT (i and ii), Rag2$^{-/-}$γc$^{-/-}$ (iii and iv) and K14 TSLP$^{+/-}$ Rag2$^{-/-}$γc$^{-/-}$ (v and vi) mice and stained for Cytokeratin-8 (CK8, green), Cytokeratin-5 (CK5, red) and Aire (blue; Aire was only stained in the right panel). Scale bar represents 50µm **B)** Aire, CD80 and xCL1 expression are shown as relative expression to EpCAM; median values + interquartile range; **P<0.01, ****P<0.0001.

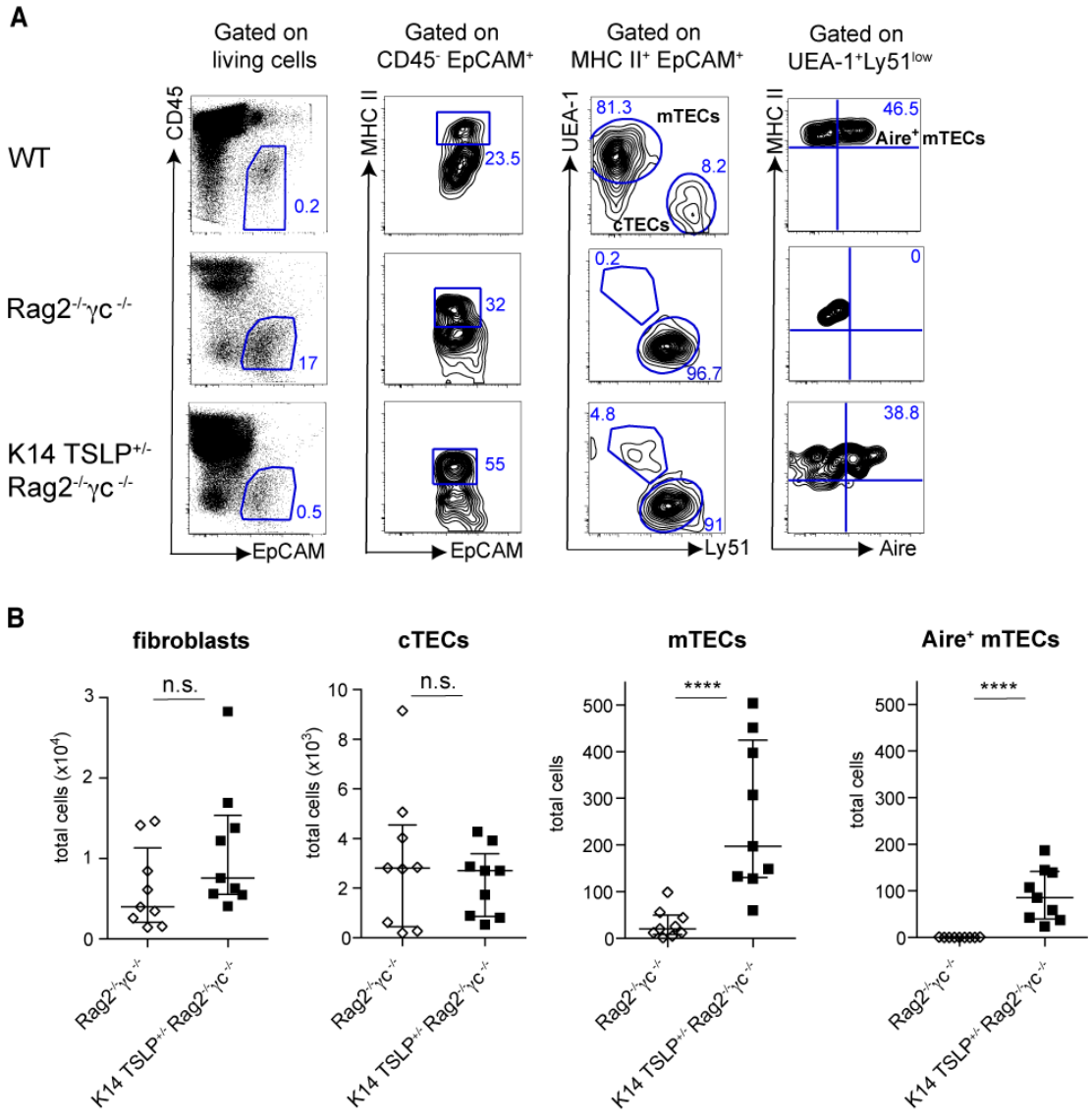

Figure 10: TSLPtg increases mTEC numbers in Rag2$^{-/-}$ γc$^{-/-}$ mice. A) Gating strategy for thymic epithelial cells. Numbers in dot plots represent frequencies. **B)** Absolute cell numbers of fibroblasts (CD45^{-} EpCAM^{-} MHC II^{-} Ly51^{+}), cortical epithelial cells (cTECs), and medullary epithelial cells (mTECs); n = 9 from 3 independent experiments; median values + interquartile range; n.s.= not significant, ****P<0.0001.

TECs are sources of many different cytokines and chemokines essential for recruitment, growth and survival of thymocyte[60-64]. To investigate whether improved thymic stromal patterning in K14 TSLP$^{+/-}$ Rag2$^{-/-}\gamma c^{-/-}$ mice alters cytokine and chemokine expression, qRT PCR analysis was performed on total thymus for IL-7, stem cell factor (SCF), CCL21, CCL25 and CCL19. Except for CCL21, which was significantly downregulated in K14 TSLP$^{+/-}$ Rag2$^{-/-}\gamma c^{-/-}$ mice, none of the factors was affected by TSLP overexpression (Fig. 11).

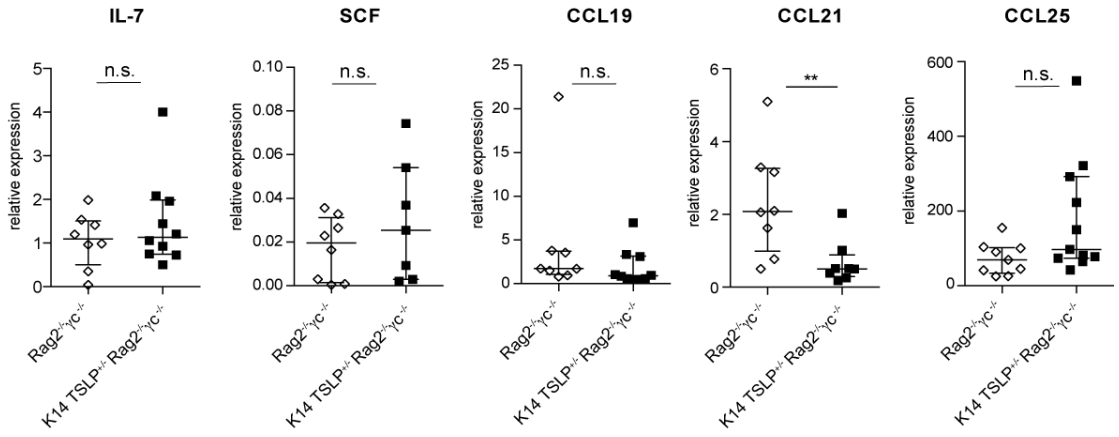

Figure 11: Cytokine and chemokine expression in total thymus normalized to the epithelial marker EpCAM. IL-7, SCF, CCL19, CCL21 and CCL25 are shown as relative expression to EpCAM; n = 7-11; median values + interquartile range; n.s. = not significant, **P<0.01.

Similarly, when mRNA levels were normalized to the fibroblast marker PDGFRα instead of EpCAM, there was no difference in transcript level for IL-7, SCF and CCL19 between the mouse strains. However, K14 TSLP$^{+/-}$ Rag2$^{-/-}\gamma c^{-/-}$ mice showed a 9-fold increase in CXCL12, which has a role in thymocyte expansion[63] and a 3-fold increase in CCL25 (Fig. 12). Also mRNA levels for fibroblast growth factors KGF and FGF 10 did not differ between Rag2$^{-/-}\gamma c^{-/-}$ and K14 TSLP$^{+/-}$ Rag2$^{-/-}\gamma c^{-/-}$ mice (Fig. 12).

Taken together, TSLPtg expression in Rag2$^{-/-}\gamma c^{-/-}$ mice increases the number of DN thymocytes and promotes Aire expression. However, the improved thymic stromal patterning in K14 TSLP$^{+/-}$ Rag2$^{-/-}\gamma c^{-/-}$ mice does not alter growth factor expression, but has a significant effect on the upregulation of CXCL12 and CCL25 in mesenchymal as well as down modulation of CCL21 in epithelial cells.

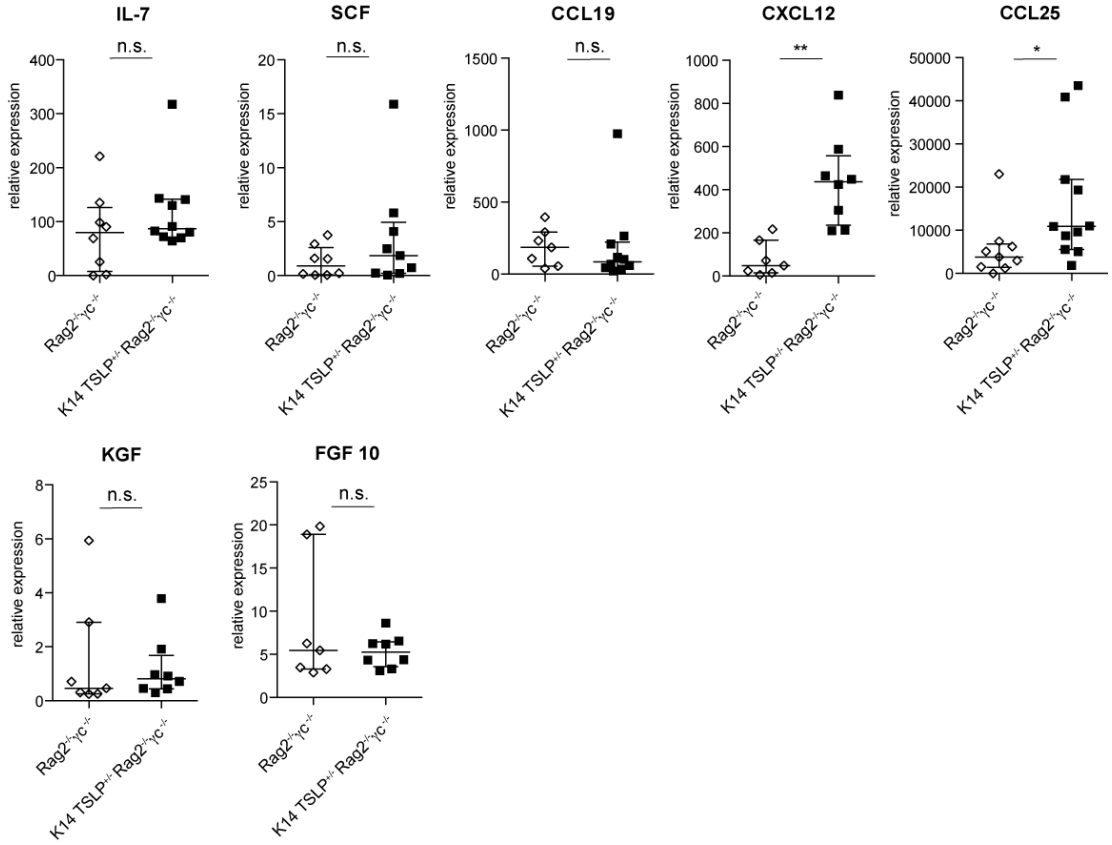

Figure 12: Cytokine and chemokine expression in total thymus normalized to fibroblast marker PDGFRα. IL-7, SCF, CCL19, CXL12, CCL25, KGF and FGF 10 are shown as relative expression to PDGFRα; n = 7-11, median values + interquartile range; n.s. = not significant, *P<0.05, **P<0.01.

5.1.3 TSLP has no direct effect on mTEC differentiation and Aire expression

mTEC development and Aire expression during embryogenesis is dependent on LTi cells and γδ T cell precursors via Rank - RankL interaction[75,76], whereas mTEC maintenance in adults is mediated by signals from αβ T cells[77-81]. Since K14 TSLP$^{+/-}$ Rag2$^{-/-}$γc$^{-/-}$ mice are T cell deficient, it was investigated whether TSLP overexpression has a direct effect on the development and maintenance of mTECs.

This question was addressed with fetal thymus organ cultures (FTOC). In WT mice, mTECs appear around E16[201]. Therefore, WT E14.5 thymi before the onset of mTEC development were used. Culturing of WT thymic lobes without treatment for

11 days showed normal cTEC and mTEC development, the latter also expressing Aire (Fig. 13A) due to the presence of LTi cells and normal thymopoiesis. To remove developing T cells, thymic lobes were treated with 2'-Deoxyguanosine (dGuo) and subsequently cultured for 5 days in the presence of RankL, different concentrations of recombinant TSLP or left unstimulated. Analysis by flow cytometry showed that treatment with dGuo inhibits mTEC development, whereas subsequent treatment with RankL initiates mTECs. Treatment with 25, 50 or 100 ng/mL TSLP did not increase the frequency of mTECs (Fig. 13B). Another approach to test whether TECs are TSLP responsive was monitoring of STAT5 phosphorylation in response to TSLP stimulation *in situ.* The biological activity of TSLP was assessed on BM cells from $Rag2^{-/-}$ mice. After stimulation with 50ng/mL TSLP, 9% of $CD19^{+}$ B cell precursor phosphorylated STAT5. This was 3.5 times lower than with the growth factor IL-7 (Fig. 13C), but confirmed the biological activity of TSLP at low concentrations.

WT TECs were isolated and stimulated with 25, 50 and 100 ng/mL TSLP. As there was no difference in STAT5 phosphorylation of unstimulated and stimulated TECs (Fig. 13D), there is no evidence for a direct effect of TSLP on mTEC development.

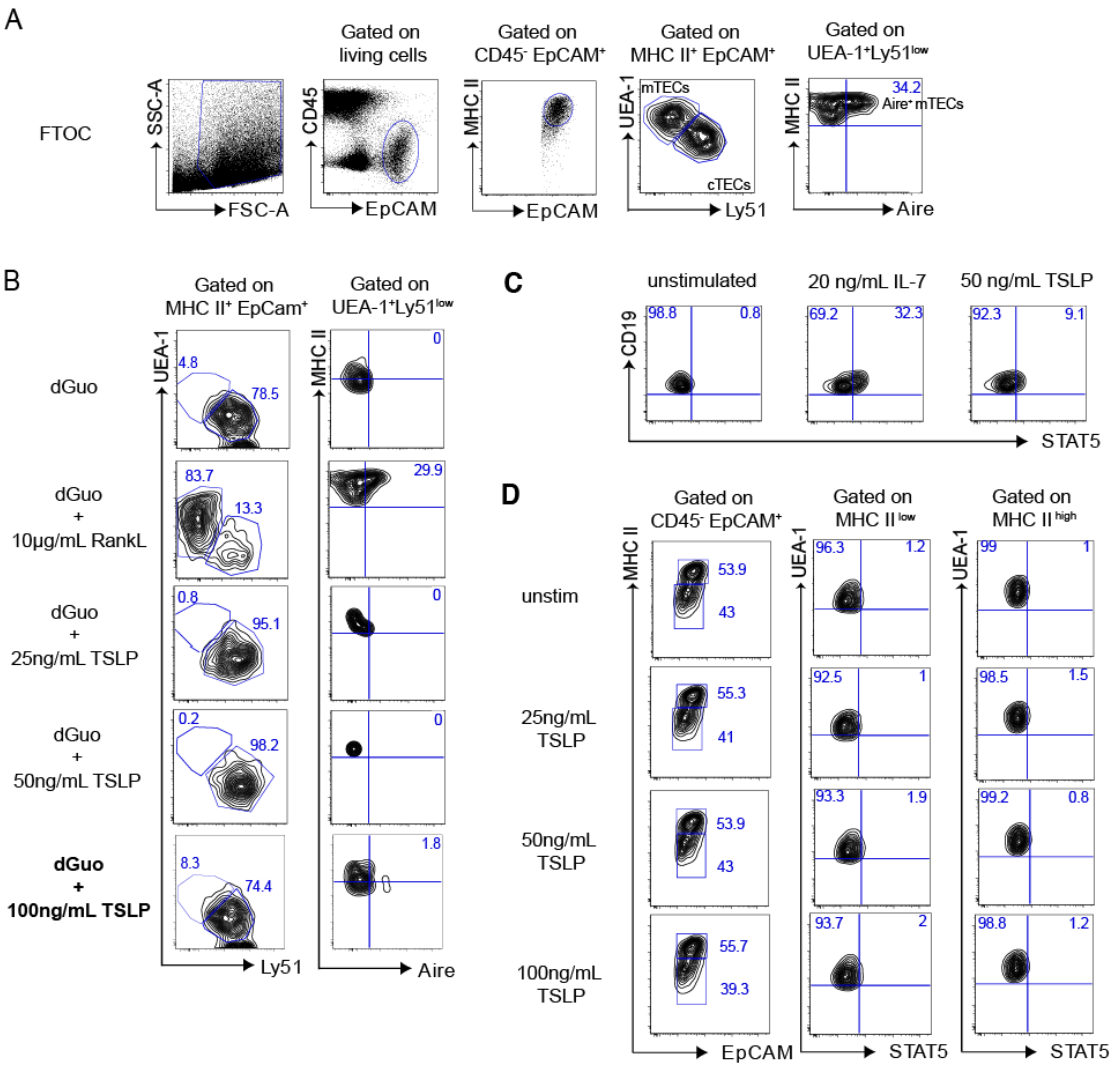

Figure 13: TSLP has no direct influence on mTEC development: A) Flow cytometry analysis of the TEC compartment in FTOCs after 11 days of culture. **B)** Analysis of the TEC compartment in dGuo treated FTOCs cultured in the presence of RankL, different concentrations of TSLP or without stimulation for 5 days. **A-B)** Numbers in dot plots represent frequencies of a representative experiment from 5 independent experiments. **C)** $Rag2^{-/-}$ BM cells were stimulated with 20 ng/mL IL-7, 50 ng/mL TSLP or left unstimulated. **D)** WT TECs were stimulated with different concentrations of TSLP or left unstimulated. **C-D)** Levels of STAT5 phosphorylation was assessed by flow cytometry analysis; Numbers in dot plots represent frequencies of a representative experiment from 2 independent experiments.

It was reported, that in the absence of T cells Rank - RankL interaction plays an important role in mTEC development and Aire induction[75,76]. Therefore, the expression of RankL was assessed by qRT PCR on total thymus of K14 $TSLP^{+/-}$ $Rag2^{-/-}\gamma c^{-/-}$ and $Rag2^{-/-}\gamma c^{-/-}$ mice. Indeed, RankL transcript levels were significantly higher in K14 $TSLP^{+/-}$ $Rag2^{-/-}\gamma c^{-/-}$ compared to $Rag2^{-/-}\gamma c^{-/-}$ mice (Fig. 14A). Possible

candidates, which express RankL in an adult T cell deficient thymus, are ILC3s. Therefore, K14 TSLP$^{+/-}$ Rag2$^{-/-}\gamma c^{-/-}$, Rag2$^{-/-}\gamma c^{-/-}$ as well as WT and ROR$\gamma t^{-/-}$ mice as controls were investigated for the presence of ILC3s in the thymus. (Fig. 7 B). Since ILC3s require γc signaling cytokines such as IL-7 for their development and survival[136], Rag2$^{-/-}\gamma c^{-/-}$ mice are almost devoid of ILC3s. However, TSLP overexpression increased ILC3s in the thymus of Rag2$^{-/-}\gamma c^{-/-}$ mice (Fig. 14B-C) as already observed for spleen and mLN[138]. qRT PCR on total thymus demonstrated that in line with the increased numbers of ILC3s, K14 TSLP$^{+/-}$ Rag2$^{-/-}\gamma c^{-/-}$ mice showed also an elevated level of IL-22 in the thymus (Fig. 14D). Other cellular subsets expressing RankL are DN2s and DN3s (Fig. 14E), but to lower extend than ILC3s[78]. Nevertheless DN2s and DN3s could potentially contribute to mTEC development in K14 TSLP$^{+/-}$ Rag2$^{-/-}\gamma c^{-/-}$ mice.

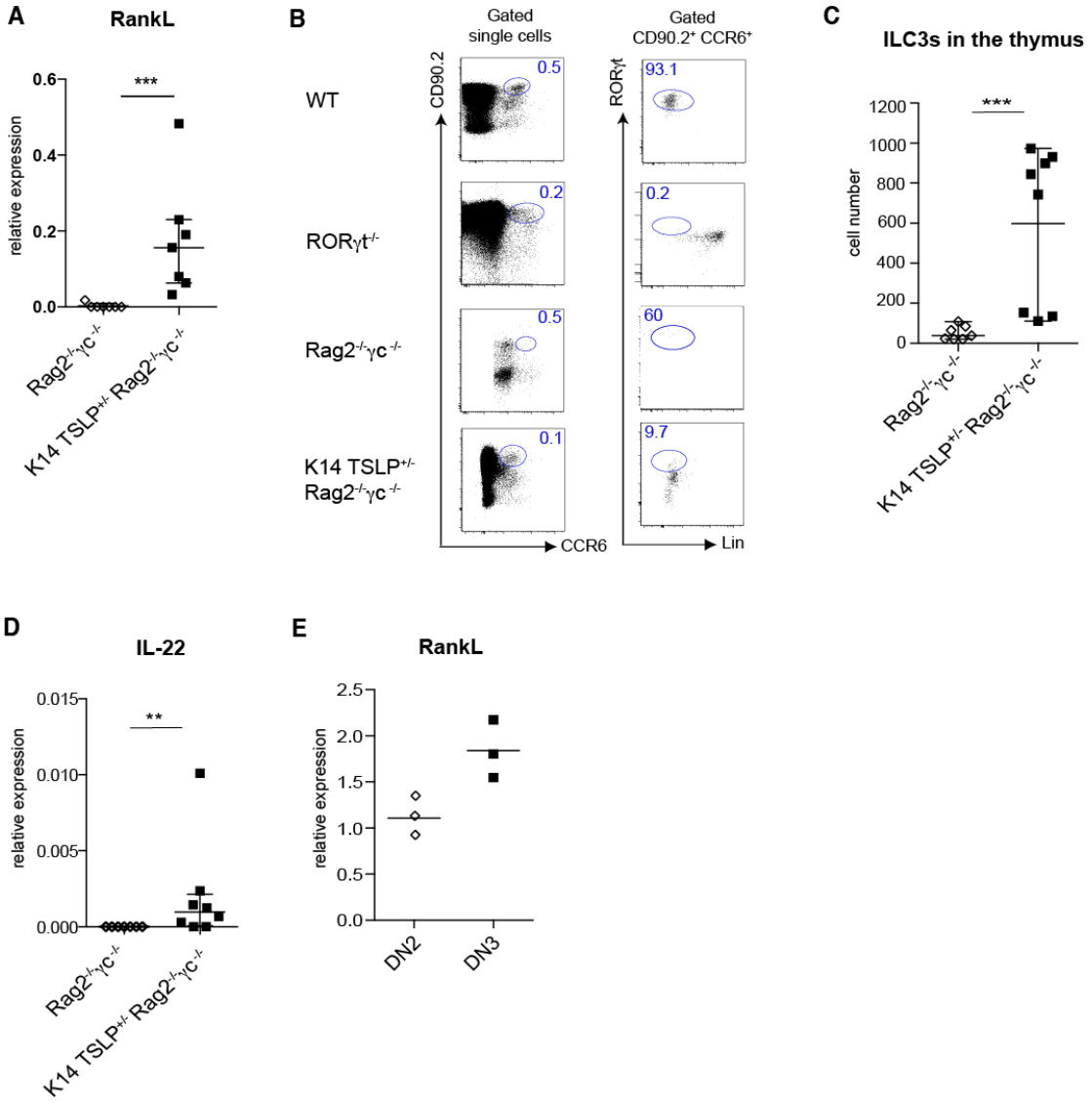

Figure 14: ILC3s are increased in K14 TSLP$^{+/-}$ Rag2$^{-/-}$γc$^{-/-}$ mice. A) RankL expression on total thymus shown as relative expression to TBP **B)** Gating strategy for ILC3s in the thymus; Lin includes CD3ε, CD8α, CD11c, CD19, B220, TCRαβ, TCRγδ, GR-1 and NK1.1. Numbers in dot plots represent frequencies of a representative experiment **C)** Absolute cell numbers of ILC3s in Rag2$^{-/-}$γc$^{-/-}$ and K14 TSLP$^{+/-}$ Rag2$^{-/-}$γc$^{-/-}$ mice **D)** IL-22 expression on total thymus shown as relative expression to TBP; **A, C-D)** n = 7 - 8; median values + interquartile range; **P<0.01, ***P<0.001. **E)** RankL expression of sorted DN2 (CD3ε^{-}, c-kit^{high} CD25^{+} CD44^{+}) and DN3s (CD3ε^{-}, CD25^{+} CD44^{-}) of K14 TSLP$^{+/-}$ Rag2$^{-/-}$γc$^{-/-}$ mice shown as relative expression to TBP; mean values.

The notion that not only ILC3 but also DN3 numbers were 16 - fold and approximately 450 - fold increased, respectively, raised the question whether DN3s and adult ILC3s were able to promote mTEC development in the absence of T cells. Therefore, $CD45^-$ cells from WT E14.5 thymi were re - aggregated at a 1:2 ratio with DN3s or with LP derived ILC3s isolated from $Rag2^{-/-}$ mice. Cells were isolated from $Rag2^{-/-}$ mice to ensure that DN3s cannot differentiate beyond DN3s. Furthermore have $Rag2^{-/-}$ mice higher ILC3 numbers due to the absence of T and B cells.

Re - aggregated thymus organ cultures (RTOC) of $CD45^-$ $TER119^-$ cells + DN3s and $CD45^-$ $TER119^-$ cells + ILC3s were cultured for 4d, disaggregated and analysed by flow cytometry. Direct analysis of sorted $CD45^-$ $TER119^-$ cells showed 95% cTECs, as mTEC development has not started at E14.5 (Fig 15 upper row). Re - aggregation of total disaggregated thymus ($CD45^-$ + $CD45^+$ cells) resulted in the development of 34% mTEC and 62% cTECs (second row). Re - aggregation of $CD45^-$ cells with DN3s showed maintenance of ~78% cTECs and development of 11% mTECs whereas re - aggregation with LPL ILC3s resulted in a strong commitment of mTECs (85%). CD80 expression of mTECs was not affected by DN3s or ILC3s, as the frequency of $CD80^+$ mTECs was comparable to the control in the second row (Fig 15). These data indicate that DN3s are able to induce mTEC development but to lesser extend than ILC3s, which might be due to different expression levels of RankL or by an additional unknown mechanism.

In summary, TSLP overexpression does not have a direct effect on mTEC development. However, ILC3s and to lesser extent DN3s are able to promote mTEC development.

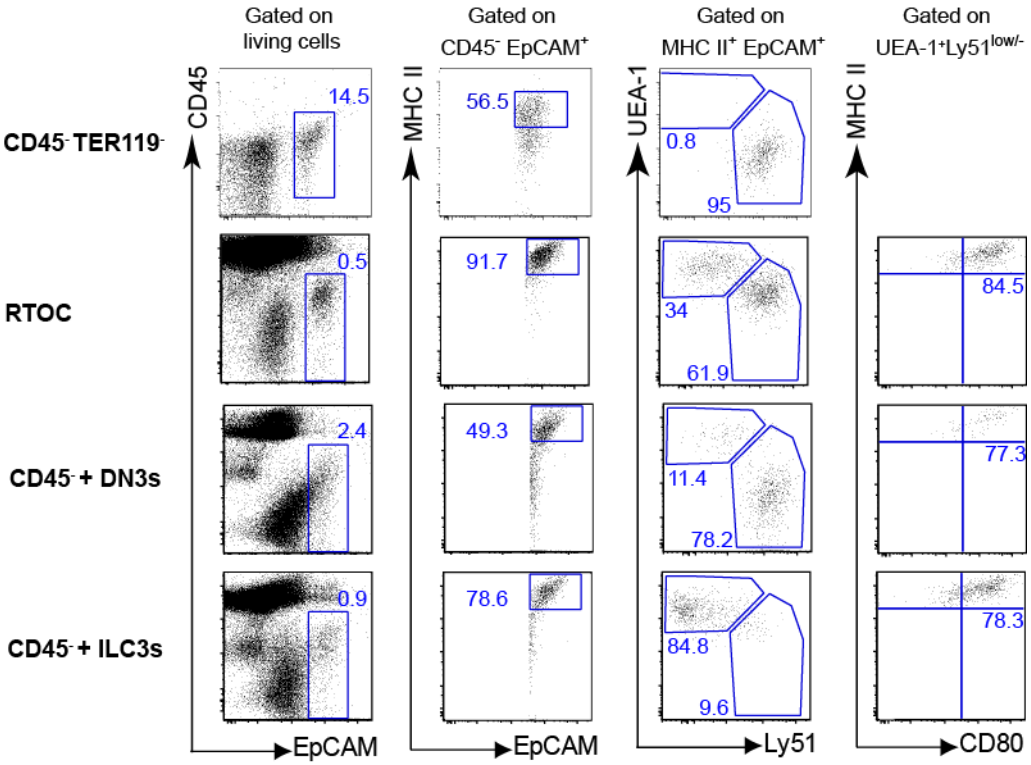

Figure 15: DN3s and LP derived ILC3s promote mTEC development: Flow cytometric analysis of TEC compartment at E14.5 (upper row), after re - aggregation of disaggregated total WT E14.5 thymi in 4d RTOCS and 4d RTOCs of WT E14.5 CD45$^-$ cells with either DN3s or LP derived ILC3s from Rag2$^{-/-}$ mice. Numbers in dot plots represent frequencies from one experiment.

3.1.4 TSLPtg expression increases myeloid cells in peripheral organs

TSLP increases the number of myeloid cells[174]. DCs respond to TSLP by upregulation of MHC II and co-stimulatory molecules CD40, CD80 and CD86[164,202]. Due to the interaction of OX40$^+$ T cells and OX40L expressed by TSLP conditioned DCs, TSLP can polarize CD4$^+$ T cells towards the Th2 lineage[87]. To address the question whether TSLP overexpression in Rag2$^{-/-}\gamma c^{-/-}$ mice has an effect on antigen presenting cells (APCs), peripheral organs were analysed in Rag2$^{-/-}\gamma c^{-/-}$ and K14 TSLP$^{+/-}$ Rag2$^{-/-}\gamma c^{-/-}$ mice for total cell numbers of GR1$^+$ CD11b$^+$ cells, CD11c$^+$ DCs, CD11c$^-$ MΦ and co-stimulatory molecules by CD11c$^+$ DCs. In the spleen, K14 TSLP$^{+/-}$ Rag2$^{-/-}\gamma c^{-/-}$ mice had significant higher GR1$^+$ CD11b$^+$ myeloid cells (~3.6x10^6 cells in K14 TSLP$^{+/-}$ Rag2$^{-/-}\gamma c^{-/-}$ mice and 1x10^6 in Rag2$^{-/-}\gamma c^{-/-}$ mice) (Fig. 16A-B),

whereas the size of the myeloid compartment in the BM did not differ between Rag2$^{-/-}\gamma c^{-/-}$ and K14 TSLP$^{+/-}$ Rag2$^{-/-}\gamma c^{-/-}$ mice (Fig. 16A-B). Further characterization of the myeloid compartment in the spleen by flow cytometry demonstrated that the CD11c^{+} CD11b^{+} MHC II^{+} DC subset was 3 times higher in K14 TSLP$^{+/-}$ Rag2$^{-/-}\gamma c^{-/-}$ mice, whereas there was no difference in the CD11c^{-} CD11b^{+} MΦ subsets (Fig 16C-D). Using flow cytometry, the expression of the co - stimulatory molecules CD40, CD80 as well as CD86 was analysed in CD11c^{+} MHC II^{+} DCs and no difference could be detected between Rag2$^{-/-}\gamma c^{-/-}$ and K14 TSLP$^{+/-}$ Rag2$^{-/-}\gamma c^{-/-}$ mice (Fig. 16E).

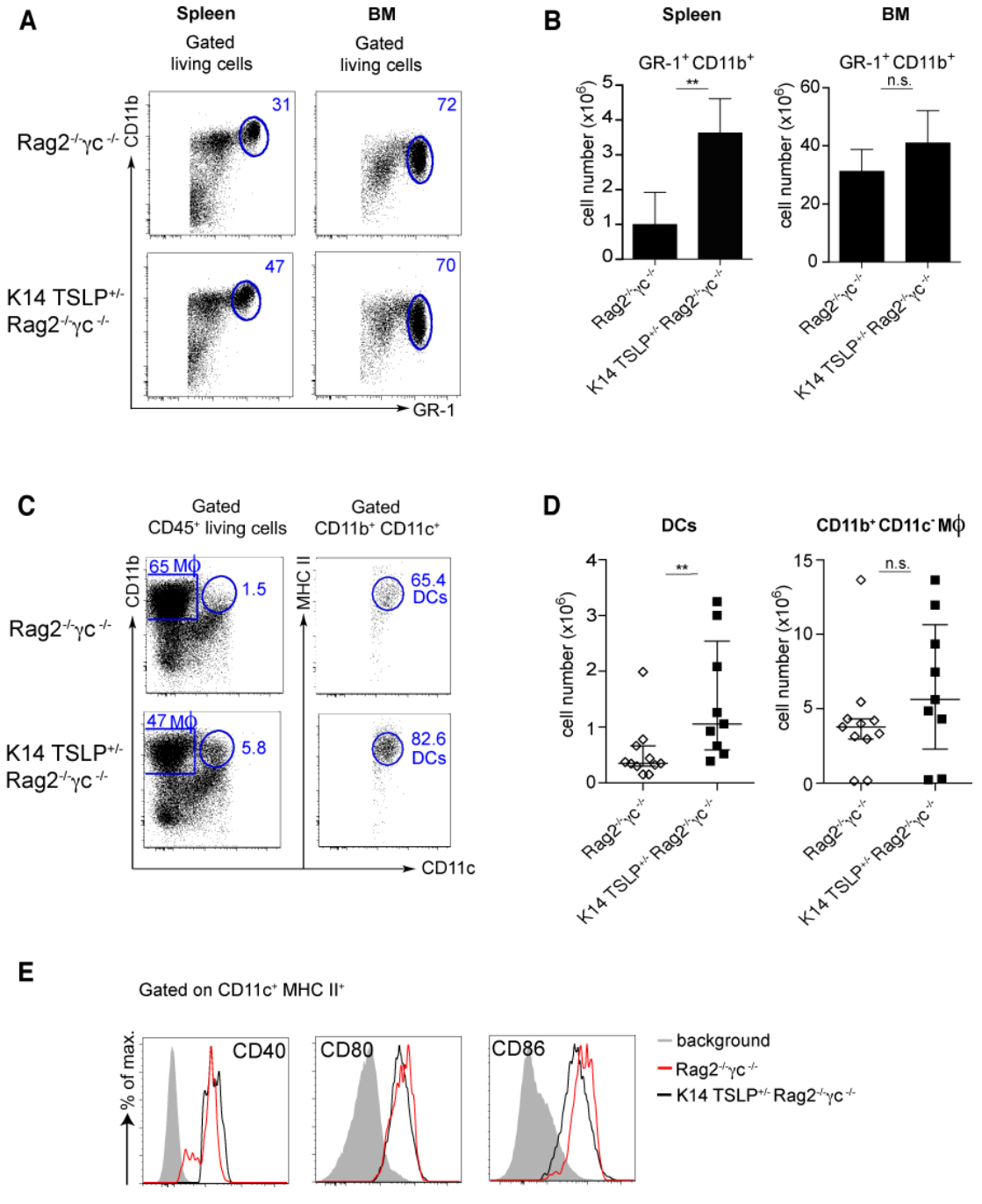

Figure 16: TSLPtg increases myeloid cells in the spleen: A) Gating strategy for myeloid cells in spleen and BM. **B)** Absolute cell numbers for GR1$^+$ CD11b$^+$ cells in spleen and BM; n = 7 - 11; median values + range; n.s. = not significant, **P<0.01. **C)** Gating strategy for DCs (CD11c$^+$ CD11b$^+$ MHC II$^+$) and MΦ (CD11c$^-$ CD11b$^+$). **D)** Absolute cell numbers for DCs and MΦ; n = 7 - 11; median values + range; n.s. = not significant, **P<0.01. **E)** Representative histograms of co - stimulatory molecule expression of CD11c$^+$ CD11b$^+$ MHC II$^+$ subset. **A+C)** Numbers in dot plots represent frequencies of a representative experiment.

DC and MΦ numbers as well as the expression of their co - stimulatory molecules were also quantified in the small intestine (SI) and colon. K14 TSLP$^{+/-}$ Rag2$^{-/-}\gamma c^{-/-}$ mice showed a small but significant increase in the number of MHC II^{+} CD11c^{+} DCs in the SI as well as in the colon (Fig. 17A-B, Fig. 18A-B). In the colon this was associated with an increase in the number of CD103^{+} DCs (Fig. 18B). The number of CD103^{low} DCs and CD11c^{-} MΦ as well as the expression of co - stimulatory molecules CD40, CD80 and CD86 on CD11c^{+} DCs did not differ between Rag2$^{-/-}\gamma c^{-/-}$ and K14 TSLP$^{+/-}$ Rag2$^{-/-}\gamma c^{-/-}$ mice in the SI and colon (Fig. 17C and 18C).

Altogether, these results indicate that TSLP overexpression promotes the accumulation of myeloid cells in the spleen and to lower extend also in the intestine. However, TSLP overexpression in Rag2$^{-/-}\gamma c^{-/-}$ mice has no impact on the expression of co - stimulatory molecules on DCs.

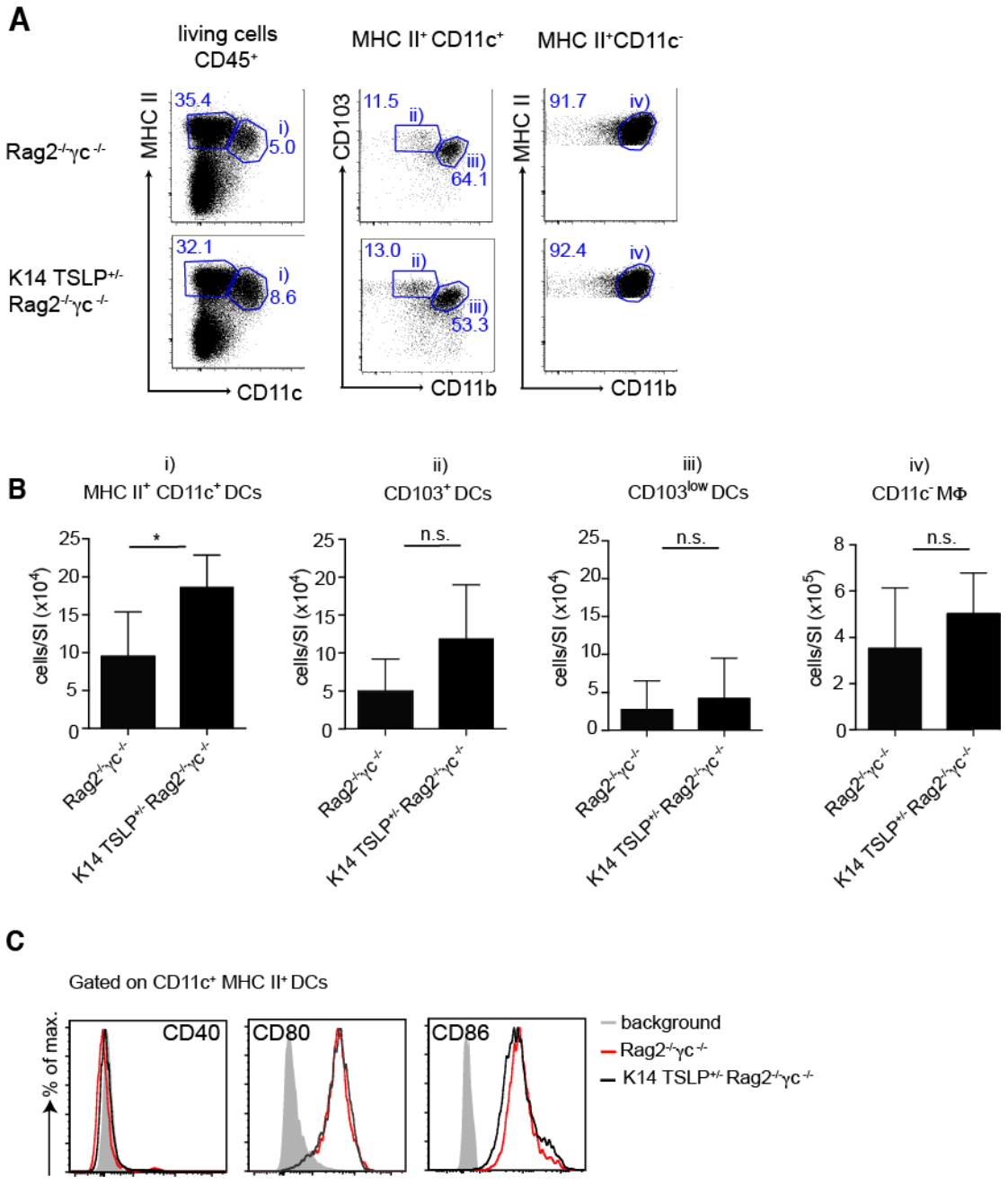

Figure 17: TSLP increases DC numbers in the small intestine: A) Gating strategy for DCs (MHC II$^+$ CD11c$^+$), CD103$^+$ DCs, CD103^{low} DCs and MΦ (MHC II$^+$ CD11c$^-$ CD11b$^+$); Numbers in dot plots represent frequencies of a representative experiment. **B)** Absolute cell numbers for DC subsets and MΦ; n = 6; median values + range; n.s. = not significant, *P<0.05. **C)** Representative histograms of co - stimulatory molecule expression of CD11c$^+$ MHC II$^+$ subset.

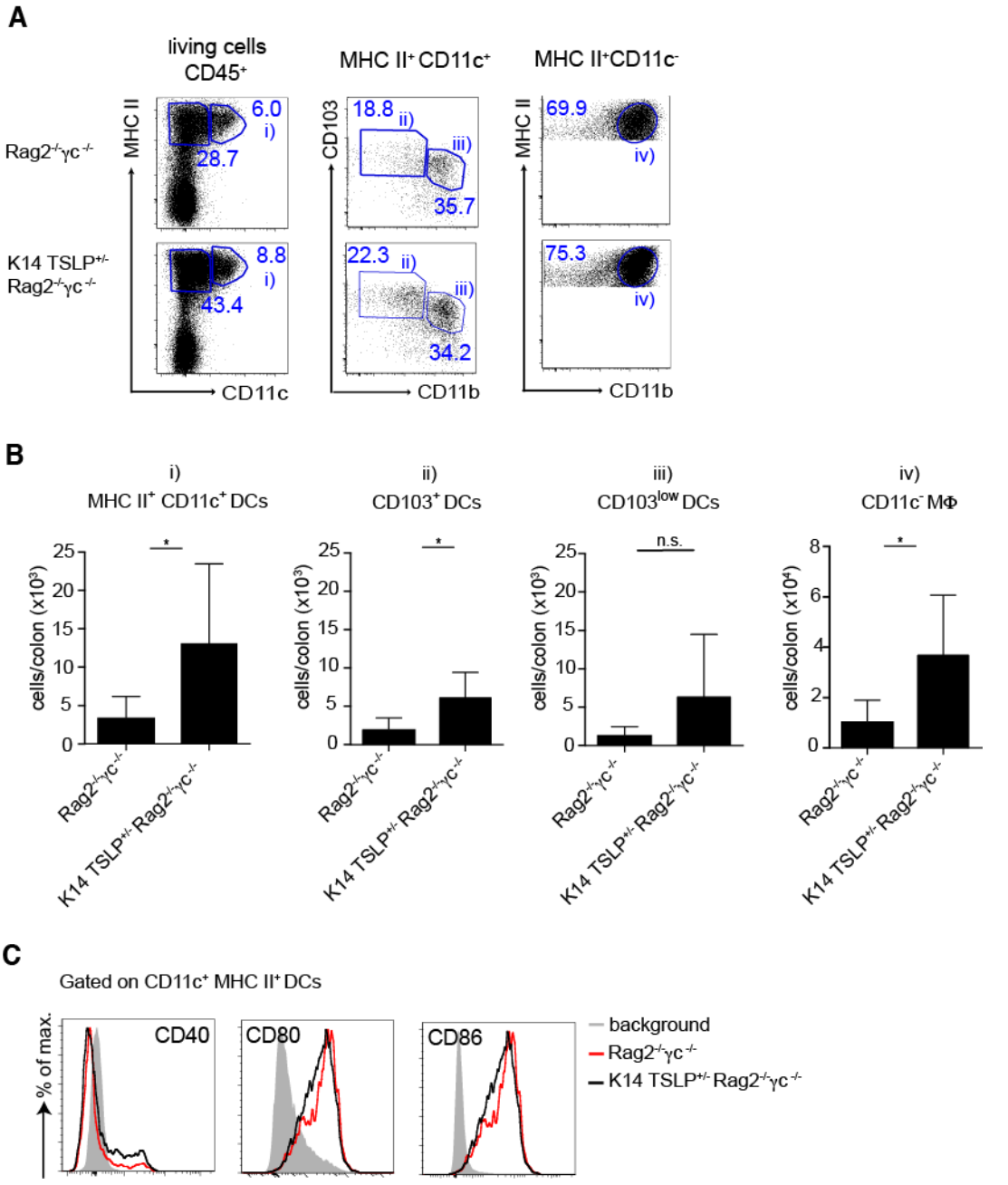

Figure 18: TSLP increases DC numbers in the colon: A) Gating strategy for DCs (MHC II$^+$ CD11c$^+$), CD103$^+$ DCs, CD103^{low} DCs and MΦ (MHC II$^+$ CD11c$^-$ CD11b$^+$); Numbers in dot plots represent frequencies of a representative experiment. **B)** Absolute cell numbers for DC subsets and MΦ; n = 6; median values + range; n.s. = not significant, *P<0.05.
C) Representative histograms of co-stimulatory molecule expression of CD11c$^+$ MHC II$^+$ subset.

3.1.5 TSLPtg expression increases ILC numbers in the intestine

The intestinal immune system has to keep the balance between tolerating commensal bacteria and mounting immune responses against potential pathogens. ILC3s in the intestine were reported to give substantial help for the maintenance of intestinal immune homeostasis[203] by creating an anti - pathological platform[146,147,151]. As a major source of IL-22[204], ILC3s can protect intestinal epithelial cells by giving survival and proliferation signals[159,205] and induce anti - microbial Reg proteins, which are targets of IL-22 signaling[151]. On the other side, NCR^- ILC3s are shown to be involved in intestinal inflammation by production of IL-17 and IFN-γ [145,206]. The role of ILC2s under steady state conditions is not clear yet[188]. However, ILC2s can be important Th2 cytokine producers after activation[207]. To investigate, whether increased numbers of ILCs alter the intestinal microenvironment, the intestinal ILC subsets and their cytokine profile were analysed.

Analysis of LP derived ILCs from SI showed that TSLP overexpression resulted in a higher frequency of ILC2s and ILC3s in K14 $TSLP^{+/-}$ $Rag2^{-/-}$ $\gamma c^{-/-}$mice (14% ILC2s, 67% ILC3s) compared to $Rag2^{-/-}$ $\gamma c^{-/-}$mice (7% ILC2s, 39% ILC3s) (Fig. 19A). This difference in frequencies is also depicted in absolute cell numbers, as K14 $TSLP^{+/-}$ $Rag2^{-/-}$ $\gamma c^{-/-}$mice have an 86-fold increase in ILC2s (Lin^- $CD90.2^+$ $GATA3^+$), 18-fold increase in NCR^- and 36-fold increase in NCR^+ ILC3s (Lin^- $CD90.2^+$ $ROR\gamma t^+$) (Fig. 19A). In line with higher ILC3 numbers in K14 $TSLP^{+/-}$ $Rag2^{-/-}$ $\gamma c^{-/-}$ mice are qRT PCR data on SI tissue, which showed a highly significant increase in RankL (Fig. 19B).

Approximately 50% of SI - ILC3s showed IL-22 production under steady state conditions in both mouse strains. Treatment of ILC3s with IL-23 raised IL-22 production by at least 20% in $Rag2^{-/-}$ $\gamma c^{-/-}$ and K14 $TSLP^{+/-}$ $Rag2^{-/-}$ $\gamma c^{-/-}$mice (Fig. 19C). IL-17 production was lower compared to IL-22 production under steady state conditions and did not significantly differ between $Rag2^{-/-}$ $\gamma c^{-/-}$ and K14 $TSLP^{+/-}$ $Rag2^{-/-}$ $\gamma c^{-/-}$ mice. However, IL-17 production was upregulated in $Rag2^{-/-}$ $\gamma c^{-/-}$ and K14 $TSLP^{+/-}$ $Rag2^{-/-}\gamma c^{-/-}$ mice upon IL-23 treatment (Fig. 19C). ILC3s were also reported to produce granulocyte macrophage colony-stimulating factor (GM-CSF), which is an important mechanism to promote tolerance in the intestine by increasing DC and Treg function[152]**.** Upon stimulation with PMA and Ionomycin, ILC3s derived from SI of both mouse strains showed GM-CSF and IFN-γ production but did not differ between $Rag2^{-/-}$ $\gamma c^{-/-}$ and K14 $TSLP^{+/-}$ $Rag2^{-/-}\gamma c^{-/-}$ mice (Fig. 19D).

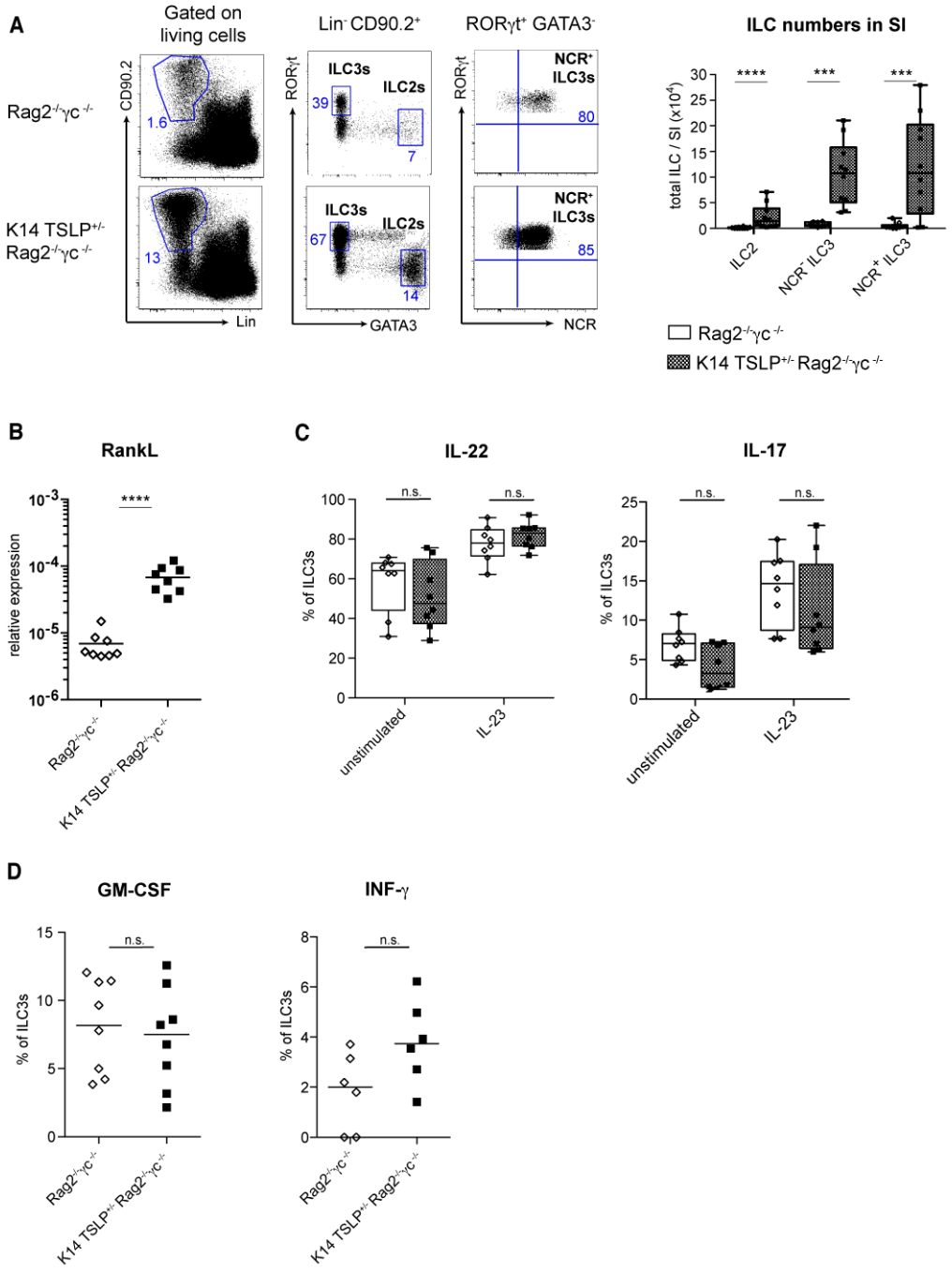

Figure 19: TSLPtg increases ILC numbers in the SI: A) Gating strategy and absolute cell numbers of ILC subsets. Lin includes CD3ε, CD8α, CD11c, B220, NK1.1 and GR - 1; numbers in dot plots represent frequencies of a representative experiment; n = 9 - 11; median values + interquartile range; ***P<0.001, ****P<0.0001 **B**) RankL expression is shown as relative expression to β-Actin; n = 8; median values, ****P<0.0001. **C)** Cytokine production of ILC3s after 4h stimulation with 20ng/mL IL-23 and incubation with Brefeldin A (10µg/mL) for 2h **D)** Cytokine production of ILC3s after 4h stimulation with 50ng/mL PMA and 2.5µg/mL Ionomycin and incubation with Brefeldin A for 2h; **C - D)** n = 6-8; median values + interquartile range; n.s. = not significant.

Although ILC3s of K14 TSLP$^{+/-}$ Rag2$^{-/-}\gamma c^{-/-}$ mice did not show a difference in IL-22 production, the increased number of ILC3s is likely responsible for the significantly higher amount of IL-22 transcripts in total SI in K14 TSLP$^{+/-}$ Rag2$^{-/-}\gamma c^{-/-}$ mice (Fig 20A). Also the mRNA expression of the natural IL-22 regulator IL-22Rα2 was 39-fold increased in SI of K14 TSLP$^{+/-}$ Rag2$^{-/-}\gamma c^{-/-}$ mice as analysed by qRT PCR. IL-22 is known to initiate anti-microbial peptide expression[151] and indeed, K14 TSLP$^{+/-}$ Rag2$^{-/-}\gamma c^{-/-}$ mice showed ~3 fold increase in Reg3β and Reg3γ production in the SI (Fig. 20B).

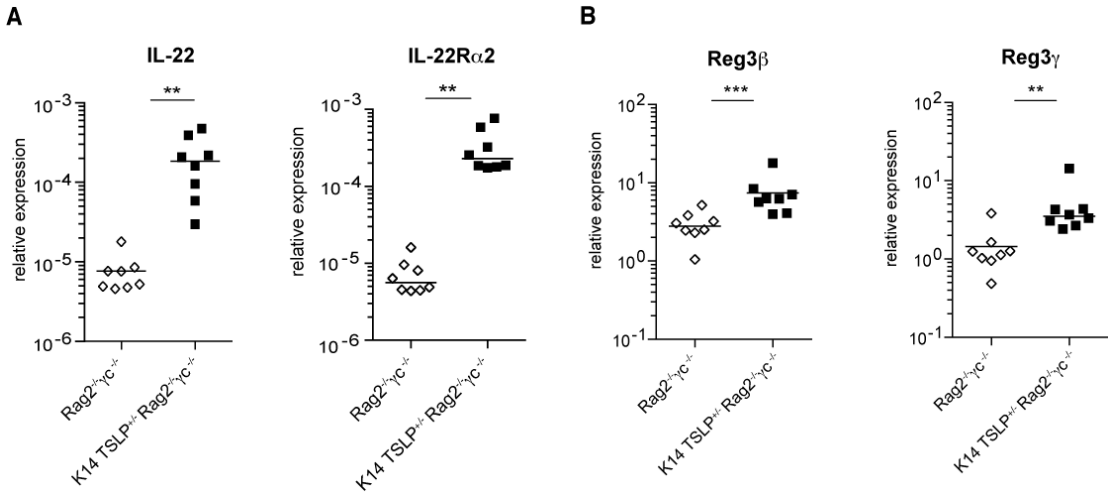

Figure 20: TSLPtg increases IL-22 and anti - microbial peptide expression in SI: A) IL-22 and IL-22Rα2 mRNA expression are shown as relative expression to β-Actin**; B)** Reg3β and Reg3γ mRNA expression are shown as relative expression to β-Actin**; A-B)** n = 8; median; **P<0.01, ***P<0.001.

In the colon, TSLP overexpression favours the increase in frequencies and absolute numbers of ILC2s compared to ILC3s. Although there is also an increase in the frequency of NCR$^+$ ILC3s, there is no significant difference in absolute cell numbers in NCR$^+$ ILC3s and only a minor increase in the NCR$^-$ ILC3 compartment (Fig. 21A). In Rag2$^{-/-}\gamma c^{-/-}$ mice, there is a prominent cell population, which is Lin$^-$ CD90.2$^+$ but negative for ILC2 and ILC3 transcription factors GATA3 and RORγt (Fig. 21A). This cell population could also be observed in the small intestine and might indicate an ILC precursor, which has a higher potential to differentiate by TSLP overexpression.

Taken together, these results demonstrate, that TSLP overexpression in the intestine increases the proportion and absolute cell numbers of ILC2s and ILC3s but has no effect on IL-22, IL-17, GM-CSF or IFN-γ production. However, increased numbers of ILC3s result in higher IL-22 levels and hence, higher amounts of anti-microbial peptides.

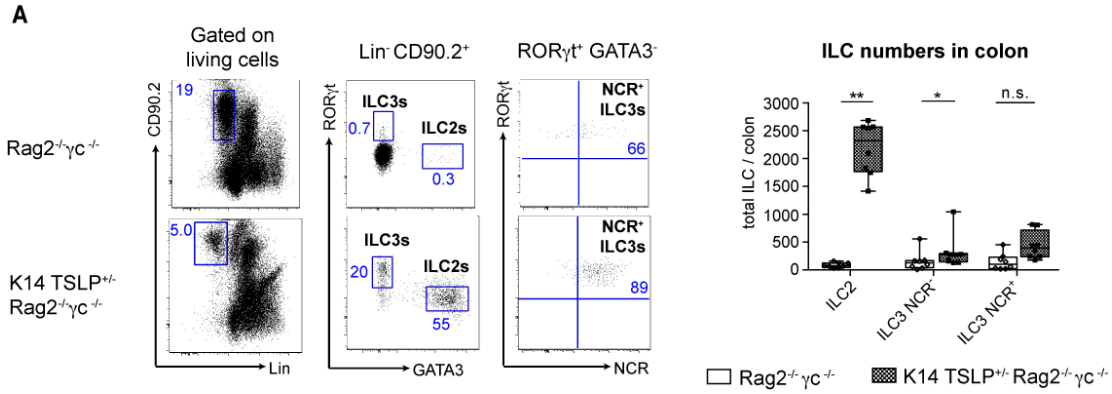

Figure 21: TSLP increases ILC numbers in the colon: Gating strategy and absolute cell numbers for ILC subsets. Lin includes CD3ε, CD8α, CD11c, B220, NK1.1 and GR-1. Numbers in dot plots represent frequencies of a representative experiment. n = 6 - 8; median + interquartile range; n.s. = not significant, *P<0.05 **P<0.01.

3.1.6 Colonization of BM and spleen in K14 TSLP$^{+/-}$ Rag2$^{-/-}$γc$^{-/-}$ mice is normal

IL-7 is crucial for the proliferation and differentiation of B-cell lineage cells[33,34,206]. However, in the absence of IL-7, TSLP can rescue the effect of IL-7 and drives precursor cells into B cell commitment[162,177,178]. Due to TSLP overexpression, K14 TSLP$^{+/-}$ Rag2$^{-/-}$γc$^{-/-}$ mice accumulate B cell precursors Pro - /Pre - B I (CD19^{+} CD117^{+}) and Pre - B II (CD19^{+} CD25^{+}) cells in the BM, whereas these cells are almost undetectable in Rag2$^{-/-}$γc$^{-/-}$ mice (Fig. 22A - B). To exclude that some B cell precursors had occupied niches for donor HSC in the later transplantation experiments, carboxyfluorescein succinimidyl ester (CFSE) - labelled TSLPR$^{-/-}$ BM cells were injected into Rag2$^{-/-}$γc$^{-/-}$ and in K14 TSLP$^{+/-}$ Rag2$^{-/-}$γc$^{-/-}$ mice. After 24h, BM cells were harvested and CFSE^{+} cells were quantified by flow cytometry. There was no significant difference in the number of CFSE^{+} cells in the BM between both mouse

strains (Fig. 22C). Also in the spleen, there was no significant difference in CFSE^{+} cell numbers between Rag2$^{-/-}$γc$^{-/-}$ and K14 TSLP$^{+/-}$ Rag2$^{-/-}$γc$^{-/-}$ mice (Fig 22D). This indicates that the recruitment of progenitor cells to the BM and the circulation through the spleen is not impaired in K14 TSLP$^{+/-}$ Rag2$^{-/-}$γc$^{-/-}$ mice.

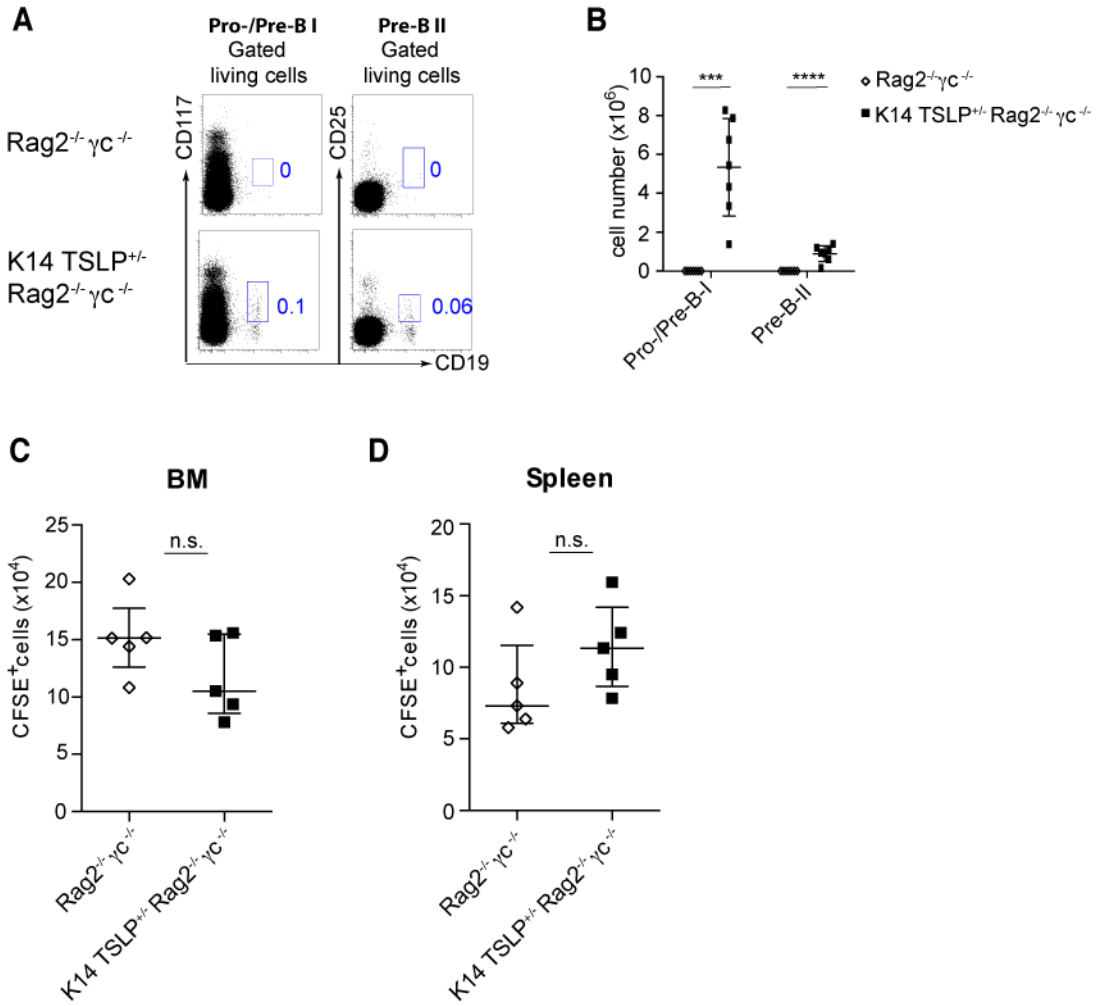

Figure 22: Increased numbers of B cell precursors in the BM of K14 TSLP$^{+/-}$ Rag2$^{-/-}$ γc$^{-/-}$ mice do not impair recruitment of progenitor cells. A) Gating strategy for Pro - /Pre - B I and Pre-B II cells; numbers in dot plots represent frequencies of a representative experiment. **B)** Absolute cell numbers of Pro - / Pre - B I and Pre-B II. **C)** Analysis of CFSE^{+} cells after 24h in the BM and **D)** spleen; **B-D)** n = 5 - 7 median values + interquartile range; n.s. = not significant, ***P<0.001, ****P<0.0001.

5.2 Reconstitution of the adaptive immune system with FL cells

To study the previously described effects of TSLPtg expression and the presence of LNs on the efficiency of HSCT, Rag2$^{-/-}\gamma c^{-/-}$ and K14 TSLP$^{+/-}$ Rag2$^{-/-}\gamma c^{-/-}$ mice were reconstituted with FL HSCs. To exclude a direct effect of TSLP on donor cells, TSLPR$^{-/-}$ FL HSC were used. The experimental approach included the injection of 5x10^6 E14.5 total FL cells and subsequent analysis of the reconstitution kinetics from 3 - 6 weeks in BM, thymus, spleen, LN and intestine of recipients (Fig. 23).

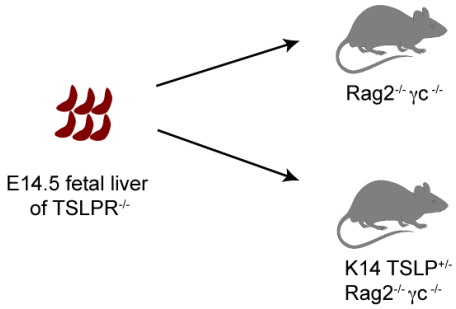

Figure 23: Transplantation model: Rag2$^{-/-}\gamma c^{-/-}$ and K14 TSLP$^{+/-}$ Rag2$^{-/-}\gamma c^{-/-}$ mice were transplanted with E14.5 TSLPR$^{-/-}$ total FL cells.

5.2.1 Efficiency of progenitor cell reconstitution in the BM

As the BM is the primary site for B cell development, several progenitor B cell subsets were analysed in reconstituted Rag2$^{-/-}\gamma c^{-/-}$ and K14 TSLP$^{+/-}$ Rag2$^{-/-}\gamma c^{-/-}$ mice 3 to 6 weeks after transplantation. While the total BM cellularity was stable during reconstitution and cell numbers did not differ between Rag2$^{-/-}\gamma c^{-/-}$ and K14 TSLP$^{+/-}$ Rag2$^{-/-}\gamma c^{-/-}$ mice (Fig. 24A), K14 TSLP$^{+/-}$ Rag2$^{-/-}\gamma c^{-/-}$ mice showed 6 weeks after transplantation a significant increase in the myeloid compartment (Fig 24B). In the B cell precursor subset was a significant increase in Pro - / Pre - B I and Pre - B II cells in K14 TSLP$^{+/-}$ Rag2$^{-/-}\gamma c^{-/-}$ mice 3 weeks after transplantation (Fig. 24C), which is likely due to the elevated cell numbers of the recipient. Pre - B II cells did not differ

between Rag2$^{-/-}\gamma c^{-/-}$ and K14 TSLP$^{+/-}$ Rag2$^{-/-}\gamma c^{-/-}$ mice until a significant decline in week 5 in K14 TSLP$^{+/-}$ Rag2$^{-/-}\gamma c^{-/-}$ mice (Fig. 24C). Investigation of B220^{+} IgM^{+} B cells, which include immature and mature B cells in the BM diminished in K14 TSLP$^{+/-}$ Rag2$^{-/-}\gamma c^{-/-}$ mice 5 and 6 weeks after transplantation (Fig. 24C).

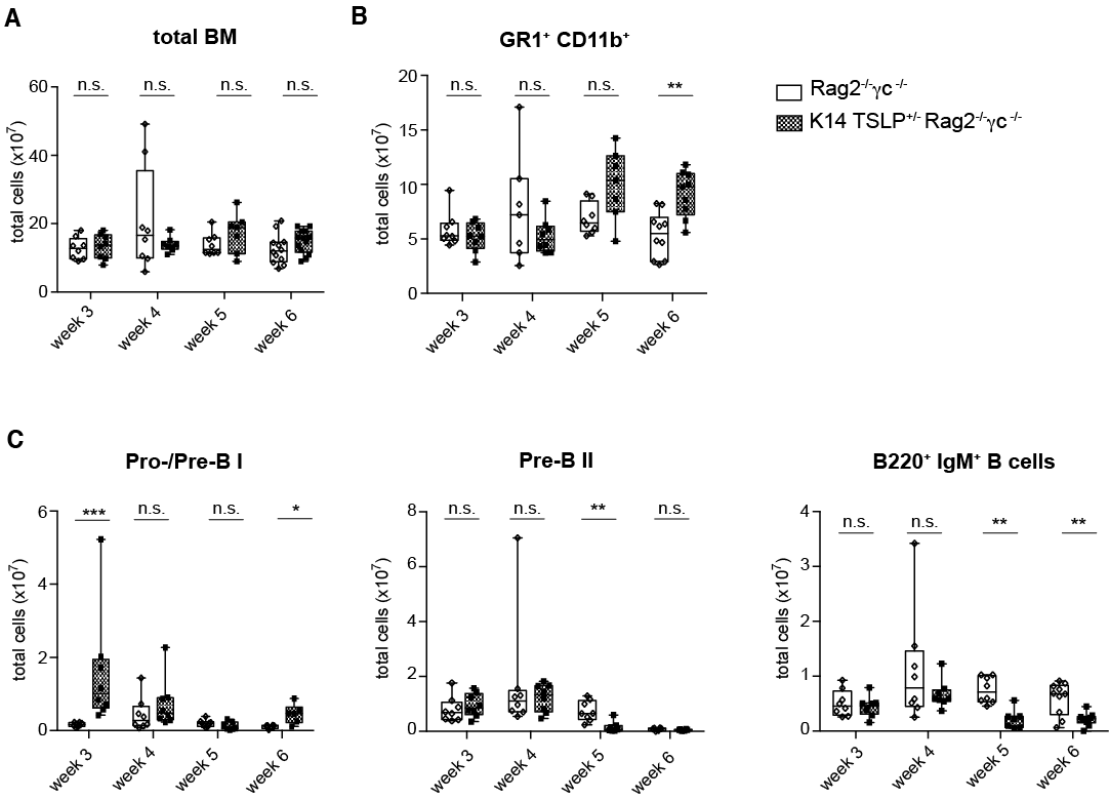

Figure 24: Myeloid and B cell subsets in the BM 3 - 6 weeks after transplantation. A) Number of total BM cells. **B)** Number of GR1^{+} CD11b^{+} myeloid cells in the BM. **C)** Number of Pro - / Pre - B I (CD19^{+} CD117^{+}), Pre - B II (CD19^{+} CD25^{+}) and B220^{+} IgM^{+} B cells in the BM; **A - C)** n = 8 - 13; median values + interquartile range; n.s. = not significant, *P<0.05, **P<0.01, ***P<0.001.

5.2.2 Efficiency of thymocyte development after FL HSCT

After transplantation of total FL cells from TSLPR$^{-/-}$ mice, the thymus size increased over time in Rag2$^{-/-}\gamma c^{-/-}$ and K14 TSLP$^{+/-}$ Rag2$^{-/-}\gamma c^{-/-}$ mice as illustrated in Fig. 25A.

Prior transplantation, K14 TSLP$^{+/-}$ Rag2$^{-/-}\gamma c^{-/-}$ mice had higher numbers of DN thymocytes in the thymus compared to Rag2$^{-/-}\gamma c^{-/-}$ mice (Fig. 8D). This could account for the higher total cell numbers 3 weeks after transplantation of FL cells (Fig. 25B). From week 4 onwards, thymic cellularity of reconstituted mice exceeded the number of thymocytes, which indicates the start of T cell development from donor precursors (Fig. 25B). 6 weeks after transplantation, there was a 6-fold increase in total cellularity, suggesting faster T cell reconstitution in K14 TSLP$^{+/-}$ Rag2$^{-/-}\gamma c^{-/-}$ mice compared to Rag2$^{-/-}\gamma c^{-/-}$ mice (Fig. 25B).

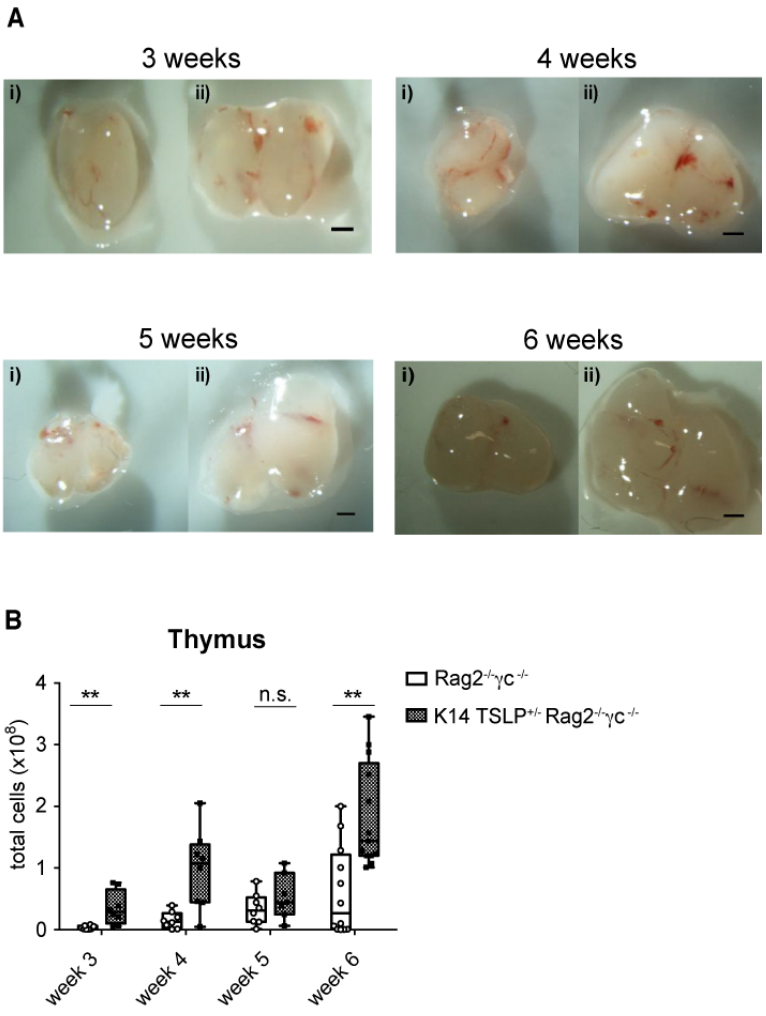

Figure 25: TSLPtg increases total cellularity in the thymus after HSC transplantation. **A)** Representative photographic picture of thymi from $Rag2^{-/-}\gamma c^{-/-}$ (i) and K14 $TSLP^{+/-}$ $Rag2^{-/-}\gamma c^{-/-}$ (ii) mice 3, 4, 5 and 6 weeks after reconstitution. Scale bar represents 1mm. **B)** Absolute cell numbers of total thymus; n = 8 - 13; median values + interquartile range; n.s. = not significant, **P<0.01.

Flow cytometry analysis of different T cell compartments in the thymi of transplanted Rag2$^{-/-}\gamma c^{-/-}$ and K14 TSLP$^{+/-}$ Rag2$^{-/-}\gamma c^{-/-}$ mice showed that T cell development started between week 3 and 4 and further increased in both Rag2$^{-/-}\gamma c^{-/-}$ and K14 TSLP$^{+/-}$ Rag2$^{-/-}\gamma c^{-/-}$ mice. DP T cells were already significantly increased 4 weeks after transplantation in K14 TSLP$^{+/-}$ Rag2$^{-/-}\gamma c^{-/-}$ mice (Fig. 26A). This was followed by a significant increase of CD4^{+} as well as CD8^{+} SP T cell subsets 5 weeks after transplantation (Fig. 26A). Further discrimination into immature (CD69^{+}) and mature (CD69^{-}) CD4^{+} and CD8^{+} SP T cells (Fig. 26B-C) showed no specific impairment in the regulation of CD69 expression in Rag2$^{-/-}\gamma c^{-/-}$ mice. This indicates that the differentiation into mature T cells is possible in both mouse strains but occurs more efficiently in K14 TSLP$^{+/-}$ Rag2$^{-/-}\gamma c^{-/-}$ mice. Tregs (TCRβ^{+} CD4^{+} CD25^{+} Foxp3^{+}) were detectable in thymi of recipient mice from weeks 3 onwards and were significantly higher with TSLP overexpression after week 5 (Fig 26D).

Together, these data demonstrate that TSLP overexpression in Rag2$^{-/-}\gamma c^{-/-}$ mice results in accelerated T cell reconstitution after HSC transplantation compared to Rag2$^{-/-}\gamma c^{-/-}$ mice.

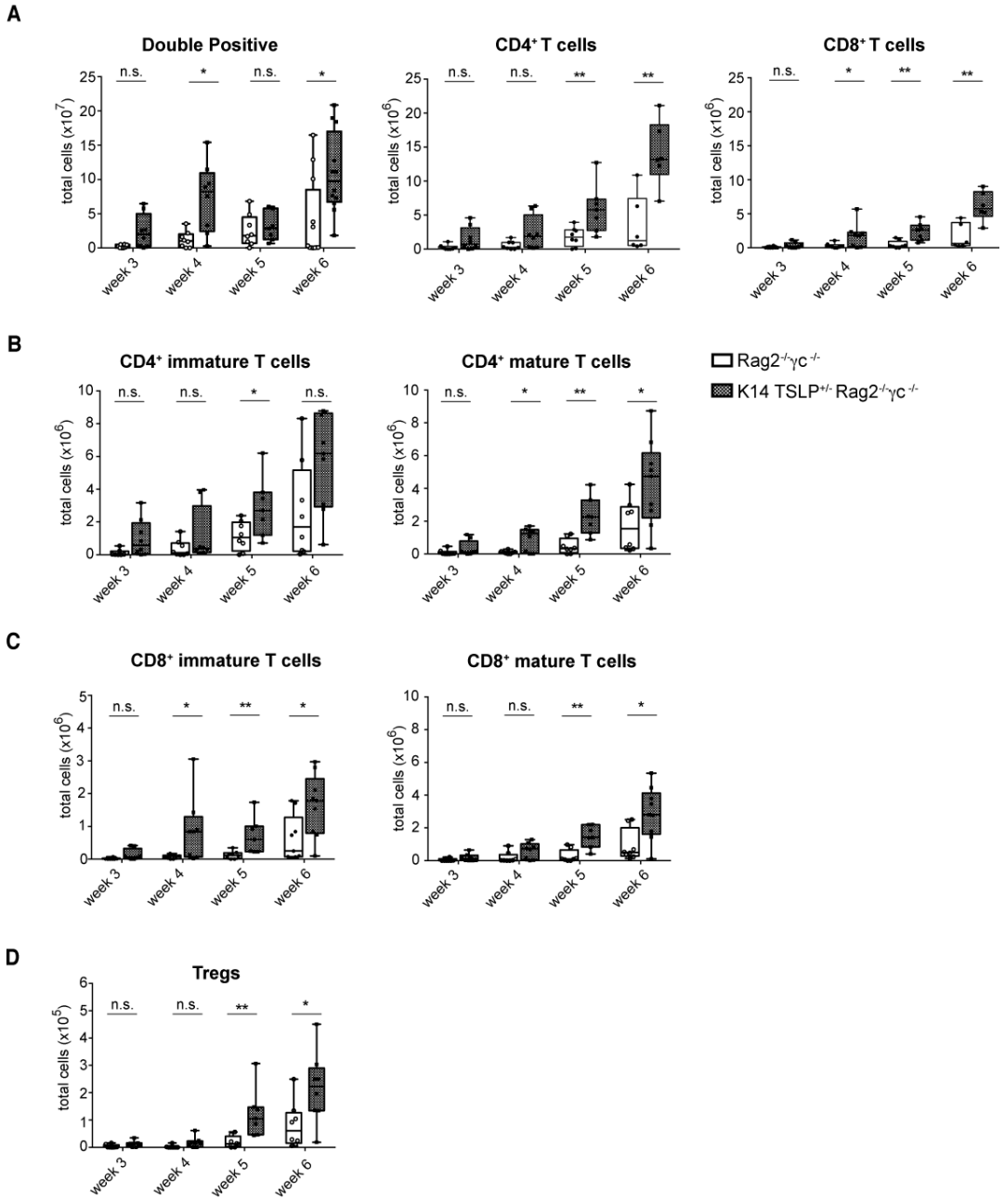

Figure 26: TSLPtg increases T cell subsets in the thymus after reconstitution: T cell subsets 3 - 6 weeks after reconstitution **A)** Number of double positive ($CD4^+$ $CD8^+$), $CD4^+$ ($TCR\beta^+$ $CD4^+$ $CD8^-$) and $CD8^+$ ($TCR\beta^+$ $CD4^-$ $CD8^+$) T cells **B)** Number of $CD4^+$ immature ($CD69^+$) and mature ($CD69^-$) T cells **C)** Number of $CD8^+$ immature ($CD69^+$) and mature ($CD69^-$) T cells **D)** Number of regulatory T cells (Tregs) ($TCR\beta^+$ $CD4^+$ $CD25^+$ $Foxp3^+$); **A - D)** n = 8 - 13; median values + interquartile range; n.s. = not significant, *P<0.05, **P<0.01.

5.2.3 Reconstitution of the spleen after FL HSCT

After adoptive transfer of FL HSCs into Rag2$^{-/-}\gamma c^{-/-}$ and K14 TSLP$^{+/-}$ Rag2$^{-/-}\gamma c^{-/-}$ mice spleens increased in size in both mouse strains (Fig. 27A). In line with the organ enlargement is the increase in total number of splenocytes. From week 3 to week 6 after transplantation, the total number of splenocytes was higher in K14 TSLP$^{+/-}$ Rag2$^{-/-}\gamma c^{-/-}$ mice compared to Rag2$^{-/-}\gamma c^{-/-}$ mice, reaching statistical significance at week 3 and week 6 (Fig. 27B).

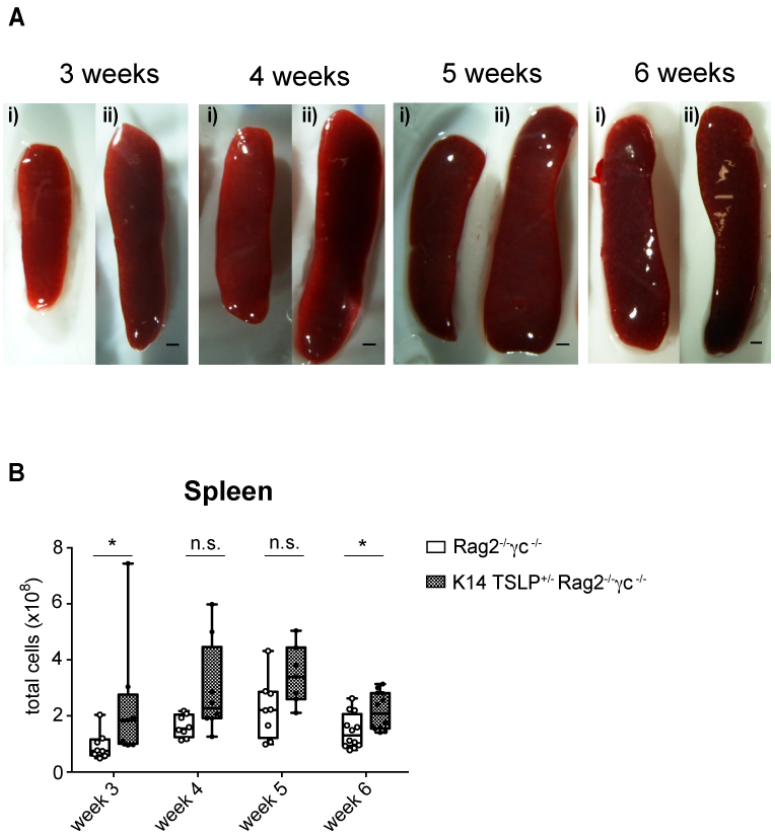

Figure 27: TSLPtg increases total cellularity in the spleen A) Representative photographic picture of spleens from Rag2$^{-/-}\gamma c^{-/-}$ (i) and K14 TSLP$^{+/-}$ Rag2$^{-/-}\gamma c^{-/-}$ (ii) mice 3, 4, 5 and 6 weeks after transplantation. Scale bar represents 1mm. **B)** Cell numbers of total spleen; n = 8 - 13; median values + interquartile range; n.s. = not significant, *P<0.05.

In addition, the total number of natural killer (NK) cells, DCs, GR1$^+$ CD11b$^+$ myeloid cells as well as B and T cells was analysed in spleens from Rag2$^{-/-}\gamma c^{-/-}$ and K14 TSLP$^{+/-}$ Rag2$^{-/-}\gamma c^{-/-}$ mice after transplantation. While the number of NK cells was only significantly increased at 3 weeks after transplantation by TSLP overexpression,

the GR1$^+$ CD11b$^+$ myeloid cells reached statistical significance at 5 weeks after HSC transplantation in K14 TSLP$^{+/-}$ Rag2$^{-/-}\gamma c^{-/-}$ mice (Fig. 28A). CD11c$^+$ DCs numbers did not differ between Rag2$^{-/-}\gamma c^{-/-}$ and K14 TSLP$^{+/-}$ Rag2$^{-/-}\gamma c^{-/-}$ mice (Fig. 28A). These results demonstrate that NK cells as well as myeloid cells, beside small differences, differentiated equally. Hence TSLP overexpression plays no major role in the regulation of these cellular subsets.

In the spleen, B cells can be divided into marginal zone (Mz) and follicular (fol) B cells. Mz B cells did not develop earlier than 4 weeks after transplantation. Therefore, total CD19$^+$ B cells were compared 3 weeks after transplantation between Rag2$^{-/-}\gamma c^{-/-}$ and K14 TSLP$^{+/-}$ Rag2$^{-/-}\gamma c^{-/-}$ mice. The latter had a significant increase in total CD19$^+$ cells (Fig. 28B), whereas Mz and fol B cell numbers did not differ between week 4 and 6 after transplantation in both mouse strains (Fig. 28B).

In summary, these data suggest that the reconstitution of the B cell compartment was equally efficient and not influenced by TSLP overexpression

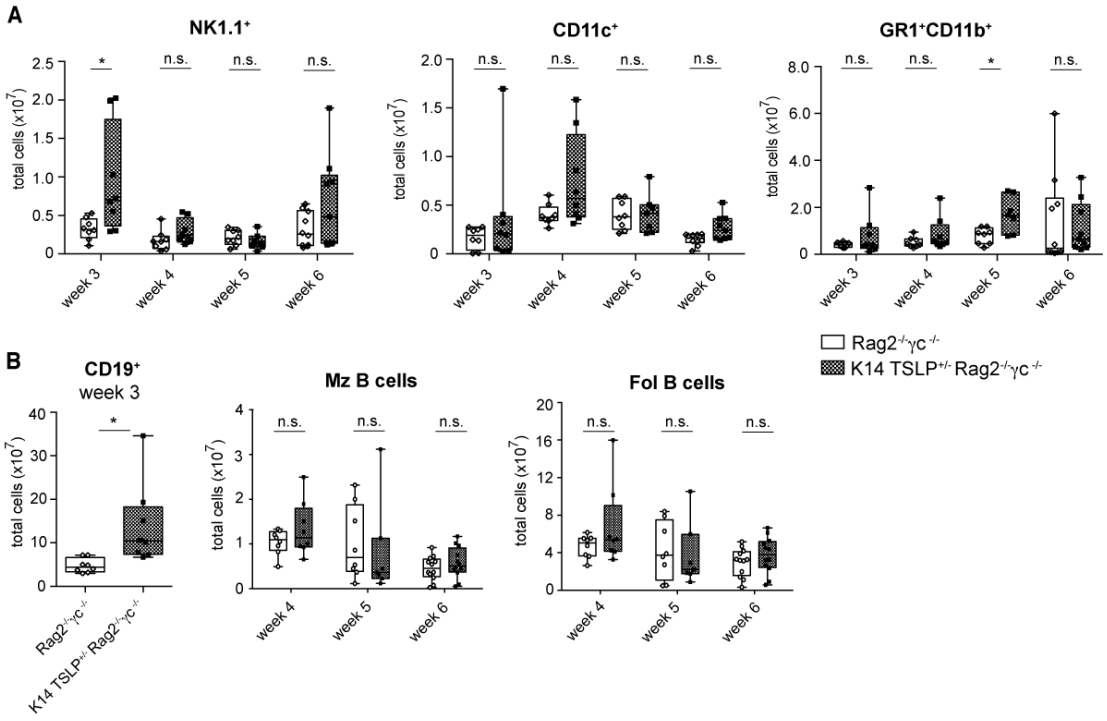

Figure 28: Myeloid and B cell subsets in the spleen A) Number of NK cells, CD11c$^+$ DCs and GR1$^+$ CD11b$^+$ cells. **B)** Number of total B cells (week 3) and B cell subsets Mz and Fol B cells (weeks 4-6); n = 8 - 13; median values + interquartile range; n.s. = not significant, *P<0.05.

Although there was no difference beyond 3 weeks of reconstitution in the splenic myeloid and B cell compartment of Rag2$^{-/-}\gamma c^{-/-}$ and K14 TSLP$^{+/-}$ Rag2$^{-/-}\gamma c^{-/-}$ mice, there were significant differences in T cell numbers. 5 weeks after transplantation the number of CD4$^+$ and CD8$^+$ T cells was significant higher in spleens of K14 TSLP$^{+/-}$ Rag2$^{-/-}\gamma c^{-/-}$ (CD4$^+$: ~ 3.6x10^7; CD8$^+$: ~ 9.3x10^7) compared to Rag2$^{-/-}\gamma c^{-/-}$mice (CD4$^+$: ~ 0.7x10^7; CD8$^+$: ~ 1.7x10^7) (Fig. 29A). Tregs were already detectable 4 weeks after reconstitution in both mouse strains with approximately 5-fold increase of Tregs in K14 TSLP$^{+/-}$ Rag2$^{-/-}\gamma c^{-/-}$ mice 5 weeks after transplantation (Fig. 29B). Staining for Helios, an intracellular transcription factor, which discriminates thymic from peripheral induced Tregs[94], showed high deviations but no significant difference in the frequency of Helios$^+$ Tregs (Fig. 29B). This indicates that Helios$^-$ Tregs were generated in the periphery of Rag2$^{-/-}\gamma c^{-/-}$ and K14 TSLP$^{+/-}$ Rag2$^{-/-}\gamma c^{-/-}$ mice with a comparable efficiency (Fig. 29B). Investigation of the memory compartments for CD4$^+$ and CD8$^+$ T cells showed no significant difference in the frequency of naïve (CD62L$^+$ CD44$^-$) or central memory (CM) (CD62L$^+$ CD44$^+$) T cells and also not in CD8$^+$ effector memory (EM) (CD62L$^-$ CD44$^+$) T cells. However, a significant decrease in the CD4$^+$ EM compartment in the spleen of K14 TSLP$^{+/-}$ Rag2$^{-/-}\gamma c^{-/-}$ mice (Fig. 29C) was observed.

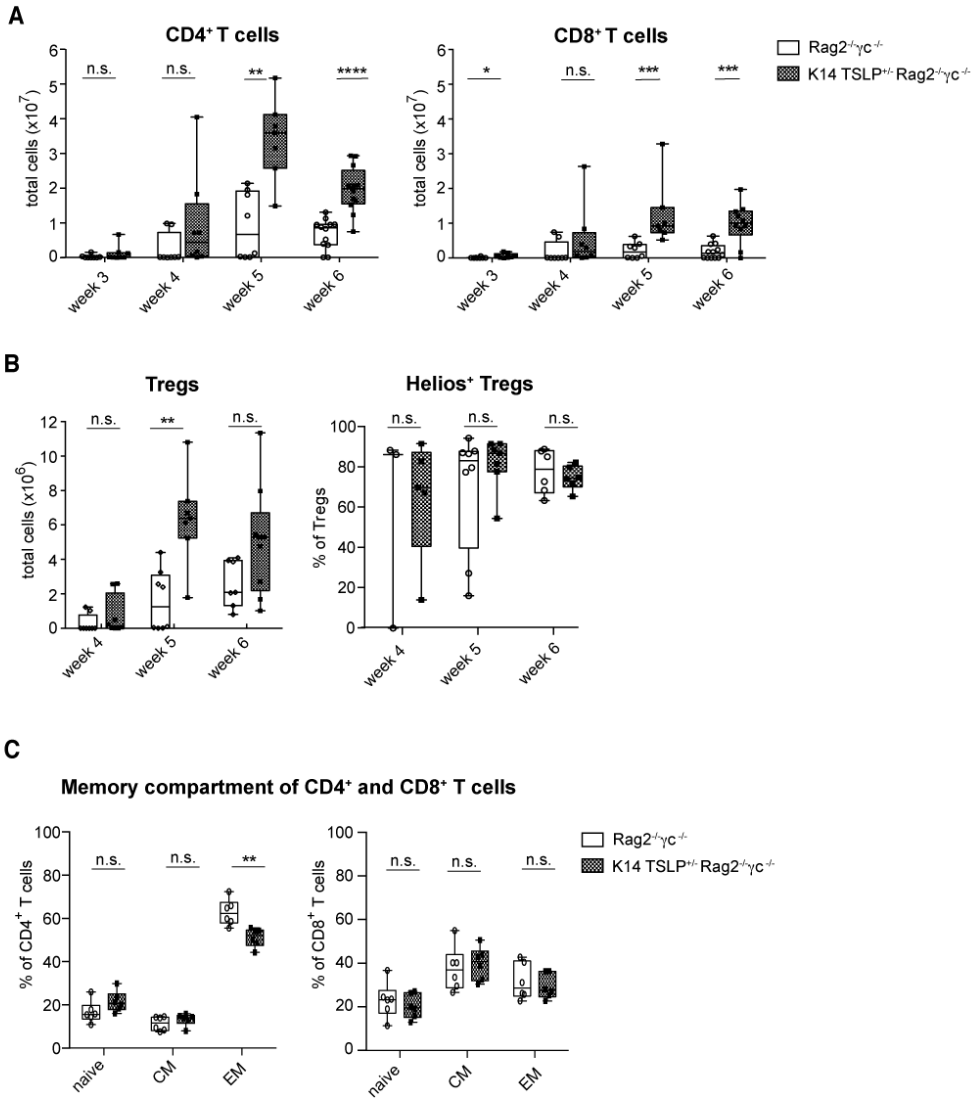

Figure 29: TSLPtg increases T cells in the spleen after reconstitution. A) Number of $CD4^+$ and $CD8^+$ T cells in the spleen of $Rag2^{-/-}\gamma c^{-/-}$ and K14 $TSLP^{+/-}$ $Rag2^{-/-}\gamma c^{-/-}$ mice **B)** Number of Tregs and frequency of $Helios^+$ Tregs; **C)** Frequencies of $CD4^+$ and $CD8^+$ naïve ($CD62L^+$ $CD44^-$), central memory (CM) ($CD62L^+$ $CD44^+$) and effector memory (EM) ($CD62L^-$ $CD44^+$) T cells; n = 6 - 8; median values + interquartile range; n.s. = not significant, *P<0.05, **P<0.01, ***P<0.001 ****P<0.0001.

5.2.4 Reconstitution of mesenteric lymph nodes

Rag2$^{-/-}\gamma c^{-/-}$ mice have severe defects in LN development due to the lack of LTi cells. It was previously described that this defect can be rescued by TSLP overexpression[138]. To investigate the reconstitution of LNs, mLNs were analysed, as mLN anlagen are present in most of the Rag2$^{-/-}\gamma c^{-/-}$ mice. mLNs were larger in size upon HSC transplantation in both mouse strains (Fig. 30A - B). However, at week 3 and 4 after transplantation, mLNs showed a significantly higher total cell number in K14 TSLP$^{+/-}$ Rag2$^{-/-}\gamma c^{-/-}$ compared to Rag2$^{-/-}\gamma c^{-/-}$ mice (Fig. 30A - B).

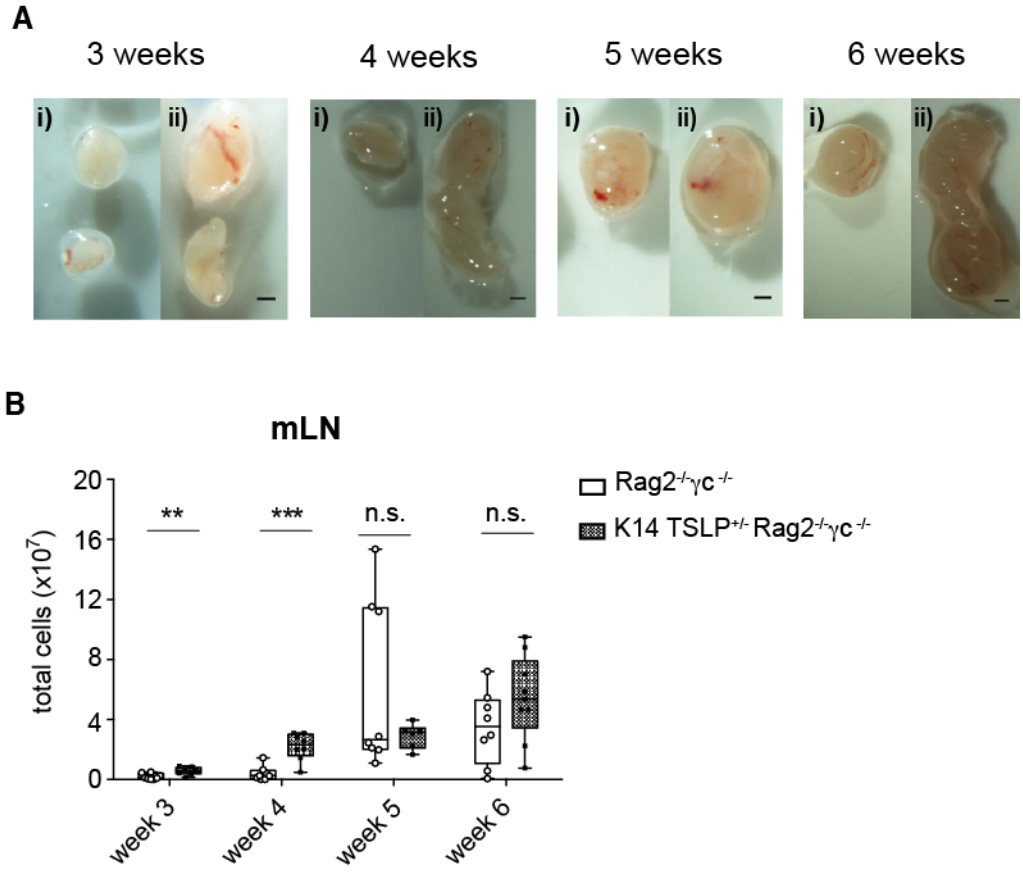

Figure 30: TSLPtg increases total cellularity in mLNs A) Representative photographic picture of mLNs from Rag2$^{-/-}\gamma c^{-/-}$ (i) and K14 TSLP$^{+/-}$ Rag2$^{-/-}\gamma c^{-/-}$ (ii) mice 3, 4, 5 and 6 weeks after reconstitution. Scale bar represents 1mm. **B)** Cell numbers of total mLNs; n = 6 - 13; median values + interquartile range; n.s. = not significant, **P<0.01, ***P<0.001.

Similar to the spleen there was no significant difference in the B cell compartment between reconstituted Rag2$^{-/-}\gamma c^{-/-}$ and K14 TSLP$^{+/-}$ Rag2$^{-/-}\gamma c^{-/-}$ mice (Fig. 31A). The number of CD4$^+$ and CD8$^+$ T cells in mLN increased between week 4 and 6 in both mouse strains. However, the rate of this increase appeared to be higher in K14 TSLP$^{+/-}$ Rag2$^{-/-}\gamma c^{-/-}$ mice (Fig. 31B). Tregs could be found 4 weeks after reconstitution and numbers were significantly higher after 5 weeks in K14 TSLP$^{+/-}$ Rag2$^{-/-}\gamma c^{-/-}$ (median: 0.47x10^6 cells) compared to Rag2$^{-/-}\gamma c^{-/-}$ mice (median: 0.064x10^6 cells). In agreement with the observation in the spleen, the frequency of Helios$^+$ cells was comparable in both mouse strains (Fig. 31C). Investigation of the memory compartment showed neither a difference in CD4$^+$ naïve, CM or EM nor in the CD8$^+$ memory subsets (Fig. 31D).

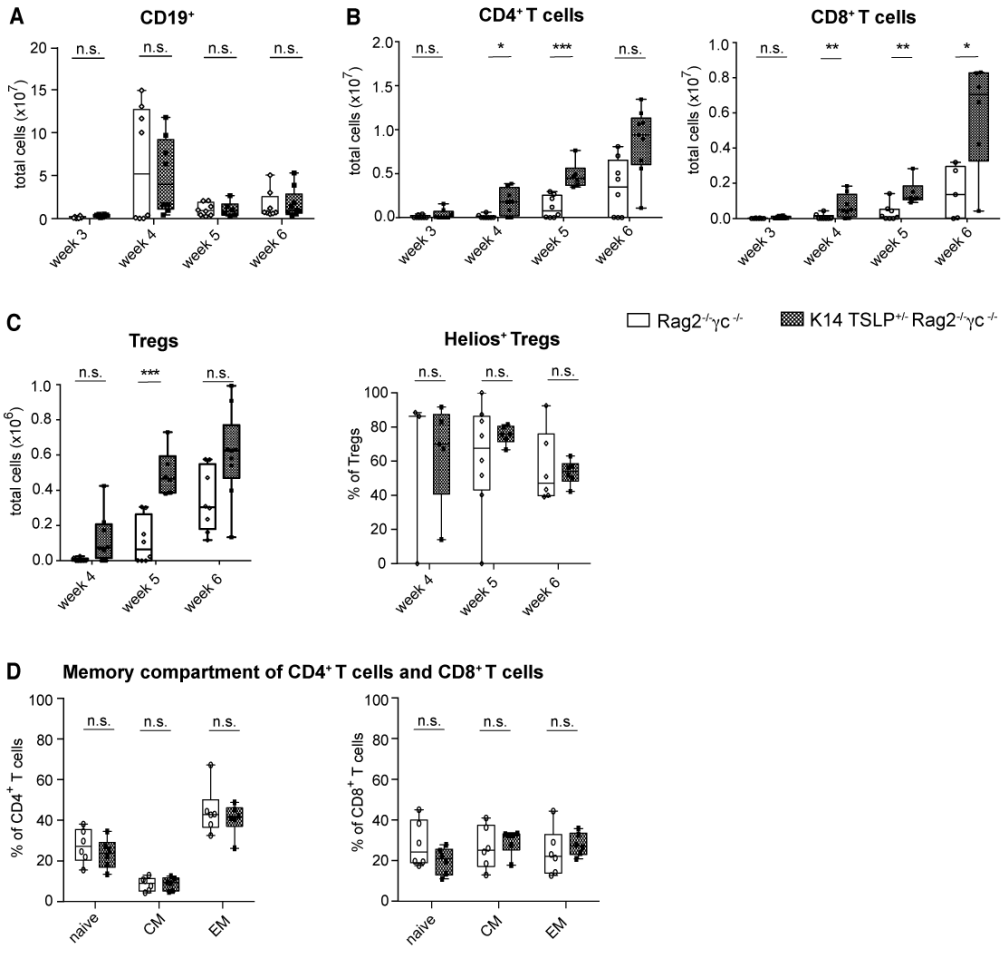

Figure 31: TSLPtg increases T cells in the mLN after reconstitution A) Absolute number of CD19$^+$ B cells **B)** Absolute number of CD4$^+$ and CD8$^+$ T cells **C)** Absolut number of Tregs and frequency of Helios$^+$ Tregs; **D)** Frequencies of CD4$^+$ and CD8$^+$ naïve (CD62L$^+$ CD44$^-$), CM (CD62L$^+$ CD44$^+$) and EM (CD62L$^-$ CD44$^+$) T cells; n = 6 - 8; median values + interquartile range; n.s. = not significant, *P<0.05, **P<0.01, ***P<0.001.

5.2.5 Reconstitution of the intestine after FL HSCT

To investigate the effect of TSLPtg expression on the efficiency of lymphocyte reconstitution in the intestine, lamina propria lymphocytes (LPLs) were isolated from SI and colon 3 - 6 weeks after FL HSC transplantation. Total LPL numbers were significantly increased 5 weeks after transplantation in K14 TSLP$^{+/-}$ Rag2$^{-/-}\gamma c^{-/-}$ mice compared to Rag2$^{-/-}\gamma c^{-/-}$ mice (Fig. 32A). The difference was also observed in the T cells subsets. Here, numbers of CD4^{+} T cells were approximately 6-fold, CD8^{+} T cells 40-fold (Fig. 32B) and Tregs 13-fold (Fig. 32C) increased in K14 TSLP$^{+/-}$ Rag2$^{-/-}\gamma c^{-/-}$ mice compared to Rag2$^{-/-}\gamma c^{-/-}$ mice. As seen in other organs, Helios expression did not differ between both mouse strains (Fig. 32C).

In the colon, there was no such difference observed in cell numbers and frequency of the different T cell subsets upon HSC transplantation (Fig. 33A - C).

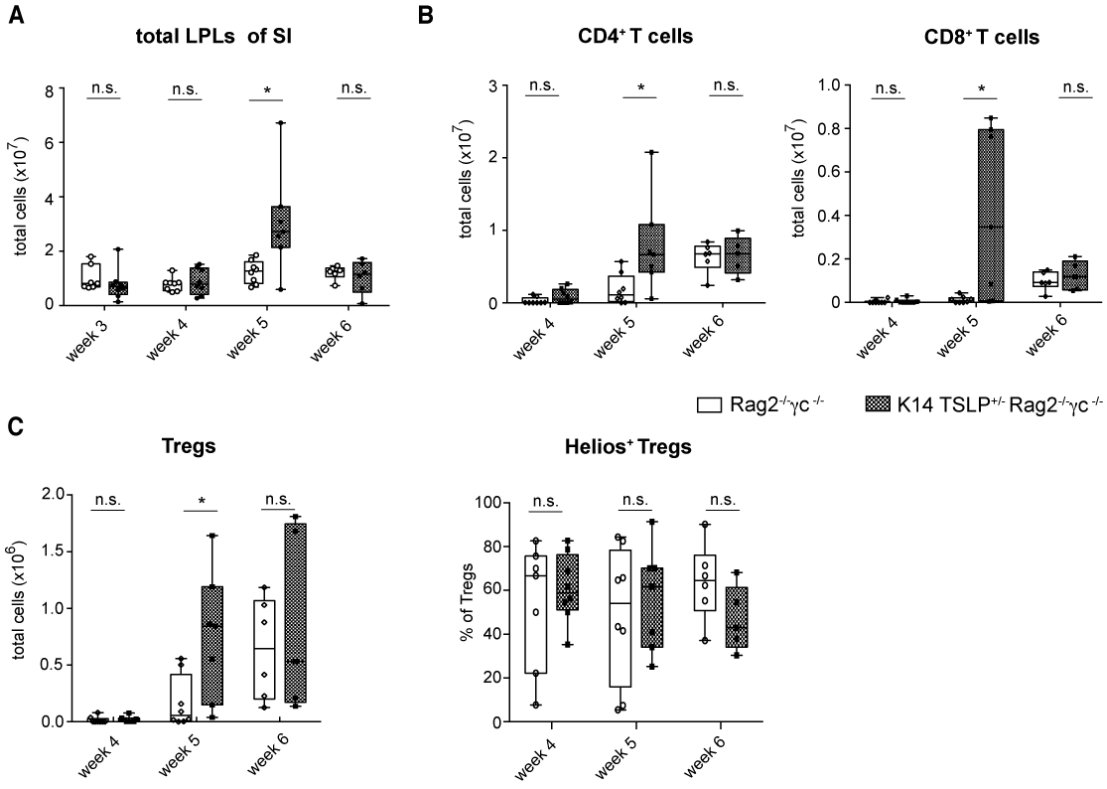

Figure 32: T cell compartment in lamina propria of SI after HSC transplantation A) Absolute number of total LPLs in SI **B)** Absolute number of CD4^{+} and CD8^{+} T cells **C)** Absolut number of Tregs and frequency of Helios^{+} Tregs; n = 6 - 8; median values + interquartile range; n.s. = not significant, *P<0.05

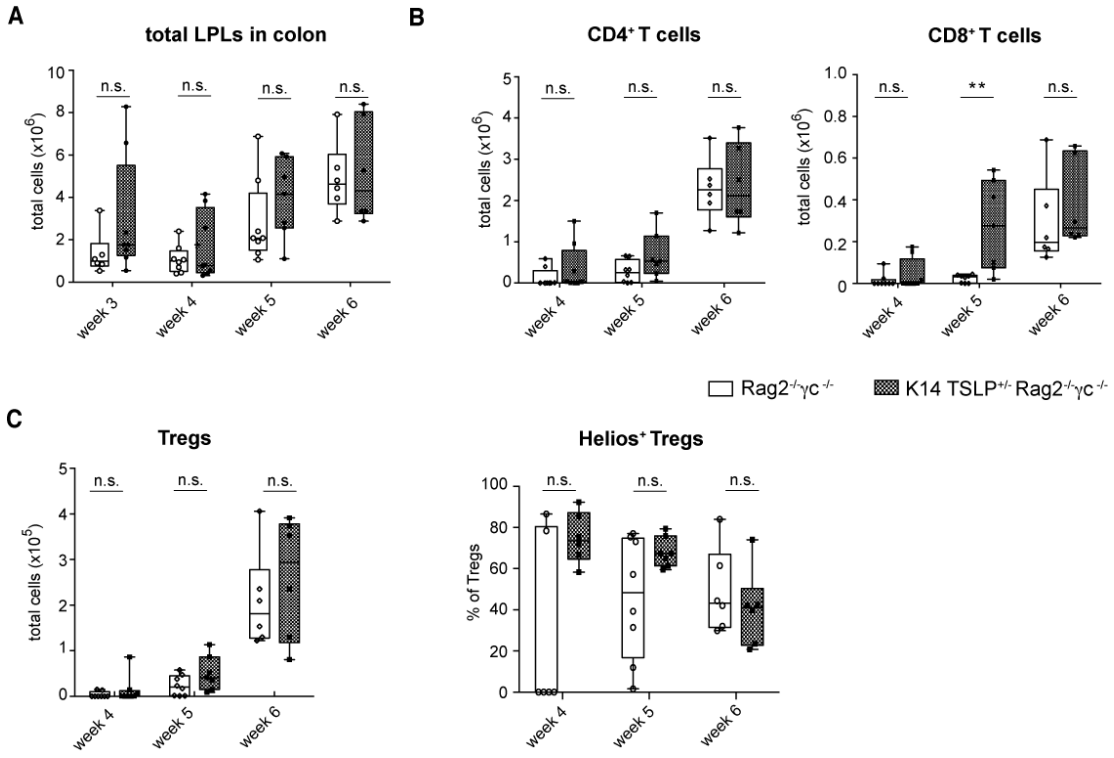

Figure 33: T cell compartment in lamina propria of colon after transplantation A) Number of total LP - derived cells in colon **B)** Number of $CD4^+$ and $CD8^+$ T cells **C)** Number of Tregs and frequency of $Helios^+$ Tregs; n = 6 - 8; median values + interquartile range; n.s. = not significant.

Taken together, TSLP overexpression in $Rag2^{-/-}\gamma c^{-/-}$ mice resulted in faster T cell reconstitution in thymus and peripheral organs after FL HSC transplantation from $TSLPR^{-/-}$ mice. B cell reconstitution was not significantly different in $Rag2^{-/-}\gamma c^{-/-}$ compared to K14 $TSLP^{+/-}$ $Rag2^{-/-}\gamma c^{-/-}$ mice indicating that the reconstitution itself was equally efficient.

5.2.6 Immunization with T-dependent antigen after FL HSCT

The previous described characterization of differences during reconstitution showed that the T cell compartment was faster reconstituted in K14 $TSLP^{+/-}$ $Rag2^{-/-}\gamma c^{-/-}$ than in $Rag2^{-/-}\gamma c^{-/-}$ mice. To investigate whether these T cells were also able to support B cell antibody (Ab) production during an immune response, reconstituted $Rag2^{-/-}\gamma c^{-/-}$ and K14 $TSLP^{+/-}$ $Rag2^{-/-}\gamma c^{-/-}$ mice were immunized with the T-

dependent antigen NP-Ovalbumin (NP-(18)-OVA). 6 weeks after transplantation with FL HSCs from TSLPR$^{-/-}$ mice, recipient mice were injected intraperitoneally (i.p.) with NP-OVA in Alum followed by a second injection 12 days after the initial immunization (boost). Total IgM and IgG levels were measured by ELISA in the serum before and after immunization. NP-OVA specific IgG was analysed 7 days after second immunization (Fig. 34A).

First, analysis of total IgM and IgG levels 42 days after reconstitution revealed that total IgM levels did not differ between Rag2$^{-/-}\gamma c^{-/-}$ and K14 TSLP$^{+/-}$ Rag2$^{-/-}\gamma c^{-/-}$ mice (Fig. 34A). In contrast, TSLP overexpression led to a higher total IgG level (Fig. 34B). As a response to NP-OVA injection both mouse strains generated NP-OVA specific IgGs in comparable amounts (Fig. 34C). These data suggest that T cells in both Rag2$^{-/-}\gamma c^{-/-}$ and K14 TSLP$^{+/-}$ Rag2$^{-/-}\gamma c^{-/-}$ mice could support Ag specific IgG production and hence give B cell help during an immune response in similar ranges.

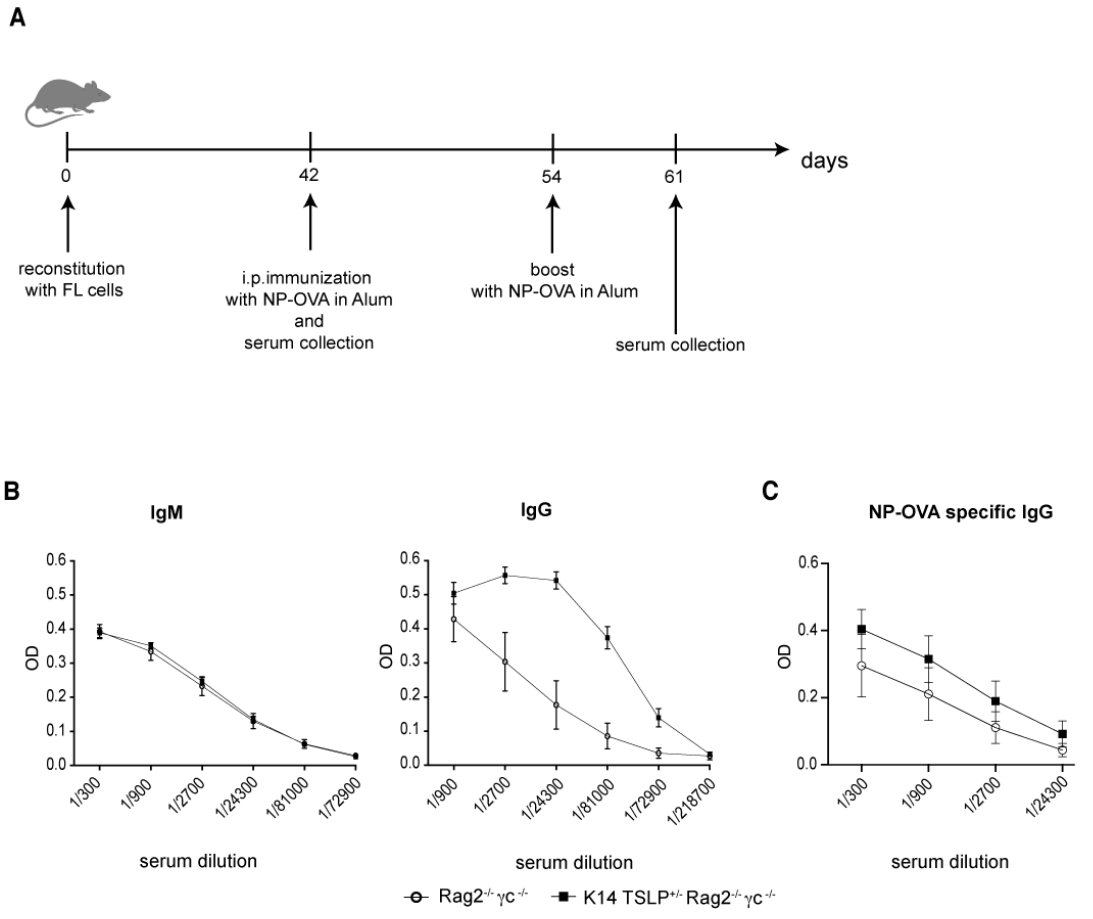

Figure 34: Immunization with NP-OVA after reconstitution A) Scheme of experimental procedure **B) Total** IgM and IgG titers of Rag2$^{-/-}\gamma c^{-/-}$ and K14 TSLP$^{+/-}$ Rag2$^{-/-}\gamma c^{-/-}$ mice 6 weeks after reconstitution **C)** NP-OVA specific IgG titers 7 days after boost with NP-OVA in Alum (day 61); n = 6 of one experiment; mean + SEM;

5.3 The influence of secondary lymphoid organs on peripheral T cell homeostasis

5.3.1 Characterization of stromal cell compartments in secondary lymphoid organs

Secondary lymphoid organs are important niches for T cells, as they provide cytokines and chemokines for migration, proliferation, and survival. Since TSLPR is also expressed by LN stromal cells, we asked whether TSLP overexpression had an effect on the stromal environment either directly via higher TSLP - TSLPR interaction or indirectly by increasing ILC3 numbers. Therefore, stromal compartments of mLNs and spleen were analysed for total cell numbers and cytokine expression. The stromal compartment of LNs consists of T zone reticular cells (TRCs: $CD45^-$ $CD31^-$ $gp38^+$), lymphatic endothelial cells (LECs: $CD45^-$ $CD31^+$ $gp38^+$), blood endothelial cells (BECs: $CD45^-$ $CD31^+$ $gp38^-$) (Fig. 35A) and double negative stromal cells (DNSCs)[109]. The role of DNSCs is still unrevealed and were not analysed in this study. To investigate the stromal compartment of mLNs, mLNs from 3 $Rag2^{-/-}\gamma c^{-/-}$ mice were pooled in order to obtain sufficient cell numbers. There was no difference in frequencies of TRCs and LECs and only a minor but significant increase in BECs in K14 $TSLP^{+/-}$ $Rag2^{-/-}\gamma c^{-/-}$ compared to $Rag2^{-/-}\gamma c^{-/-}$ mice (Fig. 35B). Total numbers of TRCs, LECs and BECs were not significantly different in $Rag2^{-/-}\gamma c^{-/-}$ compared to K14 $TSLP^{+/-}$ $Rag2^{-/-}\gamma c^{-/-}$ mice (Fig. 35A - B). These stromal subsets were also analysed in brachial LNs 4 weeks after transplantation, whereby numbers of TRCs and LECs but not BECs were significantly increased in K14 $TSLP^{+/-}$ $Rag2^{-/-}\gamma c^{-/-}$ compared to $Rag2^{-/-}\gamma c^{-/-}$ (Fig. 36A).

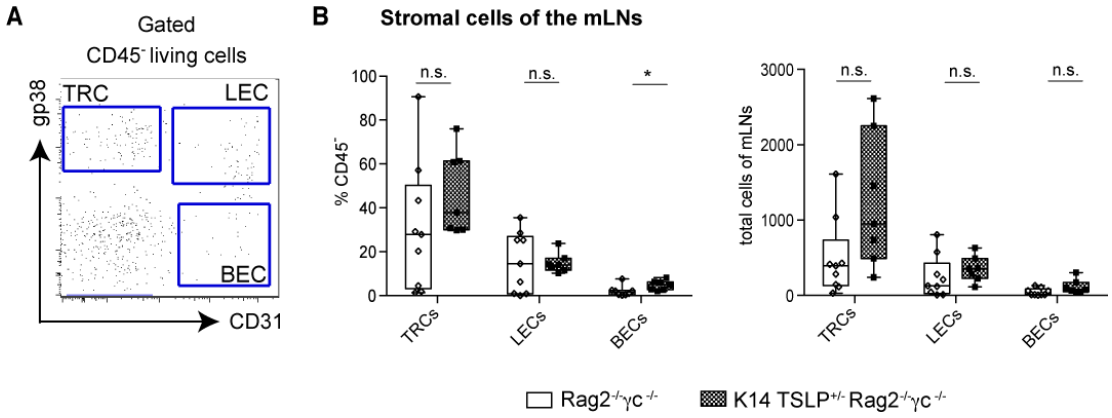

Figure 35: Characterization of mLN stromal compartment A) Gating strategy for stromal subsets **B)** Frequency and total numbers of TRCs (CD45$^-$ Gp38$^+$ CD31$^-$), LECs (CD45$^-$ Gp38$^+$ CD31$^+$) and BECs (CD45$^-$ Gp38$^-$ CD31$^+$) in Rag2$^{-/-}$ γc$^{-/-}$ and K14 TSLP$^{+/-}$ Rag2$^{-/-}$ γc$^{-/-}$ mice; n = 7 - 9 from 3 independent experiments; median values + interquartile range; n.s. = not significant, *P<0.05.

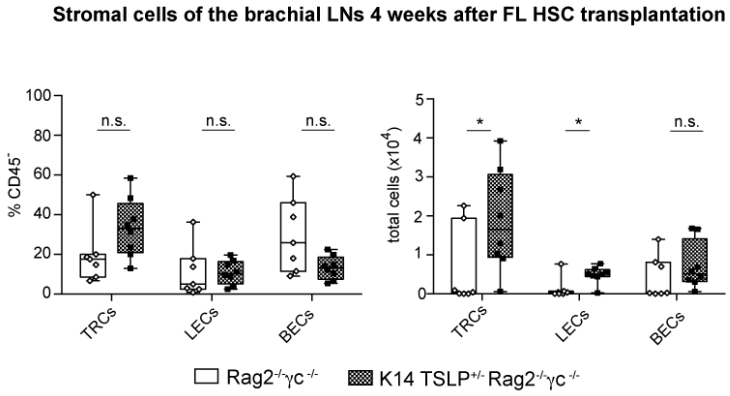

Figure 36: Stromal compartment of brachial LNs 4 weeks after transplantation: Frequency and total numbers of TRCs (CD45$^-$ Gp38$^+$ CD31$^-$), LECs (CD45$^-$ Gp38$^+$ CD31$^+$) and BECs (CD45$^-$ Gp38$^-$ CD31$^+$) in Rag2$^{-/-}$ γc$^{-/-}$ and K14 TSLP$^{+/-}$ Rag2$^{-/-}$ γc$^{-/-}$ mice; n = 8 from 2 independent experiments; median values + interquartile range; n.s. = not significant, *P<0.05.

The stromal compartment of the spleen was also analysed for TRCs and BECs. There was no significant difference in numbers of TRCs (median: 827 cells / spleen in K14 TSLP$^{+/-}$ Rag2$^{-/-}$γc$^{-/-}$ compared to 548 cells / spleen in Rag2$^{-/-}$γc$^{-/-}$ mice) or BECs (median: 597 cells / spleen in K14 TSLP$^{+/-}$ Rag2$^{-/-}$γc$^{-/-}$ compared to 195 cells / spleen in Rag2$^{-/-}$γc$^{-/-}$ mice) comparing Rag2$^{-/-}$γc$^{-/-}$ and K14 TSLP$^{+/-}$ Rag2$^{-/-}$γc$^{-/-}$ mice (Fig. 37A).

To test whether splenic TRCs and BECs from both mouse strains differ in their ability to produce cytokines for T cell proliferation and survival, TRCs and BECs were sorted and analysed for IL-7 and IL-15 transcript levels. There was no difference in IL-7 or IL-15 mRNA expression between Rag2$^{-/-}\gamma c^{-/-}$ and K14 TSLP$^{+/-}$ Rag2$^{-/-}\gamma c^{-/-}$ mice (Fig. 37B). However, IL-7 mRNA levels were 4-fold increased in total spleen of K14 TSLP$^{+/-}$ Rag2$^{-/-}\gamma c^{-/-}$ compared to Rag2$^{-/-}\gamma c^{-/-}$ mice, whereas there was no difference in IL-15 mRNA (Fig. 37C).

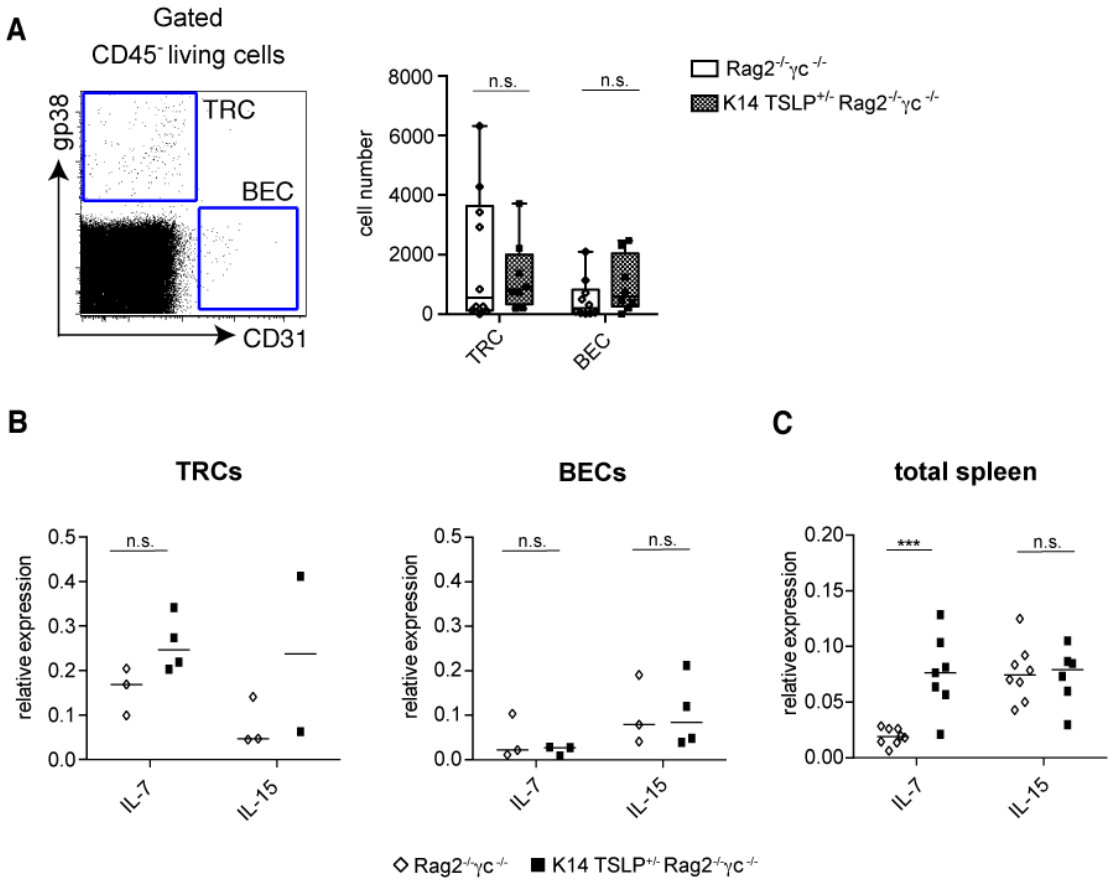

Figure 37: Characterization of splenic stromal compartment: A) Gating strategy and total number of TRCs and BECs; n = 7 - 9 from 3 independent experiments **B)** IL-7 and IL-15 transcript levels normalized to TBP on sorted TRCs and BECs, n = 2 - 4 from 2 independent experiments; n.s. = not significant **C)** IL-7 and IL-15 transcript levels normalized to TBP in total spleen; n = 7 - 8 from 3 independent experiments; median values; n.s. = not significant, ***P<0.001.

The results suggest that the stromal compartment did not contribute to the significant increase of IL-7 transcripts in K14 TSLP$^{+/-}$ Rag2$^{-/-}\gamma c^{-/-}$ mice. We further

asked, which other cell types could express IL-7 leading to the observed difference in IL-7 expression in the spleen of K14 TSLP$^{+/-}$ Rag2$^{-/-}\gamma c^{-/-}$ mice. One cell subset, which responds to TSLP overexpression by increasing their number, is the DC subset. qRT PCR data suggest no difference in IL-7 mRNA between DCs from Rag2$^{-/-}\gamma c^{-/-}$ and K14 TSLP$^{+/-}$ Rag2$^{-/-}\gamma c^{-/-}$ mice (Fig 38). However, the increased number of DCs in K14 TSLP$^{+/-}$ Rag2$^{-/-}\gamma c^{-/-}$ compared to Rag2$^{-/-}\gamma c^{-/-}$ mice may account for the 4-fold increase of IL-7 transcripts in the spleen of K14 TSLP$^{+/-}$ Rag2$^{-/-}\gamma c^{-/-}$ mice.

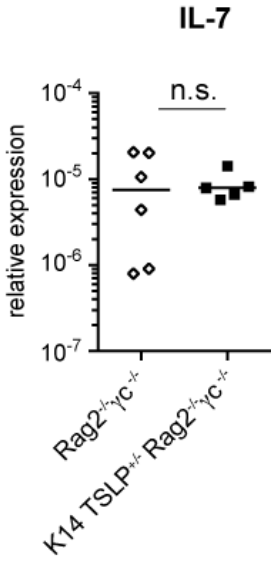

Figure 38: TSLPtg does not alter IL-7 production of DCs: IL-7 transcript levels normalized to β – actin on sorted CD11c$^+$ MHC II$^+$ DCs; n = 5 - 6 from 2 independent experiments; median values; n.s. = not significant.

Follicular dendritic cells (FDCs) found in secondary lymphoid organs are of mesenchymal origin and produce survival factors and chemoattractants for B cells[208]. The development of FDCs requires LTβR signaling, which can be provided by LT$\alpha\beta^+$ B cells[209,210]. Previous studies also described the requirement of LTi cells for the development of FDC precursors (preFDCs) in the absence of lymphocytes[211]. Rag2$^{-/-}\gamma c^{-/-}$ mice are B cell deficient, but TSLP overexpression increases the number of ILC3s, which could provide LT$\alpha\beta$. In line with this, analysis of total ILC3s in the spleen showed that NCR$^-$ ILC3s but not NCR$^+$ ILC3s were significantly increased in K14 TSLP$^{+/-}$ Rag2$^{-/-}\gamma c^{-/-}$ mice (Fig 39A). Investigation of preFDCs (CD45$^-$ CD140α^+ CD21/35$^-$ CD54$^+$ CD106$^+$) and mature FDCs (CD45$^-$ CD140α^{low} CD21/35$^+$ CD54$^+$ CD106^{low}) in Rag2$^{-/-}\gamma c^{-/-}$ and K14 TSLP$^{+/-}$ Rag2$^{-/-}\gamma c^{-/-}$ mice (Fig. 39B - C) did not show significant differences in numbers (Fig 39C), indicating that FDC development in Rag2$^{-/-}\gamma c^{-/-}$ mice was not controlled by TSLP overexpression or ILC3s.

Taken together, TSLPtg expression has no influence on the absolute cell numbers of stromal subsets in LNs and spleen before transplantation. However, 4 weeks after transplantation, TRCs and LECs were significantly increased in K14 TSLP$^{+/-}$ Rag2$^{-/-}\gamma c^{-/-}$ mice (Fig. 36). This effect is likely due to increased T cell numbers in K14 TSLP$^{+/-}$ Rag2$^{-/-}\gamma c^{-/-}$ mice, since naïve T cells were reported to be sufficient for the induction of TRC expansion[212]. Whether this is the same mechanism for LEC expansion or whether LEC numbers are regulated in a different way by TSLP overexpression during reconstitution remains to be tested.

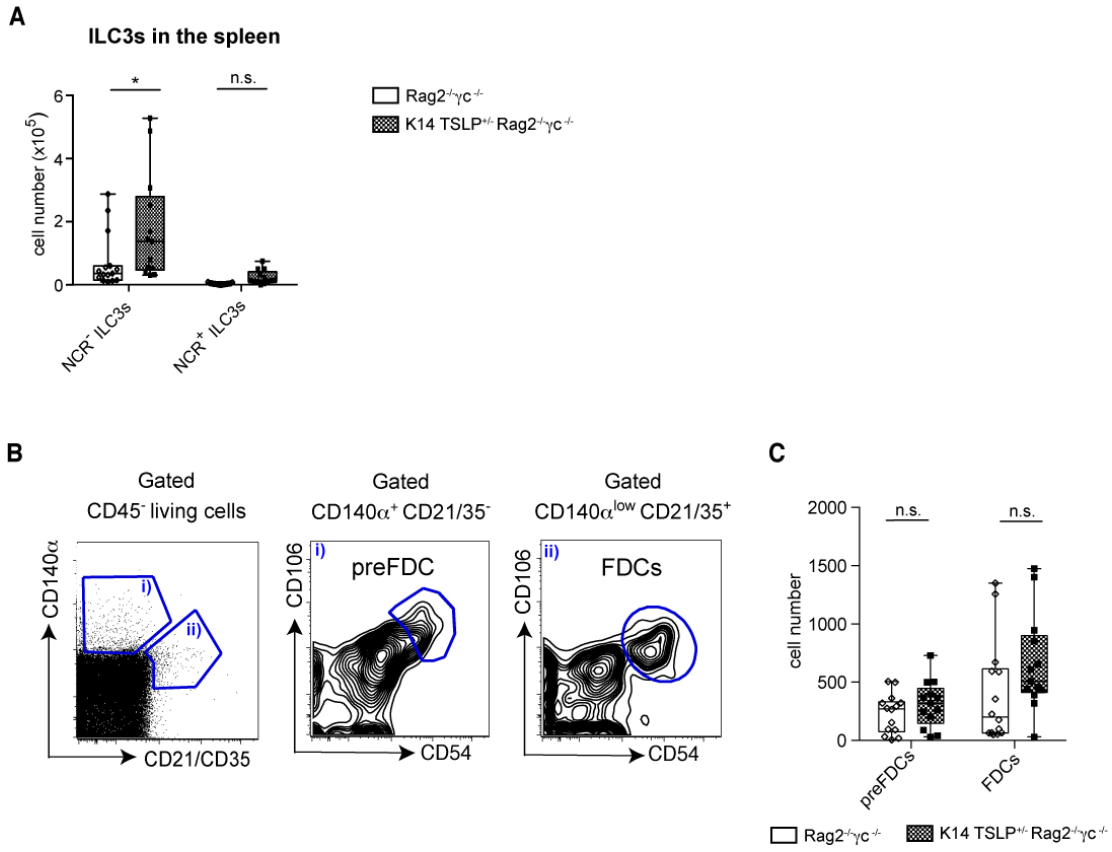

Figure 39: FDCs are not affected by TSLPtg expression: A) Total numbers of NCR$^-$ and NCR$^+$ ILC3s in the spleen; n = 8 - 16 from at least 3 independent experiments; median values + interquartile range; n.s. = not significant, *P<0.05. **B)** Gating strategy for i) FDC precursor (preFDC; CD45$^-$ CD140α^+ CD21/35$^-$ CD54$^+$ CD106$^+$) and ii) FDCs **(**CD45$^-$ CD140α^{low} CD21/35$^+$ CD54$^+$ CD106^{low}). **C)** Total numbers of preFDCs and FDCs in Rag2$^{-/-}\gamma c^{-/-}$ and K14 TSLP$^{+/-}$ Rag2$^{-/-}\gamma c^{-/-}$ mice; n = 8 - 16 from at least 3 independent experiments; median values + interquartile range; n.s. = not significant.

5.3.2 TSLPtg increases T cell proliferation in secondary lymphoid organs

Previous experiments showed that TSLP overexpression increases IL-7 expression in the spleen of $Rag2^{-/-}\gamma c^{-/-}$ mice (Fig. 37C). Since IL-7 promotes T cell proliferation and survival, T cell proliferation was investigated in $Rag2^{-/-}\gamma c^{-/-}$ and K14 $TSLP^{+/-}$ $Rag2^{-/-}\gamma c^{-/-}$ mice. In a first approach, CFSE-labelled $CD4^+$ and $CD8^+$ T cells from $TSLPR^{-/-}$ mice were injected i.v. in a 1:2 ratio. Total T cell numbers and CFSE proliferation was analysed in the spleen, total LNs and BM 4 and 14 days after T cell transfer.

After 4 days, T cells transferred into K14 $TSLP^{+/-}$ $Rag2^{-/-}\gamma c^{-/-}$ mice showed a higher proliferation index in the spleen compared to $Rag2^{-/-}\gamma c^{-/-}$ mice (Fig 40A). While approximately 14% $CD4^+$ T cells were CFSE low or negative in $Rag2^{-/-}\gamma c^{-/-}$ mice, 43% of $CD4^+$ T cells were $CFSE^{low\ /\ neg}$ in TSLP overexpressing mice. $CD8^+$ T cells proliferated generally faster than $CD4^+$ T cells. However, also here TSLP overexpression further enhanced proliferation, since 82% of $CD8^+$ T cells were $CFSE^{low\ /\ neg}$ in K14 $TSLP^{+/-}$ $Rag2^{-/-}\gamma c^{-/-}$ mice compared to 38% in $Rag2^{-/-}\gamma c^{-/-}$ mice (Fig. 40A). In contrast to splenic $CD4^+$ T cells, most of the LN $CD4^+$ T cells were $CFSE^-$ (K14 $TSLP^{+/-}$ $Rag2^{-/-}\gamma c^{-/-}$: 71%; $Rag2^{-/-}\gamma c^{-/-}$: 86%) speaking for a higher proliferation of $CD4^+$ T cells in LNs compared to spleen. However, the proliferation of $CD4^+$ T cells as well as $CD8^+$ T cells did not differ between $Rag2^{-/-}\gamma c^{-/-}$ and K14 $TSLP^{+/-}$ $Rag2^{-/-}\gamma c^{-/-}$ mice (Fig. 40A). Absolute $CD4^+$ and $CD8^+$ T cell numbers in total LNs were significantly higher in K14 $TSLP^{+/-}$ $Rag2^{-/-}\gamma c^{-/-}$ ($CD4^+$: ~ $0.27x10^6$ cells; $CD8^+$: $3.2x10^6$ cells) compared to $Rag2^{-/-}\gamma c^{-/-}$ mice ($CD4^+$: ~ $0.02x10^6$ cells; $CD8^+$: $0.1x10^6$ cells) (Fig. 40B). This difference was most likely due to the fact that LN numbers were increased in K14 $TSLP^{+/-}$ $Rag2^{-/-}\gamma c^{-/-}$ mice, hence naïve T cells had a higher chance to enter LNs. 14 days after T cell transfer, all injected T cells became $CFSE^-$ in both mouse strains (Fig. 40C), indicating that all injected naïve T cells underwent >8 divisions. Analysis 14 days after T cell transfer showed an increase in T cell numbers in both mouse strains compared to the 4 days time point, suggesting ongoing proliferation. However, absolute $CD4^+$ and $CD8^+$ T cell numbers in the spleen and LNs were significantly higher in K14 $TSLP^{+/-}$ $Rag2^{-/-}\gamma c^{-/-}$ mice compared to $Rag2^{-/-}\gamma c^{-/-}$ mice (Fig. 40D).

In summary, TSLP overexpression increases proliferation of T cells leading to higher T cell numbers in LNs. This effect must be driven indirectly by TSLP, since T cells were derived from $TSLPR^{-/-}$ mice.

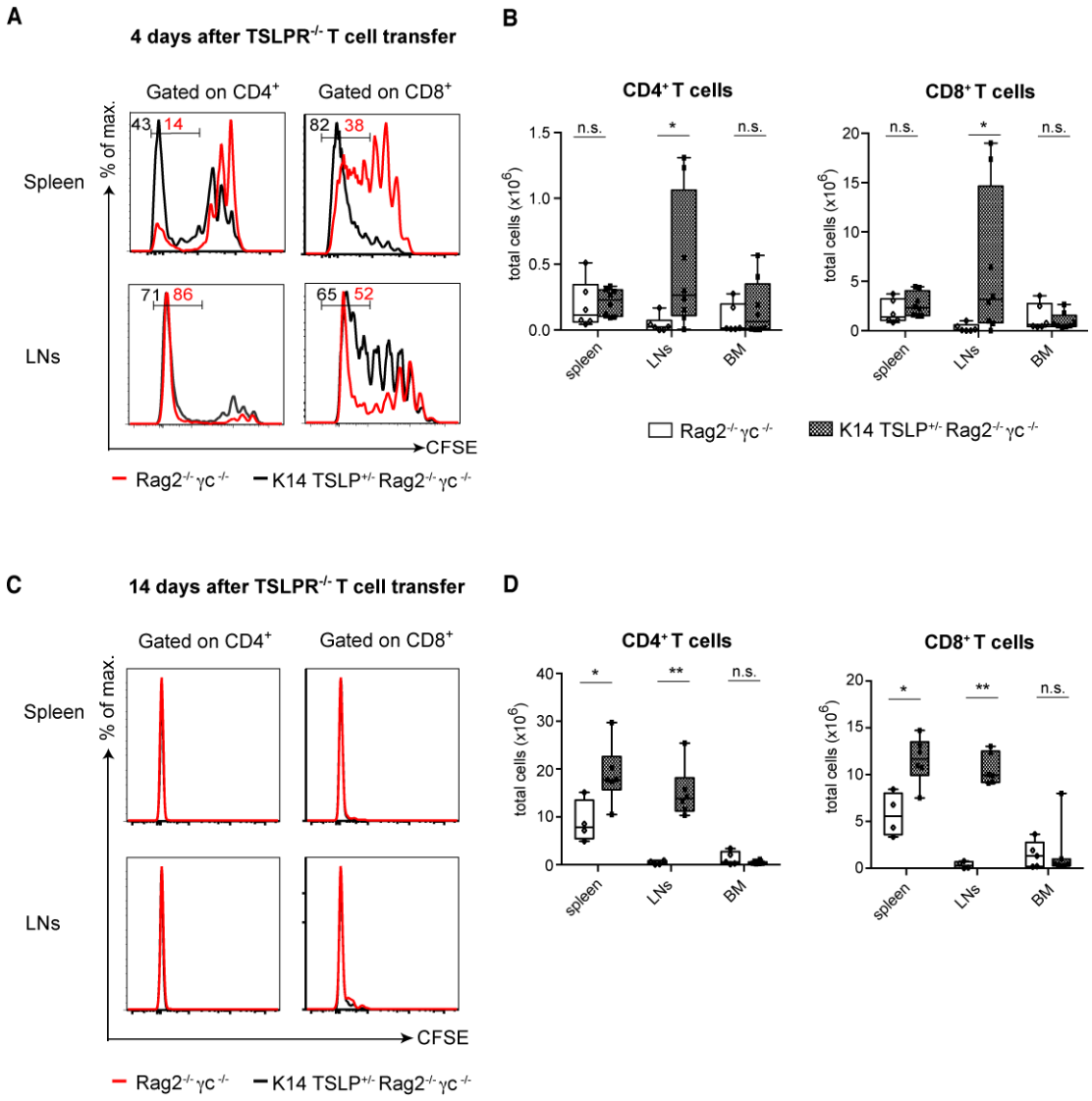

Figure 40: Increased T cell numbers after adoptive T cell transfer by TSLPtg expression. 1x10^7 CFSE - labeled T cells from TSLPR $^{-/-}$ mice were injected into Rag2$^{-/-}$γc$^{-/-}$ and K14 TSLP$^{+/-}$ Rag2$^{-/-}$γc$^{-/-}$ mice. Mice were analysed 4 days and 14 days after transfer **A)** Representative histograms of CD4$^+$ and CD8$^+$ T cell proliferation in the spleen and LNs 4d after T cell transfer. Numbers represent frequencies of CFSE$^{low/-}$ T cells **B)** Total cell numbers of CD4$^+$ and CD8$^+$ T cells in spleen, LNs and BM 4 days after T cell transfer. **C)** Representative histograms of CD4$^+$ and CD8$^+$ T cell proliferation in the spleen and LNs 14 days after T cell transfer **D)** Total numbers of CD4$^+$ and CD8$^+$ T cells in spleen, LNs and BM 14 days after T cell transfer. **A-D**) n = 5 - 8 from 2 independent experiments; n.s. = not significant, *P<0.05, **P<0.01.

To investigate proliferation of naïve T cells, $2x10^6$ sorted naïve ($CD62L^+$ $CD44^{low}$) $CD4^+$ and $CD8^+$ T cells from $TSLPR^{-/-}$ mice were injected i.v. in a 1:2 ratio into $Rag2^{-/-}\gamma c^{-/-}$ and K14 $TSLP^{+/-}$ $Rag2^{-/-}\gamma c^{-/-}$ mice. Total T cell numbers were analysed in spleen, peripheral LNs, BM and thymus 14 or 28 days after T cell transfer. After 14 days, T cell numbers were higher in LNs of K14 $TSLP^{+/-}$ $Rag2^{-/-}\gamma c^{-/-}$ mice ($CD4^+$: ~ $5.5x10^5$ cells; $CD8^+$: ~ $1.3x10^6$ cells) compared to $Rag2^{-/-}\gamma c^{-/-}$ mice ($CD4^+$: ~ $0.5x10^5$ cells; $CD8^+$: $0.1x10^6$ cells) (Fig. 41A). A difference was also observed 28 days after T cell transfer but did not reach statistical significance (Fig. 41B). Although, there was no difference in $CD4^+$ T cell numbers neither in the spleen and LNs nor in the thymus between $Rag2^{-/-}\gamma c^{-/-}$ and K14 $TSLP^{+/-}$ $Rag2^{-/-}\gamma c^{-/-}$ mice (Fig. 41B), TSLP overexpression increased $CD8^+$ T cells in the spleen and thymus (Fig. 41B).

While naïve T cells undergo homeostasis - driven proliferation in lymphopenic hosts, they acquire a memory-like phenotype by down regulating CD62L and up regulating CD44[212]. This was seen 28 days after T cell transfer in the spleen. Beside significantly elevated frequencies of effector memory (EM) in $Rag2^{-/-}\gamma c^{-/-}$ mice compared to K14 $TSLP^{+/-}$ $Rag2^{-/-}\gamma c^{-/-}$ mice, the majority of $CD4^+$ and $CD8^+$ T cells in both mice strains had a memory-like phenotype (Fig. 41C). A similar picture was seen for the $CD4^+$ compartment in the LNs, whereas approximately 40% of $CD8^+$ T cells resembled a naïve phenotype (Fig. 41D).

Taken together, TSLP overexpression increased naïve T cell numbers in LNs of K14 $TSLP^{+/-}$ $Rag2^{-/-}\gamma c^{-/-}$ mice mainly in the early phase of reconstitution. In contrast, TSLP overexpression had only a minor effect on the memory T cell compartment in peripheral lymphoid organs.

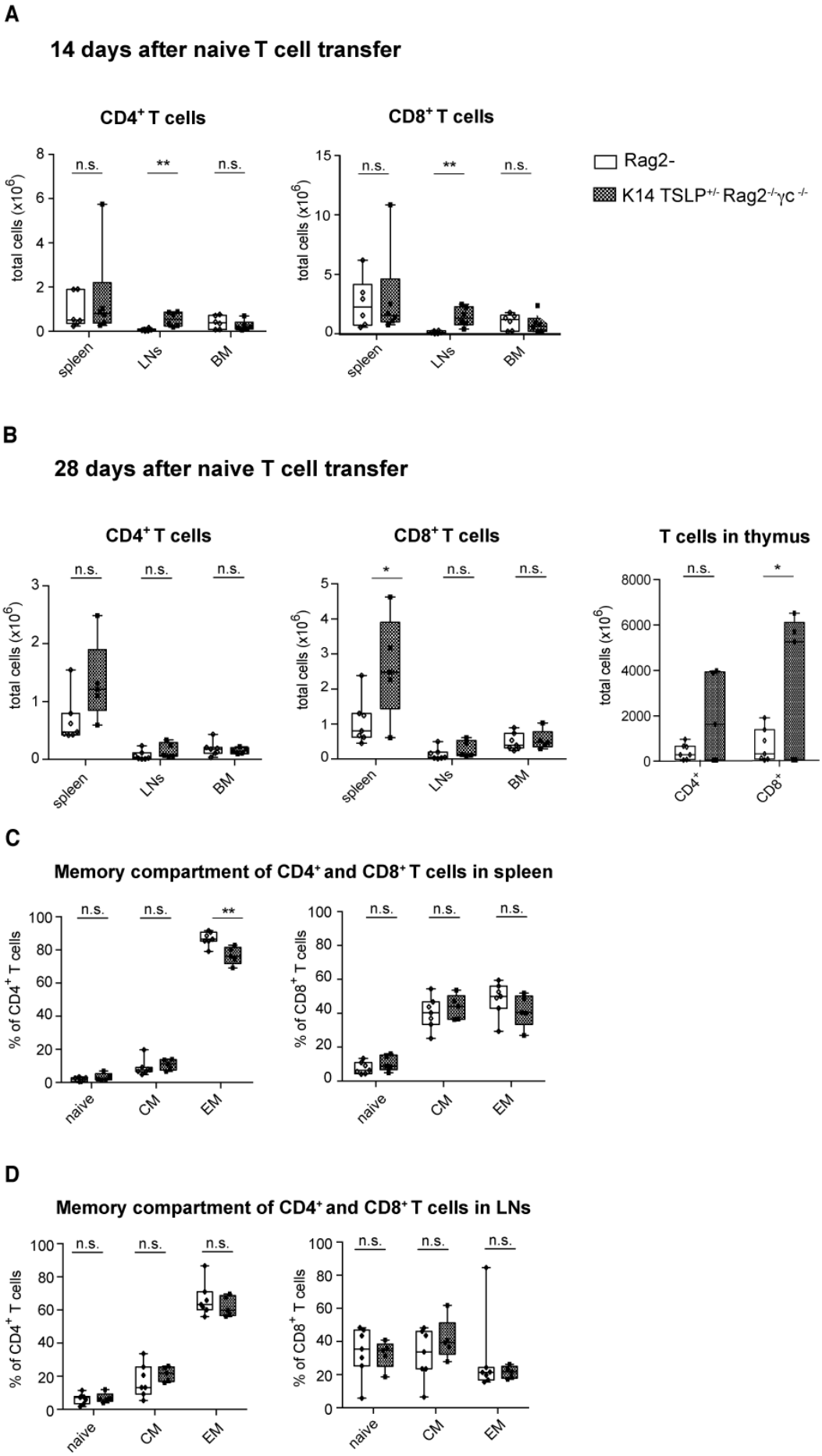
A
14 days after naive T cell transfer
CD4+ T cells
CD8+ T cells
total cells (x10^6)
n.s.
**
n.s.
spleen
LNs
BM
Rag2-
K14 TSLP+/- Rag2-/-γc-/-
B
28 days after naive T cell transfer
CD4+ T cells
CD8+ T cells
T cells in thymus
*
CD4+
CD8+
C
Memory compartment of CD4+ and CD8+ T cells in spleen
% of CD4+ T cells
% of CD8+ T cells
naive
CM
EM
D
Memory compartment of CD4+ and CD8+ T cells in LNs

Figure 41: Naïve T cell transfer into TSLPtg mice increases T cell numbers. $2x10^6$ naïve CFSE - labeled T cells from TSLPR $^{-/-}$ mice were injected into $Rag2^{-/-}\gamma c^{-/-}$ and K14 $TSLP^{+/-}$ $Rag2^{-/-}\gamma c^{-/-}$ mice. Mice were analysed 14 days and 28 days after transfer. **A)** Total cell numbers of $CD4^+$ and $CD8^+$ T cells in spleen, LNs and BM 14 days after naïve T cell ($CD62L^+$ $CD44^{low}$) transfer **B)** Total cell numbers of $CD4^+$ and $CD8^+$ T cells in spleen, LNs, BM and thymus 28d after naïve T cell ($CD62L^+$ $CD44^{low}$) transfer. Frequencies of $CD4^+$ and $CD8^+$ naïve ($CD62L^+$ $CD44^-$), central memory (CM) ($CD62L^+$ $CD44^+$) and effector memory (EM) ($CD62L^-$ $CD44^+$) T cells in **C)** spleen and **D)** LNs, 28d after naïve T cell transfer; **A - D**) n = 5 - 7 from 2 independent experiments; n.s. = not significant, *P<0.05, **P<0.01.

6 Discussion

Despite advances in improving transplantation conditions for patients suffering from immunodeficiency, the re-establishment of a functional immune system after HSCT, which is essential for the patient's life quality and survival, is still a major clinical issue. Especially *de novo* generation of an adequate T cell pool is dependent of pretransplantational conditions. For example, cytotoxic drugs and radiotherapy before transplantation damage the thymic environment, hence perturbing normal T cell development. There are two different strategies to increase T cell numbers after HSCT. Firstly, homeostatic proliferation of donor T cells in the periphery and secondly improvement of *de novo* T cell development in the thymus. Increasing peripheral T cell numbers after HSCT is achieved by homeostatic proliferation of donor T cells which on one hand keep opportunistic and potential pathogens in check but on the other hand increase the risk for GVHD. T cell development in the thymus requires bilateral communication of the lympho – stromal compartment. This interaction ensures correct T cell development and selection as well as development and differentiation of TECs.

ILC3s play an essential role in the development of LNs and have an effect on thymic medulla development before birth. I therefore investigated the effect of a cytokine - driven increase in ILC3 numbers and LNs on the reconstitution of the adaptive immune system after HSCT in immunodeficient mice. To address this question I characterized and reconstituted $Rag2^{-/-}\gamma c^{-/-}$ mice with severe defects in LN development and K14 $TSLP^{+/-}$ $Rag2^{-/-}\gamma c^{-/-}$ mice, which show almost full LN restoration due to increased numbers of ILC3s.

I could show that TSLP overexpression in $Rag2^{-/-}\gamma c^{-/-}$ mice increased the number of DN thymocytes and improved the thymic epithelium architecture with the development of $Aire^{+}$ mTECs in the absence of T cells. Furthermore, T cell reconstitution was accelerated in the thymus and in peripheral organs of K14 $TSLP^{+/-}$ $Rag2^{-/-}\gamma c^{-/-}$ mice after transplantation with FL cells from $TSLPR^{-/-}$ mice. Moreover, I could demonstrate that K14 $TSLP^{+/-}$ $Rag2^{-/-}\gamma c^{-/-}$ mice had higher T cell numbers in secondary lymphoid organs compared to $Rag2^{-/-}\gamma c^{-/-}$ mice. T cells from $TSLPR^{-/-}$ mice showed a higher proliferation rate in the spleen of K14 $TSLP^{+/-}$ $Rag2^{-/-}\gamma c^{-/-}$ compared to $Rag2^{-/-}\gamma c^{-/-}$ mice. This was associated with higher IL-7 mRNA levels in K14 $TSLP^{+/-}$

Rag2$^{-/-}$ γc$^{-/-}$ mice suggesting that IL-7 promoted the relative enrichment of T cells in K14 TSLP$^{+/-}$ Rag2$^{-/-}$ γc$^{-/-}$ either through better survival or proliferation.

6.1 TSLPtg improves thymic stroma and T cell development

Before reconstitution, Rag2$^{-/-}$ γc$^{-/-}$ and K14 TSLP$^{+/-}$ Rag2$^{-/-}$ γc$^{-/-}$ mice were analysed in detail to see the effect of transgenic TSLP overexpression in lymphoid organs.

The characterization of Rag2$^{-/-}$ γc$^{-/-}$ and K14 TSLP$^{+/-}$ Rag2$^{-/-}$ γc$^{-/-}$ thymi confirmed previous published observations that TSLP overexpression in the absence of IL-7 signaling leads to an increase of DN2 and DN3s[180]. DNs are involved in the three-dimensional patterning of the thymus and promote cTEC proliferation and maturation[68,213]. Immunofluorescence analysis in WT showed compartmentalization of the thymus in cortex (CK5^{-} CK8^{+}) and medulla (CK5^{+} CK8^{-}) containing Aire^{+} mTECs. In Rag2$^{-/-}$ γc$^{-/-}$ mice, I found predominantly CK5^{+} CK8^{+} cells. This double positive cell type was recently reported to be a precursor, which gives rise to CK5^{-} CK8^{+} progeny in the cortex in the presence of DN2s and DN3s[214]. These data suggest that CK5^{-} CK8^{+} cells in the thymus of K14 TSLP$^{+/-}$ Rag2$^{-/-}$γc$^{-/-}$ mice are a consequence of elevated numbers of DN2 and DN3s compared to Rag2$^{-/-}$ γc$^{-/-}$ mice. Analysis of TECs by flow cytometry indicated a 9-fold increase in mTEC numbers in K14 TSLP$^{+/-}$ Rag2$^{-/-}$γc$^{-/-}$ mice compared to Rag2$^{-/-}$γc$^{-/-}$ mice. Although mature mTECs are defined as MHC II^{high} [215] in WT, K14 TSLP$^{+/-}$ Rag2$^{-/-}$γc$^{-/-}$ mice showed Aire^{+} mTECs with only intermediate expression levels of MHC II, a phenotype, which might be linked to missing T cell interaction. Nevertheless, while approximately 40% of mTECs in K14 TSLP$^{+/-}$ Rag2$^{-/-}$ γc$^{-/-}$ mice were Aire^{+}, Aire^{+} mTECs were undetectable in Rag2$^{-/-}$ γc$^{-/-}$ mice, which is line with qRT PCR data. These are interesting results because many studies showed the requirement of hematopoietic cells such as mature single positive thymocytes for the development and maintenance of mTECs in the adult system[73,77-79,81,216]. To exclude a direct effect of TSLP overexpression on mTEC development and differentiation in K14 TSLP$^{+/-}$ Rag2$^{-/-}$ γc$^{-/-}$ mice, I performed FTOCs with WT E14.5 thymi. Treatment of FTOCs with RankL could initiate the development of mTECs as published by Rossi et al.[75], whereas FTOCs treated with even high concentrations of TSLP gave no evidence for a direct effect of TSLP on mTEC development.

RankL provided by ILC3s can promote mTEC development[75] and indeed, I observed higher ILC3 numbers in the thymus of K14 TSLP$^{+/-}$ Rag2$^{-/-}$ γc$^{-/-}$ compared to Rag2$^{-/-}$ γc$^{-/-}$ mice. This is in agreement with higher mRNA levels for RankL in total thymi of K14 TSLP$^{+/-}$ Rag2$^{-/-}$ γc$^{-/-}$ mice. However, previous studies[78] and also my data demonstrated that also DN2 and DN3s expressed RankL. To test whether DN3s or adult ILC3s have the capacity to induce mTECs, DN3s and LP - derived ILC3s from Rag2$^{-/-}$ mice were re - aggregated with sorted CD45^{-} TER119^{-} cells from E14.5 WT thymus. LP - derived ILC3s have high RankL expression (unpublished observation F. Lehmann) and revealed a higher potency to promote mTEC development than DN3s, likely due to higher RankL expression. While RTOCs with LP ILC3s resulted in the generation of 10% cTECs and 85% mTECs, RTOCs with DN3s favoured cTEC development and induced only 11% mTECs. There are two possible explanations for the lack of cTECs in RTOCs with LP - ILC3s. First of all, although the initial steps of cTEC development is independent of thymocyte - derived signals[217], later cTEC stages require DN1 - 3 as these cells are known to provide signals for differentiation[213]. As DNs are absent in RTOCs with LP - derived ILC3s, cTECs might die due to missing signals provided by DNs. The second hypothesis involves an additional factor on LP - derived ILC3s, which drives the commitment of common TEC precursors or even immature cTECs into mTEC lineage. The latter hypothesis is supported with my experiments in FTOCs in which RankL application also favoured mTEC development, but showed in addition a clear cTEC population.

In summary, TSLP overexpression does not have a direct effect on mTEC development. However, adult ILC3s and to lesser extent DN3s are able to promote mTEC development *in situ*, whereas DN3s preferentially maintain cTECs. Other molecules reported to be involved in the terminal differentiation of mTECS are LTαβ/LTβR[80]. Since the ligand is expressed by ILC3s, future experiments will help to answer the question whether this pathway is also involved in the improved development of mTECs in RTOCs as well as in the thymus of K14 TSLP$^{+/-}$ Rag2$^{-/-}$ γc$^{-/-}$ mice.

Important factors during T cell development are cytokines and chemokines. They mediate survival and migration of thymocytes within the thymus and are produced by the epithelial and mesenchymal compartment. IL-7 and SCF are important mediators of thymocyte precursor proliferation and differentiation[52,218]. Nevertheless mRNA levels of IL-7 and SCF in total thymus did not differ between Rag2$^{-/-}$ γc$^{-/-}$ and K14 TSLP$^{+/-}$ Rag2$^{-/-}$ γc$^{-/-}$ mice, when normalized to EpCAM or PDGFRα. In contrast, I detected higher levels of CCL25 and CXCL12 in the thymus of

K14 TSLP$^{+/-}$ Rag2$^{-/-}$ γc$^{-/-}$ mice. CCL25 is an important chemoattractant for thymocyte precursors from the blood[60-62], while CXCL12 also favours the expansion of triple negative thymocytes and DP T cells[63,64]. CCL21 is another chemokine important for thymic colonialization. The notion that thymic CCL21 mRNA is decreased in K14 TSLP$^{+/-}$ Rag2$^{-/-}$ γc$^{-/-}$ mice indicates that this chemokine has no role in recruiting more progenitor cells to the thymus of K14 TSLP$^{+/-}$ Rag2$^{-/-}$ γc$^{-/-}$ mice. In line with this, 24h after adoptive transfer of CFSE - labeled BM cells, equal numbers of donor cells were found in thymi of Rag2$^{-/-}$ γc$^{-/-}$ and K14 TSLP$^{+/-}$ Rag2$^{-/-}$ γc$^{-/-}$ mice (data not shown). CCL21 is also produced by mTECs, which increases the accumulation of positively selected thymocytes to the medulla[69]. A previous study identified CCL21^{-} TECs as an immature mTEC precursor, whose differentiation into CCL21^{+} mTECs might be regulated by LTβR and Aire[219]. Since Aire is present in K14 TSLP$^{+/-}$ Rag2$^{-/-}$ γc$^{-/-}$ mice and the ligand LTαβ is expressed by ILC3s[129], one would expect higher CCL21 levels in thymi of K14 TSLP$^{+/-}$ Rag2$^{-/-}$ γc$^{-/-}$ compared to Rag2$^{-/-}$ γc$^{-/-}$ mice. However, it remains to be investigated whether TSLP overexpression has an effect on the CCL21^{-} mTEC population, thereby out diluting CCL21 - expressing cells. This could account for the significant decrease of CCL21 mRNA in K14 TSLP$^{+/-}$ Rag2$^{-/-}$ γc$^{-/-}$ mice.

In K14 TSLP$^{+/-}$ Rag2$^{-/-}$ γc$^{-/-}$ mice, I could show increased IL-22 expression in the thymus. IL-22 is produced by thymic ILC3s and was reported to promote epithelial cell proliferation and survival[160]. Since IL-22 is exclusively produced by ILC3s in lymphopenic mice, the higher IL-22 mRNA level is likely due to the increased number of ILC3s in K14 TSLP$^{+/-}$ Rag2$^{-/-}$ γc$^{-/-}$ mice compared to Rag2$^{-/-}$ γc$^{-/-}$ mice and might contribute to the improved thymic stromal compartment by acting on TECs as proliferation and survival factor.

Concomitant with the improved thymic architecture, K14 TSLP$^{+/-}$ Rag2$^{-/-}$ γc$^{-/-}$ mice had higher numbers of CD4^{+}, CD8^{+} and naturally occuring Tregs (nTregs) in the thymus after HSCT. In addition, K14 TSLP$^{+/-}$ Rag2$^{-/-}$ γc$^{-/-}$ mice had also higher expression levels of Aire - dependent xCL1 in the thymus. xCL1 was reported to attract tDCs to the medulla. In this study the increasing number of self - antigen presenting DCs contributed to nTreg development[220]**.** Another mechanism to foster nTreg development was described for TSLP by upregulating the co - stimulatory molecules CD80 and CD86 on tDCs[221,222]. In line with this, I found increased mRNA levels for CD80 in K14 TSLP$^{+/-}$ Rag2$^{-/-}$ γc$^{-/-}$ mice. However, transcript levels were determined on total thymus including not only potential CD80^{+} tDCs but also CD80^{+} mTECs.

5 weeks after adoptive transfer of fetal liver cells thymocyte numbers were increased in the thymus of K14 TSLP$^{+/-}$ Rag2$^{-/-}$ γc$^{-/-}$ compared to Rag2$^{-/-}$ γc$^{-/-}$ mice. This indicates an accelerated T cell development in mice with increased availability of TSLP. Since donor cells were derived from TSLPR$^{-/-}$ mice, this effect must be indirect. The improved thymic microenvironment in K14 TSLP$^{+/-}$ Rag2$^{-/-}$ γc$^{-/-}$ mice before transplantation might give a reason for the accelerated T cell reconstitution.

6.2 TSLPtg increases T cell reconstitution in secondary lymphoid organs

Besides higher thymocyte numbers in reconstituted K14 TSLP$^{+/-}$ Rag2$^{-/-}$ γc$^{-/-}$ mice, I could also detect higher T cell numbers in secondary lymphoid organs of K14 TSLP$^{+/-}$ Rag2$^{-/-}$ γc$^{-/-}$ mice after HSCT as compared to Rag2$^{-/-}$ γc$^{-/-}$ mice. Like in the thymus, Treg numbers were increased in the spleen, mLN and small intestine of K14 TSLP$^{+/-}$ Rag2$^{-/-}$ γc$^{-/-}$ mice.

Some *in vitro* studies described a role for TSLP conditioned DCs in the generation and proliferation of Tregs, which was associated with upregulation of co - stimulatory molecules on DCs[221,222]. Characterization of CD11c^{+} DCs in the spleen and intestine before transplantation did not show different expression of co - stimulatory molecules CD40, CD80 or CD86. Since also Helios expression on Tregs did not differ between Rag2$^{-/-}$ γc$^{-/-}$ and K14 TSLP$^{+/-}$ Rag2$^{-/-}$ γc$^{-/-}$ mice, there is no evidence for a difference in peripheral Treg induction between Rag2$^{-/-}$ γc$^{-/-}$ and K14 TSLP$^{+/-}$ Rag2$^{-/-}$ γc$^{-/-}$ mice. Therefore, the increase of Tregs in secondary lymphoid organs of K14 TSLP$^{+/-}$ Rag2$^{-/-}$ γc$^{-/-}$ mice most likely reflects the increase in naturally generating Tregs in the thymus.

Homeostatic proliferation of peripheral donor T cells is an important mechanism to restore the T cell compartment directly after HSCT, since *de novo* T cell development in the thymus takes about 3 to 4 weeks[223]. Analysis of reconstituted mice did not allow me to discriminate between expansion of recent thymic emigrants and peripheral T cells, which underwent homeostatic proliferation. Therefore, I studied T cell proliferation by adoptive transfer of mature TSLPR$^{-/-}$ T cells into Rag2$^{-/-}$ γc$^{-/-}$ and K14 TSLP$^{+/-}$ Rag2$^{-/-}$ γc$^{-/-}$ mice.

It is well accepted, that transferred T cells proliferate in lymphopenic mice[224]. The transfer of CFSE - labelled TSLPR$^{-/-}$ T cells showed a higher proliferation profile of

$CD4^+$ and $CD8^+$ T cells in K14 $TSLP^{+/-}$ $Rag2^{-/-}$ $\gamma c^{-/-}$ compared to $Rag2^{-/-}$ $\gamma c^{-/-}$ mice. Proliferation of naïve $CD4^+$ T cells in lymphopenic hosts was reported to have two different mechanisms of proliferation. While homeostatic proliferation is IL-7 dependent and T cells divide not more than once every 2 - 4 days, spontaneous proliferation is antigen driven, IL-7 independent and faster with more than one division per day[225]. In my adoptive T cell experiments, the majority of injected T cells divided >8 times within 14d, indicating that in addition to homeostatic proliferation also spontaneous proliferation occurred presumably driven by foreign antigens from commensal microbiota[226]. Homeostatic proliferation of $CD4^+$ T cells is IL-7 dependent. Therefore, IL-7 mRNA levels were investigated in $Rag2^{-/-}$ $\gamma c^{-/-}$ and K14 $TSLP^{+/-}$ $Rag2^{-/-}$ $\gamma c^{-/-}$ mice. I could not detect differences in mRNA expression in splenic stromal subsets but increased IL-7 mRNA levels in total spleen of K14 $TSLP^{+/-}$ $Rag2^{-/-}$ $\gamma c^{-/-}$ mice. Therefore we focused on DCs, since they were described as IL-7 producers[184,227,228]. Sorted $CD11c^+$ MHC II^+ DCs from the spleen of $Rag2^{-/-}$ $\gamma c^{-/-}$ and K14 $TSLP^{+/-}$ $Rag2^{-/-}$ $\gamma c^{-/-}$ mice did not differ in IL-7 mRNA, but the 4 - fold increase in DC numbers in the spleen of K14 $TSLP^{+/-}$ $Rag2^{-/-}$ $\gamma c^{-/-}$ mice may account for the higher IL-7 levels and hence for better homeostatic proliferation of T cells.

$CD8^+$ T cell proliferation and survival is dependent on IL-7 and IL-15. However, in my studies IL-15 mRNA was not significantly different between $Rag2^{-/-}$ $\gamma c^{-/-}$ and K14 $TSLP^{+/-}$ $Rag2^{-/-}$ $\gamma c^{-/-}$ mice, suggesting that IL-7 and not IL-15 may contribute to the higher proliferation profile and increased number of $CD8^+$ T cells in the spleen of K14 $TSLP^{+/-}$ $Rag2^{-/-}$ $\gamma c^{-/-}$ mice[100,229,230]. Moreover, homeostatic proliferation was more prominent in $CD8^+$ than in $CD4^+$ T cells, which is also reflected in the approximately 10 times higher $CD8^+$ than $CD4^+$ T cell numbers 4d after adoptive T cell transfer. As reported, this effect is not due to differences in IL-7Rα expression or its downstream signaling. It results rather of IL-7 mediated downregulation of MHC II molecules on IL-7Rα^+ DCs, hence reducing TCR / MHC II interactions and proliferation of $CD4^+$ T cells [231].

CD62L is a molecule essential for the migration of mature naïve T cells to LNs. I could show in the adoptive T cell transfer experiments, that K14 $TSLP^{+/-}$ $Rag2^{-/-}$ $\gamma c^{-/-}$ mice had higher T cell numbers in total LNs compared to $Rag2^{-/-}$ $\gamma c^{-/-}$ mice. Since TSLP overexpression could not directly modulate the expression of surface molecules on $TSLPR^{-/-}$ T cells, it is unlikely that this difference is due to changes in CD62L levels. Probably, the higher absolute T cell numbers in total LNs of K14

TSLP$^{+/-}$ Rag2$^{-/-}$ γc$^{-/-}$ mice can be ascribed to increased LN numbers compared to Rag2$^{-/-}$ γc$^{-/-}$ mice.

Adoptive T cell transfer was repeated with sorted naïve T cells. Naïve T cells, which undergo homeostatic proliferation, acquire a phenotype with high CD44 expression levels and functional properties of memory T cells[212]. Also with this approach, K14 TSLP$^{+/-}$ Rag2$^{-/-}$ γc$^{-/-}$ mice had higher T cell numbers after 14d in peripheral LNs compared to Rag2$^{-/-}$ γc$^{-/-}$ mice. However, after 28d only a minor but significant increase of CD8^{+} T cells was seen in the spleen. There was also a significant increase of CD8^{+} T cells in the thymus of K14 TSLP$^{+/-}$ Rag2$^{-/-}$ γc$^{-/-}$ mice, compared to Rag2$^{-/-}$ γc$^{-/-}$ mice. These recirculating T cells might play a beneficial role under transplantation conditions. Donor T cells could support the re - establishment of the recipient thymic microenvironment by maintaining mTECs and presenting peripheral antigens to developing thymocytes, hence contributing to positive as well as negative selection of thymocytes[232,233].

The frequency of naïve and memory T cells in the LNs between Rag2$^{-/-}$ γc$^{-/-}$ and K14 TSLP$^{+/-}$ Rag2$^{-/-}$ γc$^{-/-}$ mice after naïve T cell transfer was equal. While in WT mice more than 60% of T cells have a CD44^{-} naïve phenotype[234,235], reconstituted Rag2$^{-/-}$ γc$^{-/-}$ and K14 TSLP$^{+/-}$ Rag2$^{-/-}$ γc$^{-/-}$ mice showed a higher percentage of memory cells, which is reported for T cells undergoing proliferation in lymphopenic hosts[212,236]. In the spleen, there was a significant decrease in the CD4^{+} effector memory compartment of K14 TSLP$^{+/-}$ Rag2$^{-/-}$ γc$^{-/-}$ mice. As there was no difference in naïve or central memory T cells, it is likely that TSLP overexpression has an effect on a memory compartment, which is not described.

An increase in T cell survival rate could account for the increase of peripheral T cells in K14 TSLP$^{+/-}$ Rag2$^{-/-}$ γc$^{-/-}$ mice after HSCT. T cell survival is influenced by signals through TCR / MHC interaction and co - stimulatory molecules or through cytokines such as IL-2 and IL-7 [237,238]. Since IL-7 is produced by DCs, I investigated DC numbers after reconstitution in Rag2$^{-/-}$ γc$^{-/-}$ and K14 TSLP$^{+/-}$ Rag2$^{-/-}$ γc$^{-/-}$ mice. However, the number of CD11c^{+} DCs did not differ between Rag2$^{-/-}$ γc$^{-/-}$ mice and K14 TSLP$^{+/-}$ Rag2$^{-/-}$ γc$^{-/-}$ mice. This suggests, that TCR / self - antigen driven survival as well as increased IL-7 availability due to higher DC numbers do not account for higher T cell numbers in secondary lymphoid organs. However, to test directly the T cell survival rate, one could consider to inject T cells from a Bcl-2tg mouse on a TSLPR$^{-/-}$ background into Rag2$^{-/-}$ γc$^{-/-}$ and K14 TSLP$^{+/-}$ Rag2$^{-/-}$ γc$^{-/-}$ mice. With this approach, all T cell subsets have the same base line of survival and the role of ILC3s and secondary lymphoid organs on T cell survival could be investigated.

Taken together, the better peripheral T cell reconstitution in K14 TSLP$^{+/-}$ Rag2$^{-/-}$ γc$^{-/-}$ mice after HSC transplantation compared to Rag2$^{-/-}$ γc$^{-/-}$ mice is the interplay of several mechanisms. Due to an improved state of maturation and architecture of the thymus in K14 TSLP$^{+/-}$ Rag2$^{-/-}$ γc$^{-/-}$ mice, the thymus produces faster T cells, which leads to a higher thymic output in week 5 and 6 after HSCT. Analysis of brachial LNs in Rag2$^{-/-}$ γc$^{-/-}$ mice and K14 TSLP$^{+/-}$ Rag2$^{-/-}$ γc$^{-/-}$ mice 4 weeks after HSCT demonstrated that the absolute numbers of TRCs and LECs were higher in K14 TSLP$^{+/-}$ Rag2$^{-/-}$ γc$^{-/-}$ mice. As TRC and LECs are important IL-7 producers[109], it could be assumed that the overall availability of these cytokines is higher in LNs of K14 TSLP$^{+/-}$ Rag2$^{-/-}$ γc$^{-/-}$ mice compared to Rag2$^{-/-}$ γc$^{-/-}$ mice and could account for better homeostatic proliferation and survival of T cells.

6.3 TSLPtg increases ILC3 numbers in the intestine, which provide an anti – inflammatory environment

GVHD is a clinical issue and responsible for increased morbidity and mortality after HSCT[239]. During acute GVHD, alloreactive T cells activated against recipient antigens attack several organs such as skin, liver and gastrointestinal tract. In this setting IL-22 was reported to have beneficial effects on the intestinal mucosa protecting epithelial cells and intestinal stem cells from graft - versus - host mediated injury after bone marrow transplantation[159]. In line with this observation, IL-22 was further described to play a protective role in infection models with *Citrobacter rodentium*[152,240] and *Salmonella enterica*[241] as well as protect intestinal epithelial cells during inflammatory bowel disease (IBD) and colitis by providing a signal for epithelial cell survival, proliferation, and wound healing[242].

TSLP overexpression increases the total number of ILC3s in the intestine. ILC3s were reported to directly regulate immune homeostasis in the intestine. By presenting microbiota - derived peptides via MHC II, ILC3s induce apoptotic cell death of commensal bacteria - specific T cells similar to negative T cell selection in the thymus[243]. Besides mediating intestinal selection, ILC3s are important cytokine producers. They produce IL-22 but are also able to secrete the pro - inflammatory cytokine IL-17. Flow cytometric analysis demonstrated that TSLP overexpression had no influence on IL-22 or IL-17 production of ILC3s compared to Rag2$^{-/-}$ γc$^{-/-}$ mice. However, associated with increased numbers of ILC3s, IL-22 mRNA level was 24 times higher in K14 TSLP$^{+/-}$ Rag2$^{-/-}$ γc$^{-/-}$ mice compared to Rag2$^{-/-}$ γc$^{-/-}$ mice. IL-22 is also required for the induction of anti – microbial peptide expression in epithelial cells[151], which have anti - bacterial activity. My data showed that K14 TSLP$^{+/-}$ Rag2$^{-/-}$ γc$^{-/-}$ mice have a 2.5 and 3 fold increase in Reg3β and Reg3γ, respectively.

Besides the beneficial aspects on the intestinal epithelium, IL-22 can also act as pro - inflammatory mediator in diseases such as psoriasis and rheumatoid arthritis[244,245]. Collectively, the dual nature of IL-22 likely depends on the tissues, the cytokine milieu and the amount and duration of IL-22 presence. Therefore, it is important to have regulatory mechanisms, which control IL-22 availability. A natural regulator of IL-22 is the soluble receptor IL-22Rα2[246,247], which is secreted from a subset of immature DCs. It is most prominent under steady state conditions and not under inflammatory conditions, as mature DCs downregulate IL-22Rα2 expression[248]. Since K14 TSLP$^{+/-}$ Rag2$^{-/-}$ γc$^{-/-}$ mice have elevated numbers of IL-22 producing ILC3s, we analysed the mRNA expression of the IL-22 binding protein IL-22Rα2. The

39 - fold increase of IL-22Rα2 mRNA expression in K14 TSLP$^{+/-}$ Rag2$^{-/-}$ γc$^{-/-}$ mice is associated with higher DC numbers in the small intestine compared to Rag2$^{-/-}$ γc$^{-/-}$ mice. This indicates, that IL-22 is also tightly regulated in TSLP overexpressing mice, which reduces the risk for immunopathology. Whether levels of IL-22 and IL-22Rα2 are still significantly increased in K14 TSLP$^{+/-}$ Rag2$^{-/-}$ γc$^{-/-}$ compared to Rag2$^{-/-}$ γc$^{-/-}$ mice or alter after reconstitution remains to be investigated.

Taken together, increased numbers of ILC3s in K14 TSLP$^{+/-}$ Rag2$^{-/-}$ γc$^{-/-}$ mice together with higher Treg numbers in the small intestine, as discussed in 6.2, provides an anti – inflammatory environment, which could protect the intestinal epithelial cells by reducing the risk of GVHD and bacterial pathogens after HSCT.

6.4 TSLP as therapeutic treatment?

Treatments to improve T cell reconstitution after HSCT follows two strategies: Either by direct targeting of T cell development and proliferation with cytokines like IL-7 or IL-2 or by improving the niches mainly by stimulating the proliferation and repair of epithelial cells by e.g. KGF and IL-22[249]. The beneficial effects of cytokines are often limited and accompanied by severe side effects. IL-7 for instance is implicated in multiple autoimmune diseases[250-252] due to enhanced proliferative responses to self - antigens during lymphopenia. With this study I show the potential of TSLP as an alternative cytokine to improve the thymic microenvironment as well as the niches in secondary lymphoid organs without affecting adaptive immune cells directly. This raises the question whether TSLP is a candidate for therapeutic treatment after HSCT. My study demonstrates clear advantages of TSLP overexpression on *de novo* T cell development and peripheral T cell proliferation. However, there are also pathological issues associated with TSLP expression. TSLP is preferentially released by epithelial cells of different organs such as lung, intestine and skin and multiple studies assessed an important role for TSLP in triggering allergic airway diseases and dermatitis in the presence of antigen [189,202,253-256]. Naive CD4^{+} T cells, which were primed by TSLP conditioned DCs polarize towards Th2 phenotype, hence generating Th2 mediated diseases like allergy and asthma. Another cell type, which is associated with allergic diseases and promoting inflammation in the intestine are ILC2s, which can be activated by TSLP [257-259]. K14 TSLP$^{+/-}$ Rag2$^{-/-}$ γc$^{-/-}$ mice have also increased numbers of ILC2 in the intestine.

This together with Th2 polarized T cells after reconstitution might increase inflammatory conditions. Therefore, future experiments are needed to investigate Th cell subsets and the cytokine milieu in different organs to exclude that TSLP overexpression creates an inflammatory environment.

In order to avoid polarization of T cells towards Th2 cells one could consider the application of TSLP under sterile conditions after cytotoxic treatment and radiotherapy in patients before HSCT. This treatment would probably have the potential to amplify ILC numbers in patients with a common γ chain deficiency. In mice, ILC3 development from the BM transplants takes about 3 - 4 weeks[204]. It remains to be investigated in humans whether this time is sufficient for therapeutic TSLP - mediated improvement of thymus, peripheral lymph node and mucosal epithelial cell function.

Translating results from mouse studies into the human system is subjected to limitations because of genetic differences e.g. cell marker expression between these two species. To be closer to the human system, there are recent advances in the development of humanized mouse models. In these models, human genes or human HSCs are introduced into mice, which gives the possibility to study the human immune system in a small animal model[260]. In case of studying the role of ILC3s and secondary lymphoid organs on the reconstitution of the adaptive immune system, one could engraft human HSCs into $Rag2^{-/-}\gamma c^{-/-}$ and K14 $TSLP^{+/-}$ $Rag2^{-/-}\gamma c^{-/-}$ mice. As murine and human TSLP share only 43% amino acid identity, it is unlikely that human $TSLPR^{+}$ cells respond directly to murine TSLP. With this approach I could study whether the reconstitution of human T cells is also increased due to the restoration of lymphoid niches by TSLP overexpression. This would open a new way of pre - transplantational treatment to improve the outcome of HSCT.

References

1 Parkin, J. & Cohen, B. An overview of the immune system. *Lancet* **357**, 9270, 1777-1789, (2001).

2 Luckheeram, R. V., Zhou, R., Verma, A. D. & Xia, B. CD4(+)T cells: differentiation and functions. *Clin Dev Immunol* **2012**, 925135, (2012).

3 Janeway, C. A., Jr. & Medzhitov, R. Innate immune recognition. *Annu Rev Immunol* **20**, 197-216, (2002).

4 Georgopoulos, K., Moore, D. D. & Derfler, B. Ikaros, an early lymphoid-specific transcription factor and a putative mediator for T cell commitment. *Science* **258**, 5083, 808-812, (1992).

5 Candotti, F., Notarangelo, L., Visconti, R. & O'Shea, J. Molecular aspects of primary immunodeficiencies: lessons from cytokine and other signaling pathways. *Journal of Clinical Investigation* **109**, 10, 1261-1269, (2002).

6 Copelan, E. Hematopoietic Stem-Cell Transplantation. *N Engl J Med* **354**, 1813-1826, (2006).

7 Passweg, J. R. *et al.* Hematopoietic stem cell transplantation: a review and recommendations for follow-up care for the general practitioner. *Swiss Med Wkly* **142**, w13696, (2012).

8 Koreth J, S. R., Kopecky KJ, Honda S, Sierra J, et al. Allogeneic stem cell transplantation for acute myeloid leukemia in first complete remission: systematic review and meta-analysis of prospective clinical trials. *JAMA* **301**, 2349-2361, (2009).

9 Weinberg, K. I. *et al.* Hematopoietic stem cell transplantation for severe combined immune deficiency. *Curr Allergy Asthma Rep* **1**, 5, 416-420, (2001).

10 Cavazzana-Calvo M, A.-S. I., Dal Cortivo L, Neven B, & Hacein-Bey-Abina S, F. A. Immune reconstitution after haematopoietic stem cell transplantation: obstacles and anticipated progress. *Curr Opin Immunol* **21**, 544-548, (2009).

11 Crooks, G. M., Weinberg, K. & Mackall, C. Immune reconstitution: from stem cells to lymphocytes. *Biol Blood Marrow Transplant* **12**, 1 Suppl 1, 42-46, (2006).

12 Seggewiss, R. & Einsele, H. Immune reconstitution after allogeneic transplantation and expanding options for immunomodulation: an update. *Blood* **115**, 19, 3861-3868, (2010).

13 Ochs, L. *et al.* Late infections after allogeneic bone marrow transplantations: comparison of incidence in related and unrelated donor transplant recipients. *Blood* **86**, 10, 3979-3986, (1995).

14 Robin, M. *et al.* Risk factors for late infections after allogeneic hematopoietic stem cell transplantation from a matched related donor. *Biol Blood Marrow Transplant* **13**, 11, 1304-1312, (2007).

15 Neven, B. *et al.* Long-term outcome after hematopoietic stem cell transplantation of a single-center cohort of 90 patients with severe combined immunodeficiency. *Blood* **113**, 17, 4114-4124, (2009).

16 Marie-Cardine, A. *et al.* Transitional B cells in humans: characterization and insight from B lymphocyte reconstitution after hematopoietic stem cell transplantation. *Clin Immunol* **127**, 1, 14-25, (2008).

17 Alpdogan, O. *et al.* Keratinocyte growth factor (KGF) is required for postnatal thymic regeneration. *Blood* **107**, 6, 2453-2460, (2006).

18 Min, D. *et al.* Protection from thymic epithelial cell injury by keratinocyte growth factor: a new approach to improve thymic and peripheral T-cell

reconstitution after bone marrow transplantation. *Blood* **99**, 12, 4592-4600, (2002).
19 Rossi, S. *et al.* Keratinocyte growth factor preserves normal thymopoiesis and thymic microenvironment during experimental graft-versus-host disease. *Blood* **100**, 2, 682-691, (2002).
20 Kennedy-Nasser, A. A. *et al.* Ultra Low-Dose IL-2 for GVHD Prophylaxis after Allogeneic Hematopoietic Stem Cell Transplantation Mediates Expansion of Regulatory T Cells without Diminishing Antiviral and Antileukemic Activity. *Clinical Cancer Research* **20**, 8, 2215-2225, (2014).
21 Perales, M. A. *et al.* Recombinant human interleukin-7 (CYT107) promotes T-cell recovery after allogeneic stem cell transplantation. *Blood* **120**, 24, 4882-4891, (2012).
22 Chen, B. J., Cui, X., Sempowski, G. D. & Chao, N. J. Growth hormone accelerates immune recovery following allogeneic T-cell-depleted bone marrow transplantation in mice. *Exp Hematol* **31**, 10, 953-958, (2003).
23 Sutherland, J. S. *et al.* Enhanced immune system regeneration in humans following allogeneic or autologous hemopoietic stem cell transplantation by temporary sex steroid blockade. *Clin Cancer Res* **14**, 4, 1138-1149, (2008).
24 Riddell, S. R., Bleakley, M., Nishida, T., Berger, C. & Warren, E. H. Adoptive transfer of allogeneic antigen-specific T cells. *Biol Blood Marrow Transplant* **12**, 1 Suppl 1, 9-12, (2006).
25 Le Blanc, K. *et al.* Transplantation of mesenchymal stem cells to enhance engraftment of hematopoietic stem cells. *Leukemia* **21**, 8, 1733-1738, (2007).
26 Belizário, J. E. Immunodeficient Mouse Models: An Overview. *The Open Immunology Journal* **2**, 79-85, (2009).
27 Seymour, R., Sundberg, J. P. & Hogenesch, H. Abnormal lymphoid organ development in immunodeficient mutant mice. *Vet Pathol* **43**, 4, 401-423, (2006).
28 Carsetti, R. The development of B cells in the bone marrow is controlled by the balance between cell-autonomous mechanisms and signals from the microenvironment. *Journal of Experimental Medicine* **191**, 1, 5-8, (2000).
29 Carvalho, T. L., Mota-Santos, T., Cumano, A., Demengeot, J. & Vieira, P. Arrested B lymphopoiesis and persistence of activated B cells in adult interleukin 7(-/-) mice. *Journal of Experimental Medicine* **194**, 8, 1141-1150, (2001).
30 Peschon, J. J. *et al.* Early Lymphocyte Expansion Is Severely Impaired in Interleukin-7 Receptor-Deficient Mice. *Journal of Experimental Medicine* **180**, 5, 1955-1960, (1994).
31 Sitnicka, E. *et al.* Key role of flt3 ligand in regulation of the common lymphoid progenitor but not in maintenance of the hematopoietic stem cell pool. *Immunity* **17**, 4, 463-472, (2002).
32 Sudo, T. *et al.* Interleukin 7 production and function in stromal cell-dependent B cell development. *J Exp Med* **170**, 1, 333-338, (1989).
33 von Freeden jeffry, U. *et al.* Lymphopenia in Interleukin (Il)-7 Gene-Deleted Mice Identifies Il-7 as a Nonredundant Cytokine. *Journal of Experimental Medicine* **181**, 4, 1519-1526, (1995).
34 Waskow, C., Paul, S., Haller, C., Gassmann, M. & Rodewald, H. R. Viable c-Kit(W/W) mutants reveal pivotal role for c-kit in the maintenance of lymphopoiesis. *Immunity* **17**, 3, 277-288, (2002).
35 Nemazee, D. A. & Burki, K. Clonal deletion of B lymphocytes in a transgenic mouse bearing anti-MHC class I antibody genes. *Nature* **337**, 6207, 562-566, (1989).
36 Cambier, J. C., Gauld, S. B., Merrell, K. T. & Vilen, B. J. B-cell anergy: from transgenic models to naturally occurring anergic B cells? *Nat Rev Immunol* **7**, 8, 633-643, (2007).

37 Sukumar, S. & Schlissel, M. S. Receptor Editing as a Mechanism of B Cell Tolerance. *Journal of Immunology* **186**, 3, 1301-1302, (2011).

38 Ceredig, R. & Rolink, T. A positive look at double-negative thymocytes. *Nature Reviews Immunology* **2**, 11, 888-896, (2002).

39 Cerutti, A., Cols, M. & Puga, I. Marginal zone B cells: virtues of innate-like antibody-producing lymphocytes. *Nature Reviews Immunology* **13**, 2, 118-132, (2013).

40 Martin, F. & Kearney, J. F. Marginal-zone B cells. *Nat Rev Immunol* **2**, 5, 323-335, (2002).

41 Allman, D. & Pillai, S. Peripheral B cell subsets. *Curr Opin Immunol* **20**, 2, 149-157, (2008).

42 Ribatti, D., Crivellato, E. & Vacca, A. Miller's seminal studies on the role of thymus in immunity. *Clin Exp Immunol* **144**, 3, 371-375, (2006).

43 Takahama, Y. Journey through the thymus: stromal guides for T-cell development and selection. *Nature Reviews Immunology* **6**, 2, 127-135, (2006).

44 Gill, J. *et al.* Thymic generation and regeneration. *Immunol Rev* **195**, 28-50, (2003).

45 van Ewijk, W. *et al.* Thymic microenvironments, 3-D versus 2-D? *Semin Immunol* **11**, 1, 57-64, (1999).

46 Klug, D. B., Carter, C., Gimenez-Conti, I. B. & Richie, E. R. Cutting edge: thymocyte-independent and thymocyte-dependent phases of epithelial patterning in the fetal thymus. *J Immunol* **169**, 6, 2842-2845, (2002).

47 Lee, E. N. *et al.* Characterization of the expression of cytokeratins 5, 8, and 14 in mouse thymic epithelial cells during thymus regeneration following acute thymic involution. *Anat Cell Biol* **44**, 1, 14-24, (2011).

48 Derbinski, J., Schulte, A., Kyewski, B. & Klein, L. Promiscuous gene expression in medullary thymic epithelial cells mirrors the peripheral self. *Nat Immunol* **2**, 11, 1032-1039, (2001).

49 Farr, A. G. & Rudensky, A. Medullary thymic epithelium: a mosaic of epithelial "self"? *J Exp Med* **188**, 1, 1-4, (1998).

50 Koble, C. & Kyewski, B. The thymic medulla: a unique microenvironment for intercellular self-antigen transfer. *J Exp Med* **206**, 7, 1505-1513, (2009).

51 Nagamine, K. *et al.* Positional cloning of the APECED gene. *Nat Genet* **17**, 4, 393-398, (1997).

52 Godfrey, D. I., Zlotnik, A. & Suda, T. Phenotypic and Functional-Characterization of C-Kit Expression during Intrathymic T-Cell Development. *Journal of Immunology* **149**, 7, 2281-2285, (1992).

53 Palmer, E. & Naeher, D. Affinity threshold for thymic selection through a T-cell receptor-co-receptor zipper. *Nature Reviews Immunology* **9**, 3, 206-212, (2009).

54 Coquet, J. M. *et al.* Epithelial and dendritic cells in the thymic medulla promote CD4+Foxp3+ regulatory T cell development via the CD27-CD70 pathway. *J Exp Med* **210**, 4, 715-728, (2013).

55 Yui, M. A. & Rothenberg, E. V. Developmental gene networks: a triathlon on the course to T cell identity. *Nat Rev Immunol* **14**, 8, 529-545, (2014).

56 Radtke, F. *et al.* Deficient T cell fate specification in mice with an induced inactivation of Notch1. *Immunity* **10**, 5, 547-558, (1999).

57 Wolfer A, W. A., Nemir M, MacDonald HR, Radtke F. Inactivation of Notch1 impairs VDJbeta rearrangement and allows pre-TCR-independent survival of early alpha beta Lineage Thymocytes. *Immunity* **22**, 3, 155-160, (2002).

58 Massa, S., Balciunaite, G., Ceredig, R. & Rolink, A. G. Critical role for c-kit (CD117) in T cell lineage commitment and early thymocyte development in vitro. *Eur J Immunol* **36**, 3, 526-532, (2006).

59 Rodewald, H. R., Kretzschmar, K., Swat, W. & Takeda, S. Intrathymically Expressed C-Kit Ligand (Stem-Cell Factor) Is a Major Factor Driving Expansion of Very Immature Thymocytes in-Vivo. *Immunity* **3**, 3, 313-319, (1995).

60 Bleul CC, B. T. Chemokines define distinct microenvironments in the developing thymus. *Eur J Immunol.* **30**, 12, 3371-3379, (2000).

61 Liu, C. L. *et al.* Coordination between CCR7-and CCR9-mediated chemokine signals in prevascular fetal thymus colonization. *Blood* **108**, 8, 2531-2539, (2006).

62 Wurbel, M. A. *et al.* Mice lacking the CCR9 CC-chemokine receptor show a mild impairment of early T- and B-cell development and a reduction in T-cell receptor gammadelta(+) gut intraepithelial lymphocytes. *Blood* **98**, 9, 2626-2632, (2001).

63 Ara, T. *et al.* A role of CXC chemokine ligand 12/stromal cell-derived factor-1/pre-B cell growth stimulating factor and its receptor CXCR4 in fetal and adult T cell development in vivo. *J Immunol* **170**, 9, 4649-4655, (2003).

64 Plotkin, J., Prockop, S. E., Lepique, A. & Petrie, H. T. Critical role for CXCR4 signaling in progenitor localization and T cell differentiation in the postnatal thymus. *J Immunol* **171**, 9, 4521-4527, (2003).

65 Lind, E. F., Prockop, S. E., Porritt, H. E. & Petrie, H. T. Mapping precursor movement through the postnatal thymus reveals specific microenvironments supporting defined stages of early lymphoid development. *Journal of Experimental Medicine* **194**, 2, 127-134, (2001).

66 Ueno, T. *et al.* CCR7 signals are essential for cortex-medulla migration of developing thymocytes. *J Exp Med* **200**, 4, 493-505, (2004).

67 Ueno, T. *et al.* Role for CCR7 ligands in the emigration of newly generated T lymphocytes from the neonatal thymus. *Immunity* **16**, 2, 205-218, (2002).

68 Holländer, G. A., Wang, B., Nichogiannopoulou, A., Platenburg, P. P., van Ewijk, W., Burakoff, S. J., Gutierrez-Ramos, J. C., and Terhorst, C. Developmental control point in induction of thymic cortex regu- lated by a subpopulation of prothymocytes. *Nature* **373**, 6512, 350-353, (1995).

69 Nitta, T., Ohigashi, I., Nakagawa, Y. & Takahama, Y. Cytokine crosstalk for thymic medulla formation. *Curr Opin Immunol* **23**, 2, 190-197, (2011).

70 Shores, E. W., Van Ewijk, W. & Singer, A. Disorganization and restoration of thymic medullary epithelial cells in T cell receptor-negative scid mice: evidence that receptor-bearing lymphocytes influence maturation of the thymic microenvironment. *Eur J Immunol* **21**, 7, 1657-1661, (1991).

71 Buckley, R. H. Molecular defects in human severe combined immunodeficiency and approaches to immune reconstitution. *Annual Review of Immunology* **22**, 625-655, (2004).

72 Lomada, D., Liu, B., Coghlan, L., Hu, Y. & Richie, E. R. Thymus medulla formation and central tolerance are restored in IKKalpha-/- mice that express an IKKalpha transgene in keratin 5+ thymic epithelial cells. *J Immunol* **178**, 2, 829-837, (2007).

73 Boehm, T., Scheu, S., Pfeffer, K. & Bleul, C. C. Thymic medullary epithelial cell differentiation, thymocyte emigration, and the control of autoimmunity require lympho-epithelial cross talk via LTbetaR. *J Exp Med* **198**, 5, 757-769, (2003).

74 Zhu, M. & Fu, Y. X. Coordinating development of medullary thymic epithelial cells. *Immunity* **29**, 3, 386-388, (2008).

75 Rossi, S. W. *et al.* RANK signals from CD4(+)3(-) inducer cells regulate development of Aire-expressing epithelial cells in the thymic medulla. *J Exp Med* **204**, 6, 1267-1272, (2007).

76 Roberts, N. A. *et al.* Rank signaling links the development of invariant gammadelta T cell progenitors and Aire(+) medullary epithelium. *Immunity* **36**, 3, 427-437, (2012).

77 Akiyama, T. *et al.* The tumor necrosis factor family receptors RANK and CD40 cooperatively establish the thymic medullary microenvironment and self-tolerance. *Immunity* **29**, 3, 423-437, (2008).

78 Hikosaka, Y. *et al.* The cytokine RANKL produced by positively selected thymocytes fosters medullary thymic epithelial cells that express autoimmune regulator. *Immunity* **29**, 3, 438-450, (2008).

79 Irla, M. *et al.* Autoantigen-specific interactions with CD4+ thymocytes control mature medullary thymic epithelial cell cellularity. *Immunity* **29**, 3, 451-463, (2008).

80 White, A. J. *et al.* Lymphotoxin signals from positively selected thymocytes regulate the terminal differentiation of medullary thymic epithelial cells. *J Immunol* **185**, 8, 4769-4776, (2010).

81 White, A. J. *et al.* Sequential phases in the development of Aire-expressing medullary thymic epithelial cells involve distinct cellular input. *Eur J Immunol* **38**, 4, 942-947, (2008).

82 Bettelli, E., Korn, T., Oukka, M. & Kuchroo, V. K. Induction and effector functions of T(H)17 cells. *Nature* **453**, 7198, 1051-1057, (2008).

83 O'garra, A. T-cell differentiation: Commitment factors for T helper cells. *Current Biology* **10**, 13, R492-R494, (2000).

84 Okazawa, A. *et al.* Th1-mediated intestinal inflammation in Crohn's disease may be induced by activation of lamina propria lymphocytes through synergistic stimulation of interleukin-12 and interleukin-18 without T cell receptor engagement. *American Journal of Gastroenterology* **97**, 12, 3108-3117, (2002).

85 Leung, B. P., McInnes, I. B., Esfandiari, E., Wei, X. Q. & Liew, F. Y. Combined effects of IL-12 and IL-18 on the induction of collagen-induced arthritis. *J Immunol* **164**, 12, 6495-6502, (2000).

86 Swain, S. L., Weinberg, A. D., English, M. & Huston, G. IL-4 directs the development of Th2-like helper effectors. *J Immunol* **145**, 11, 3796-3806, (1990).

87 Ito, T. *et al.* TSLP-activated dendritic cells induce an inflammatory T helper type 2 cell response through OX40 ligand. *J Exp Med* **202**, 9, 1213-1223, (2005).

88 Kitajima, M., Lee, H. C., Nakayama, T. & Ziegler, S. F. TSLP enhances the function of helper type 2 cells. *Eur J Immunol* **41**, 7, 1862-1871, (2011).

89 Finkelman, F. D., Pearce, E. J., Urban, J. F., Jr. & Sher, A. Regulation and biological function of helminth-induced cytokine responses. *Immunol Today* **12**, 3, A62-66, (1991).

90 Robinson, D. S. *et al.* Predominant TH2-like bronchoalveolar T-lymphocyte population in atopic asthma. *N Engl J Med* **326**, 5, 298-304, (1992).

91 Zhou, B. H. *et al.* Thymic stromal lymphopoietin as a key initiator of allergic airway inflammation in mice. *Nature Immunology* **6**, 10, 1047-1053, (2005).

92 Thornton, A. M. *et al.* Expression of Helios, an Ikaros Transcription Factor Family Member, Differentiates Thymic-Derived from Peripherally Induced Foxp3(+) T Regulatory Cells. *Journal of Immunology* **184**, 7, 3433-3441, (2010).

93 Weiss, J. M. *et al.* Neuropilin 1 is expressed on thymus-derived natural regulatory T cells, but not mucosa- generated induced Foxp3(+) T reg cells. *Journal of Experimental Medicine* **209**, 10, 1723-1742, (2012).

94 Singh, K., Hjort, M., Thorvaldson, L. & Sandler, S. Concomitant analysis of Helios and Neuropilin-1 as a marker to detect thymic derived regulatory T cells in naive mice. *Sci Rep* **5**, 7767, (2015).

95 Sprent, J., Cho, J. H., Boyman, O. & Surh, C. D. T cell homeostasis. *Immunol Cell Biol* **86**, 4, 312-319, (2008).

96 Obhrai, J. S. *et al.* Effector T cell differentiation and memory T cell maintenance outside secondary lymphoid organs. *J Immunol* **176**, 7, 4051-4058, (2006).

97 Sprent, J. & Tough, D. F. T cell death and memory. *Science* **293**, 5528, 245-248, (2001).

98 Schluns, K. S., Kieper, W. C., Jameson, S. C. & Lefrancois, L. Interleukin-7 mediates the homeostasis of naive and memory CD8 T cells in vivo. *Nature Immunology* **1**, 5, 426-432, (2000).

99 Tan, J. T. *et al.* IL-7 is critical for homeostatic proliferation and survival of naive T cells. *P Natl Acad Sci USA* **98**, 15, 8732-8737, (2001).

100 Berard, M., Brandt, K., Bulfone-Paus, S. & Tough, D. F. IL-15 promotes the survival of naive and memory phenotype CD8+ T cells. *J Immunol* **170**, 10, 5018-5026, (2003).

101 Cho, J. H. *et al.* An intense form of homeostatic proliferation of naive CD8+ cells driven by IL-2. *J Exp Med* **204**, 8, 1787-1801, (2007).

102 Malek, T. R. & Bayer, A. L. Tolerance, not immunity, crucially depends on IL-2. *Nat Rev Immunol* **4**, 9, 665-674, (2004).

103 Girard, J. P., Moussion, C. & Forster, R. HEVs, lymphatics and homeostatic immune cell trafficking in lymph nodes. *Nat Rev Immunol* **12**, 11, 762-773, (2012).

104 von Andrian, U. H. & Mempel, T. R. Homing and cellular traffic in lymph nodes. *Nat Rev Immunol* **3**, 11, 867-878, (2003).

105 Batista, F. D. & Harwood, N. E. The who, how and where of antigen presentation to B cells. *Nature Reviews Immunology* **9**, 1, 15-27, (2009).

106 Cyster, J. G. *et al.* Follicular stromal cells and lymphocyte homing to follicles. *Immunological Reviews* **176**, 181-193, (2000).

107 Worbs, T., Mempel, T. R., Bolter, J., von Andrian, U. H. & Forster, R. CCR7 ligands stimulate the intranodal motility of T lymphocytes in vivo. *Journal of Experimental Medicine* **204**, 3, 489-495, (2007).

108 Marsland, B. J. *et al.* CCL19 and CCL21 induce a potent proinflammatory differentiation program in licensed dendritic cells. *Immunity* **22**, 4, 493-505, (2005).

109 Link, A. *et al.* Fibroblastic reticular cells in lymph nodes regulate the homeostasis of naive T cells. *Nature Immunology* **8**, 11, 1255-1265, (2007).

110 Surh, C. D. & Sprent, J. Regulation of mature T cell homeostasis. *Semin Immunol* **17**, 3, 183-191, (2005).

111 Onder, L. *et al.* IL-7-producing stromal cells are critical for lymph node remodeling. *Blood* **120**, 24, 4675-4683, (2012).

112 Luther, S. A., Vogt, T. K. & Siegert, S. Guiding blind T cells and dendritic cells: A closer look at fibroblastic reticular cells found within lymph node T zones. *Immunology Letters* **138**, 1, 9-11, (2011).

113 Cui, G. W. *et al.* Characterization of the IL-15 niche in primary and secondary lymphoid organs in vivo. *P Natl Acad Sci USA* **111**, 5, 1915-1920, (2014).

114 Lee, J. W. *et al.* Peripheral antigen display by lymph node stroma promotes T cell tolerance to intestinal self. *Nat Immunol* **8**, 2, 181-190, (2007).

115 Magnusson, F. C. *et al.* Direct presentation of antigen by lymph node stromal cells protects against CD8 T-cell-mediated intestinal autoimmunity. *Gastroenterology* **134**, 4, 1028-1037, (2008).

116 Fletcher, A. L. *et al.* Lymph node fibroblastic reticular cells directly present peripheral tissue antigen under steady-state and inflammatory conditions. *J Exp Med* **207**, 4, 689-697, (2010).

117 Malhotra, D. *et al.* Transcriptional profiling of stroma from inflamed and resting lymph nodes defines immunological hallmarks. *Nat Immunol* **13**, 5, 499-510, (2012).

118 Alimzhanov, M. B. *et al.* Abnormal development of secondary lymphoid tissues in lymphotoxin beta-deficient mice. *Proc Natl Acad Sci U S A* **94**, 17, 9302-9307, (1997).

119 Banks, T. A. *et al.* Lymphotoxin-alpha-deficient mice. Effects on secondary lymphoid organ development and humoral immune responsiveness. *J Immunol* **155**, 4, 1685-1693, (1995).

120 Futterer, A., Mink, K., Luz, A., Kosco-Vilbois, M. H. & Pfeffer, K. The lymphotoxin beta receptor controls organogenesis and affinity maturation in peripheral lymphoid tissues. *Immunity* **9**, 1, 59-70, (1998).

121 Fukuyama, S. *et al.* Initiation of NALT organogenesis is independent of the IL-7R, LTbetaR, and NIK signaling pathways but requires the Id2 gene and CD3(-)CD4(+)CD45(+) cells. *Immunity* **17**, 1, 31-40, (2002).

122 Georgopoulos, K. *et al.* The Ikaros Gene Is Required for the Development of All Lymphoid Lineages. *Cell* **79**, 1, 143-156, (1994).

123 Kurebayashi, S. *et al.* Retinoid-related orphan receptor gamma (RORgamma) is essential for lymphoid organogenesis and controls apoptosis during thymopoiesis. *Proc Natl Acad Sci U S A* **97**, 18, 10132-10137, (2000).

124 Wang, J. H. *et al.* Selective defects in the development of the fetal and adult lymphoid system in mice with an Ikaros null mutation. *Immunity* **5**, 6, 537-549, (1996).

125 Mebius, R. E., Rennert, P. & Weissman, I. L. Developing lymph nodes collect CD4(+)CD3(-) LT beta(+) cells that can differentiate to APC, NK cells, and follicular cells but not T or B cells. *Immunity* **7**, 4, 493-504, (1997).

126 Finke, D., Acha-Orbea, H., Mattis, A., Lipp, M. & Kraehenbuhl, J. CD4+CD3- cells induce Peyer's patch development: role of alpha4beta1 integrin activation by CXCR5. *Immunity* **17**, 3, 363-373, (2002).

127 Finke, D. Fate and function of lymphoid tissue inducer cells. *Curr Opin Immunol* **17**, 2, 144-150, (2005).

128 Nishikawa, S., Honda, K., Vieira, P. & Yoshida, H. Organogenesis of peripheral lymphoid organs. *Immunol Rev* **195**, 72-80, (2003).

129 Yoshida H, N. A., Inoue J, Satoh M, Santee-Cooper SM, Ware CF, et al. Different cytokines induce surface lymphotoxin-alphabeta on IL-7 receptor-alpha cells that differentially engender lymph nodes and Peyer's patches. *Immunity* **17**, 6, 823-833, (2002).

130 Cupedo, T., Jansen, W., Kraal, G. & Mebius, R. E. Induction of secondary and tertiary lymphoid structures in the skin. *Immunity* **21**, 5, 655-667, (2004).

131 Okuda, M., Togawa, A., Wada, H. & Nishikawa, S. Distinct activities of stromal cells involved in the organogenesis of lymph nodes and Peyer's patches. *J Immunol* **179**, 2, 804-811, (2007).

132 Vondenhoff, M. F. *et al.* LTbetaR signaling induces cytokine expression and up-regulates lymphangiogenic factors in lymph node anlagen. *J Immunol* **182**, 9, 5439-5445, (2009).

133 Mebius, R. E. Organogenesis of lymphoid tissues. *Nat Rev Immunol* **3**, 4, 292-303, (2003).

134 Spits, H. & Di Santo, J. P. The expanding family of innate lymphoid cells: regulators and effectors of immunity and tissue remodeling. *Nat Immunol* **12**, 1, 21-27, (2011).

135 Spits H, A. D., Colonna M, Diefenbach A, Di Santo JP, Eberl G, et al. Innate lymphoid cells--a proposal for uniform nomenclature. *Nature reviews Immunology* **13**, 2, 145-149, (2013).

136 Artis, D. & Spits, H. The biology of innate lymphoid cells. *Nature* **517**, 7534, 293-301, (2015).

137 Yokota, Y. *et al.* Development of peripheral lymphoid organs and natural killer cells depends on the helix-loop-helix inhibitor Id2. *Nature* **397**, 6721, 702-706, (1999).
138 Chappaz, S. & Finke, D. The IL-7 signaling pathway regulates lymph node development independent of peripheral lymphocytes. *J Immunol* **184**, 7, 3562-3569, (2010).
139 Chappaz, S., Gartner, C., Rodewald, H. R. & Finke, D. Kit ligand and Il7 differentially regulate Peyer's patch and lymph node development. *J Immunol* **185**, 6, 3514-3519, (2010).
140 Eberl, G. & Littman, D. R. Thymic origin of intestinal alphabeta T cells revealed by fate mapping of RORgammat+ cells. *Science* **305**, 5681, 248-251, (2004).
141 Eberl, G. *et al.* An essential function for the nuclear receptor RORgamma(t) in the generation of fetal lymphoid tissue inducer cells. *Nat Immunol* **5**, 1, 64-73, (2004).
142 Scandella, E. *et al.* Restoration of lymphoid organ integrity through the interaction of lymphoid tissue-inducer cells with stroma of the T cell zone. *Nature Immunology* **9**, 6, 667-675, (2008).
143 Schmutz, S. *et al.* Cutting Edge: IL-7 Regulates the Peripheral Pool of Adult ROR gamma(+) Lymphoid Tissue Inducer Cells. *Journal of Immunology* **183**, 4, 2217-2221, (2009).
144 Sonnenberg, G. F., Fouser, L. A. & Artis, D. Border patrol: regulation of immunity, inflammation and tissue homeostasis at barrier surfaces by IL-22. *Nat Immunol* **12**, 5, 383-390, (2011).
145 Buonocore, S. *et al.* Innate lymphoid cells drive interleukin-23-dependent innate intestinal pathology. *Nature* **464**, 7293, 1371-1375, (2010).
146 Pantelyushin, S. *et al.* Rorgammat+ innate lymphocytes and gammadelta T cells initiate psoriasiform plaque formation in mice. *J Clin Invest* **122**, 6, 2252-2256, (2012).
147 Powell, N. *et al.* The transcription factor T-bet regulates intestinal inflammation mediated by interleukin-7 receptor+ innate lymphoid cells. *Immunity* **37**, 4, 674-684, (2012).
148 Sawa, S. *et al.* RORgammat+ innate lymphoid cells regulate intestinal homeostasis by integrating negative signals from the symbiotic microbiota. *Nat Immunol* **12**, 4, 320-326, (2011).
149 Liang, S. C. *et al.* Interleukin (IL)-22 and IL-17 are coexpressed by Th17 cells and cooperatively enhance expression of antimicrobial peptides. *J Exp Med* **203**, 10, 2271-2279, (2006).
150 Satoh-Takayama, N. *et al.* Microbial flora drives interleukin 22 production in intestinal NKp46+ cells that provide innate mucosal immune defense. *Immunity* **29**, 6, 958-970, (2008).
151 Zheng, Y. *et al.* Interleukin-22 mediates early host defense against attaching and effacing bacterial pathogens. *Nature Medicine* **14**, 3, 282-289, (2008).
152 Sonnenberg, G. F., Monticelli, L. A., Elloso, M. M., Fouser, L. A. & Artis, D. CD4(+) lymphoid tissue-inducer cells promote innate immunity in the gut. *Immunity* **34**, 1, 122-134, (2011).
153 Kruglov, A. A. *et al.* Nonredundant function of soluble LTalpha3 produced by innate lymphoid cells in intestinal homeostasis. *Science* **342**, 6163, 1243-1246, (2013).
154 Hepworth, M. R. *et al.* Innate lymphoid cells regulate CD4+ T-cell responses to intestinal commensal bacteria. *Nature* **498**, 7452, 113-117, (2013).
155 von Burg, N. *et al.* Activated group 3 innate lymphoid cells promote T-cell-mediated immune responses. *Proc Natl Acad Sci U S A* **111**, 35, 12835-12840, (2014).

156 Goto, Y. *et al.* Innate lymphoid cells regulate intestinal epithelial cell glycosylation. *Science* **345**, 6202, 1254009, (2014).

157 Mortha, A. *et al.* Microbiota-Dependent Crosstalk Between Macrophages and ILC3 Promotes Intestinal Homeostasis. *Science* **343**, 6178, 1477-+, (2014).

158 Gladiator, A., Wangler, N., Trautwein-Weidner, K. & LeibundGut-Landmann, S. Cutting edge: IL-17-secreting innate lymphoid cells are essential for host defense against fungal infection. *J Immunol* **190**, 2, 521-525, (2013).

159 Hanash, A. M. *et al.* Interleukin-22 Protects Intestinal Stem Cells from Immune-Mediated Tissue Damage and Regulates Sensitivity to Graft versus Host Disease. *Immunity* **37**, 2, 339-350, (2012).

160 Dudakov, J. A. *et al.* Interleukin-22 Drives Endogenous Thymic Regeneration in Mice. *Science* **336**, 6077, 91-95, (2012).

161 Friend, S. L. *et al.* A thymic stromal cell line supports in vitro development of surface IgM+ B cells and produces a novel growth factor affecting B and T lineage cells. *Exp Hematol* **22**, 3, 321-328, (1994).

162 Sims J.E., W. D. E., Morrissey P.J., Garka K., Foxworthe D., Price V., Friend S., Farr A.G., Bedell M., Jenkins N.A., Copeland N.G., Grabstein K., Paxton R.J. . Molecular cloning and biological characterization of a novel lymphoid growth factor. *J. Exp. Med.* **192**, 671–680, (2000).

163 Quentmeier, H. *et al.* Cloning of human thymic stromal lymphopoietin (TSLP) and signaling mechanisms leading to proliferation. *Leukemia* **15**, 8, 1286-1292, (2001).

164 Reche, P. A. *et al.* Human thymic stromal lymphopoietin preferentially stimulates myeloid cells. *J Immunol* **167**, 1, 336-343, (2001).

165 Liu, Y. J. Thymic stromal lymphopoietin: master switch for allergic inflammation. *J Exp Med* **203**, 2, 269-273, (2006).

166 Saenz, S. A., Taylor, B. C. & Artis, D. Welcome to the neighborhood: epithelial cell-derived cytokines license innate and adaptive immune responses at mucosal sites. *Immunological Reviews* **226**, 172-190, (2008).

167 Ziegler, S. F. The role of thymic stromal lymphopoietin (TSLP) in allergic disorders. *Current Opinion in Immunology* **22**, 6, 795-799, (2010).

168 Cosman, D. *et al.* A new cytokine receptor superfamily. *Trends Biochem Sci* **15**, 7, 265-270, (1990).

169 Pandey, A. *et al.* Cloning of a receptor subunit required for signaling by thymic stromal lymphopoietin. *Nat Immunol* **1**, 1, 59-64, (2000).

170 Zhang, W. *et al.* Identification of a novel type I cytokine receptor CRL2 preferentially expressed by human dendritic cells and activated monocytes. *Biochem Biophys Res Commun* **281**, 4, 878-883, (2001).

171 Blagoev, B., Nielsen, M. M., Angrist, M., Chakravarti, A. & Pandey, A. Cloning of rat thymic stromal lymphopoietin receptor (TSLPR) and characterization of genomic structure of murine Tslpr gene. *Gene* **284**, 1-2, 161-168, (2002).

172 Park, L. S. *et al.* Cloning of the murine thymic stromal lymphopoietin (TSLP) receptor: Formation of a functional heteromeric complex requires interleukin 7 receptor. *J Exp Med* **192**, 5, 659-670, (2000).

173 Isaksen, D. E. *et al.* Requirement for Stat5 in thymic stromal lymphopoietin-mediated signal transduction. *Journal of Immunology* **163**, 11, 5971-5977, (1999).

174 Roan, F. *et al.* The multiple facets of thymic stromal lymphopoietin (TSLP) during allergic inflammation and beyond. *J Leukocyte Biol* **91**, 6, 877-886, (2012).

175 Rochman, Y. *et al.* Thymic stromal lymphopoietin-mediated STAT5 phosphorylation via kinases JAK1 and JAK2 reveals a key difference from IL-7-induced signaling. *P Natl Acad Sci USA* **107**, 45, 19455-19460, (2010).

176 Ziegler, S. F. *et al.* The Biology of Thymic Stromal Lymphopoietin (TSLP). *Immunopharmacology* **66**, 129-155, (2013).

177 Ray, R. J., Furlonger, C., Williams, D. E. & Paige, C. J. Characterization of thymic stromal-derived lymphopoietin (TSLP) in murine B cell development in vitro. *Eur J Immunol* **26**, 1, 10-16, (1996).
178 Levin, S. D. *et al.* Thymic Stromal Lymphopoietin (TSLP): A cytokine that promotes the development of IgM(+) B cells in vitro and signals via a novel mechanism. *Faseb Journal* **13**, 4, A322-A322, (1999).
179 Scheeren, F. A. *et al.* Thymic stromal lymphopoietin induces early human B-cell proliferation and differentiation. *Eur J Immunol* **40**, 4, 955-965, (2010).
180 Chappaz, S., Flueck, L., Farr, A. G., Rolink, A. G. & Finke, D. Increased TSLP availability restores T- and B-cell compartments in adult IL-7 deficient mice. *Blood* **110**, 12, 3862-3870, (2007).
181 Al-Shami, A. *et al.* A role for thymic stromal lymphopoietin in CD4(+) T cell development. *Journal of Experimental Medicine* **200**, 2, 159-168, (2004).
182 Jensen, C. T. *et al.* FLT3 ligand and not TSLP is the key regulator of IL-7-independent B-1 and B-2 B lymphopoiesis. *Blood* **112**, 6, 2297-2304, (2008).
183 Kashyap, M., Rochman, Y., Spolski, R., Samsel, L. & Leonard, W. J. Thymic Stromal Lymphopoietin Is Produced by Dendritic Cells. *Journal of Immunology* **187**, 3, 1207-1211, (2011).
184 Spadoni, I., Iliev, I. D., Rossi, G. & Rescigno, M. Dendritic cells produce TSLP that limits the differentiation of Th17 cells, fosters Treg development, and protects against colitis. *Mucosal Immunol* **5**, 2, 184-193, (2012).
185 Watanabe, N. *et al.* Human thymic stromal lymphopoietin promotes dendritic cell-mediated CD4+ T cell homeostatic expansion. *Nat Immunol* **5**, 4, 426-434, (2004).
186 Gilliet, M. *et al.* Human dendritic cells activated by TSLP and CD40L induce proallergic cytotoxic T cells. *Journal of Experimental Medicine* **197**, 8, 1059-1063, (2003).
187 Lee, H. C. & Ziegler, S. F. Inducible expression of the proallergic cytokine thymic stromal lymphopoietin in airway epithelial cells is controlled by NFkappaB. *Proc Natl Acad Sci U S A* **104**, 3, 914-919, (2007).
188 Zaph, F. A. a. C. Another Brick in the Wall: Innate Lymphoid Cells of the Intestine. *Current Immunology Reviews* **9**, 111-117, (2013).
189 Zhang, K. *et al.* Constitutive and inducible thymic stromal lymphopoietin expression in human airway smooth muscle cells: role in chronic obstructive pulmonary disease. *Am J Physiol Lung Cell Mol Physiol* **293**, 2, L375-382, (2007).
190 Wang, Y. H. *et al.* Maintenance and polarization of human TH2 central memory T cells by thymic stromal lymphopoietin-activated dendritic cells. *Immunity* **24**, 6, 827-838, (2006).
191 Allakhverdi, Z. *et al.* Thymic stfomal lymphopoietin is released by human epithelial cells in response to microbes, trauma, or inflammation and potently activates mast cells. *Journal of Experimental Medicine* **204**, 2, 253-258, (2007).
192 Kato, A., Favoreto, S., Avila, P. C. & Schleimer, R. P. TLR3- and Th2 cytokine-dependent production of thymic stromal lymphopoietin in human airway epithelial cells. *Journal of Immunology* **179**, 2, 1080-1087, (2007).
193 Li, M. *et al.* Retinoid X receptor ablation in adult mouse keratinocytes generates an atopic dermatitis triggered by thymic stromal lymphopoietin. *Proc Natl Acad Sci U S A* **102**, 41, 14795-14800, (2005).
194 Li, M. *et al.* Topical vitamin D3 and low-calcemic analogs induce thymic stromal lymphopoietin in mouse keratinocytes and trigger an atopic dermatitis. *Proc Natl Acad Sci U S A* **103**, 31, 11736-11741, (2006).
195 Li, M. *et al.* Induction of Thymic Stromal Lymphopoietin Expression in Keratinocytes Is Necessary for Generating an Atopic Dermatitis upon

Application of the Active Vitamin D3 Analogue MC903 on Mouse Skin. *J Invest Dermatol* **129**, 2, 498-502, (2009).
196 Lee, H. C., Headley, M. B., Iseki, M., Ikuta, K. & Ziegler, S. F. Cutting edge: Inhibition of NF-kappaB-mediated TSLP expression by retinoid X receptor. *J Immunol* **181**, 8, 5189-5193, (2008).
197 Demehri, S. *et al.* Notch-deficient skin induces a lethal systemic B-lymphoproliferative disorder by secreting TSLP, a sentinel for epidermal integrity. *Plos Biology* **6**, 5, 992-1005, (2008).
198 Dumortier, A. *et al.* Atopic dermatitis-like disease and associated lethal myeloproliferative disorder arise from loss of Notch signaling in the murine skin. *PLoS One* **5**, 2, e9258, (2010).
199 Sun, Z. *et al.* Requirement for RORgamma in thymocyte survival and lymphoid organ development. *Science* **288**, 5475, 2369-2373, (2000).
200 Shinkai, Y. *et al.* RAG-2-deficient mice lack mature lymphocytes owing to inability to initiate V(D)J rearrangement. *Cell* **68**, 5, 855-867, (1992).
201 Gabler, J., Arnold, J. & Kyewski, B. Promiscuous gene expression and the developmental dynamics of medullary thymic epithelial cells. *Eur J Immunol* **37**, 12, 3363-3372, (2007).
202 Soumelis, V. *et al.* Human epithelial cells trigger dendritic cell mediated allergic inflammation by producing TSLP. *Nat Immunol* **3**, 7, 673-680, (2002).
203 Sonnenberg, G. F. & Artis, D. Innate lymphoid cell interactions with microbiota: implications for intestinal health and disease. *Immunity* **37**, 4, 601-610, (2012).
204 Sawa, S. *et al.* Lineage relationship analysis of RORgammat+ innate lymphoid cells. *Science* **330**, 6004, 665-669, (2010).
205 Lindemans, C. A. *et al.* IL-22 Is an Intestinal Stem Cell Growth Factor, and IL-22 Administration in Vivo Reduces Morbidity and Mortality in Murine GvHD. *Blood* **124**, 21, (2014).
206 Geremia, A. *et al.* IL-23-responsive innate lymphoid cells are increased in inflammatory bowel disease. *Journal of Experimental Medicine* **208**, 6, 1127-1133, (2011).
207 Walker JA, B. J., McKenzie AN. Innate lymphoid cells-how did we miss them. *Nat Rev Immunol.* **13**, 2, 75-87, (2013).
208 El Shikh, M. E. & Pitzalis, C. Follicular dendritic cells in health and disease. *Front Immunol* **3**, 292, (2012).
209 Fu, Y. X., Huang, G., Wang, Y. & Chaplin, D. D. B lymphocytes induce the formation of follicular dendritic cell clusters in a lymphotoxin alpha-dependent fashion. *J Exp Med* **187**, 7, 1009-1018, (1998).
210 Tumanov, A. V., Kuprash, D. V., Mach, J. A., Nedospasov, S. A. & Chervonsky, A. V. Lymphotoxin and TNF produced by B cells are dispensable for maintenance of the follicle-associated epithelium but are required for development of lymphoid follicles in the Peyer's patches. *J Immunol* **173**, 1, 86-91, (2004).
211 Krautler, N. J. *et al.* Follicular dendritic cells emerge from ubiquitous perivascular precursors. *Cell* **150**, 1, 194-206, (2012).
212 Haluszczak, C. *et al.* The antigen-specific CD8+ T cell repertoire in unimmunized mice includes memory phenotype cells bearing markers of homeostatic expansion. *J Exp Med* **206**, 2, 435-448, (2009).
213 Shakib, S. *et al.* Checkpoints in the development of thymic cortical epithelial cells. *J Immunol* **182**, 1, 130-137, (2009).
214 Klug, D. B. *et al.* Interdependence of cortical thymic epithelial cell differentiation and T-lineage commitment. *Proc Natl Acad Sci U S A* **95**, 20, 11822-11827, (1998).
215 Gray, D. H. *et al.* Developmental kinetics, turnover, and stimulatory capacity of thymic epithelial cells. *Blood* **108**, 12, 3777-3785, (2006).

216 Palmer, D. B., Viney, J. L., Ritter, M. A., Hayday, A. C. & Owen, M. J. Expression of the Alpha-Beta-T-Cell Receptor Is Necessary for the Generation of the Thymic Medulla. *Dev Immunol* **3**, 3, 175-179, (1993).

217 Jenkinson, E. J., Anderson, G. & Owen, J. J. Studies on T cell maturation on defined thymic stromal cell populations in vitro. *J Exp Med* **176**, 3, 845-853, (1992).

218 Fry, T. J. & Mackall, C. L. The many faces of IL-7: From lymphopoiesis to peripheral T cell maintenance. *Journal of Immunology* **174**, 11, 6571-6576, (2005).

219 Lkhagvasuren, E., Sakata, M., Ohigashi, I. & Takahama, Y. Lymphotoxin beta receptor regulates the development of CCL21-expressing subset of postnatal medullary thymic epithelial cells. *J Immunol* **190**, 10, 5110-5117, (2013).

220 Lei, Y. & Takahama, Y. XCL1 and XCR1 in the immune system. *Microbes Infect* **14**, 3, 262-267, (2012).

221 Watanabe, N. *et al.* Hassall's corpuscles instruct dendritic cells to induce CD4+CD25+ regulatory T cells in human thymus. *Nature* **436**, 7054, 1181-1185, (2005).

222 Besin, G., Dupuis, G. & Amrani, A. Protection of NOD mice against diabetes by TSLP : conversion of T lymphocytes CD4+CD25-FOXP3-in T lymphocyte regulators CD4+CD25+FOXP3+in the presence of dendritic cells cultivated in the presence of TSLP. *Diabetes Metab* **34**, A51-A51, (2008).

223 Foss, D. L., Donskoy, E. & Goldschneider, I. The importation of hematogenous precursors by the thymus is a gated phenomenon in normal adult mice. *Journal of Experimental Medicine* **193**, 3, 365-374, (2001).

224 Stockinger, B., Barthlott, T. & Kassiotis, G. The concept of space and competition in immune regulation. *Immunology* **111**, 3, 241-247, (2004).

225 Min, B., Yamane, H., Hu-Li, J. & Paul, W. E. Spontaneous and homeostatic proliferation of CD4 T cells are regulated by different mechanisms. *Journal of Immunology* **174**, 10, 6039-6044, (2005).

226 Surh, C. D. & Sprent, J. Homeostasis of Naive and Memory T Cells. *Immunity* **29**, 6, 848-862, (2008).

227 de Saint-Vis, B. *et al.* The cytokine profile expressed by human dendritic cells is dependent on cell subtype and mode of activation. *Journal of Immunology* **160**, 4, 1666-1676, (1998).

228 Harnaha, J. *et al.* Interleukin-7 is a survival factor for CD4(+) CD25(+) T-cells and is expressed by diabetes-suppressive dendritic cells. *Diabetes* **55**, 1, 158-170, (2006).

229 Ku, C. C., Murakami, M., Sakamoto, A., Kappler, J. & Marrack, P. Control of homeostasis of CD8+ memory T cells by opposing cytokines. *Science* **288**, 5466, 675-678, (2000).

230 Lodolce, J. P. *et al.* IL-15 receptor maintains lymphoid homeostasis by supporting lymphocyte homing and proliferation. *Immunity* **9**, 5, 669-676, (1998).

231 Guimond, M. *et al.* Interleukin 7 signaling in dendritic cells regulates the homeostatic proliferation and niche size of CD4+ T cells. *Nat Immunol* **10**, 2, 149-157, (2009).

232 Kirberg, J., Bosco, N., Deloulme, J. C., Ceredig, R. & Agenes, F. Peripheral T lymphocytes recirculating back into the thymus can mediate thymocyte positive selection. *Journal of Immunology* **181**, 2, 1207-1214, (2008).

233 Bosco, N., Kirberg, J., Ceredig, R. & Agenes, F. Peripheral T cells in the thymus: have they just lost their way or do they do something? *Immunology and Cell Biology* **87**, 1, 50-57, (2009).

234 Raberger, J. *et al.* The transcriptional regulator PLZF induces the development of CD44 high memory phenotype T cells. *Proc Natl Acad Sci U S A* **105**, 46, 17919-17924, (2008).

235 Bjorkdahl, O. *et al.* Characterization of CC-chemokine receptor 7 expression on murine T cells in lymphoid tissues. *Immunology* **110**, 2, 170-179, (2003).

236 Goldrath, A. W., Bogatzki, L. Y. & Bevan, M. J. Naive T cells transiently acquire a memory-like phenotype during homeostasis-driven proliferation. *J Exp Med* **192**, 4, 557-564, (2000).

237 Rathmell, J. C., Farkash, E. A., Gao, W. & Thompson, C. B. IL-7 enhances the survival and maintains the size of naive T cells. *J Immunol* **167**, 12, 6869-6876, (2001).

238 Wang, R., Xie, H., Huang, Z., Shang, W. & Sun, Z. Developing and activated T cell survival depends on differential signaling pathways to regulate anti-apoptotic Bcl-x(L). *Clin Dev Immunol* **2012**, 632837, (2012).

239 Wingard, J. R. *et al.* Long-term survival and late deaths after allogeneic hematopoietic cell transplantation. *J Clin Oncol* **29**, 16, 2230-2239, (2011).

240 Tumanov, A. V. *et al.* Lymphotoxin controls the IL-22 protection pathway in gut innate lymphoid cells during mucosal pathogen challenge. *Cell Host Microbe* **10**, 1, 44-53, (2011).

241 Schulz, S. M. *et al.* Protective immunity to systemic infection with attenuated Salmonella enterica serovar enteritidis in the absence of IL-12 is associated with IL-23-dependent IL-22, but not IL-17. *J Immunol* **181**, 11, 7891-7901, (2008).

242 Pickert, G. *et al.* STAT3 links IL-22 signaling in intestinal epithelial cells to mucosal wound healing. *J Exp Med* **206**, 7, 1465-1472, (2009).

243 Hepworth, M. R. *et al.* Immune tolerance. Group 3 innate lymphoid cells mediate intestinal selection of commensal bacteria-specific CD4(+) T cells. *Science* **348**, 6238, 1031-1035, (2015).

244 Ma, H. L. *et al.* IL-22 is required for Th17 cell-mediated pathology in a mouse model of psoriasis-like skin inflammation. *Journal of Clinical Investigation* **118**, 2, 597-607, (2008).

245 Zenewicz, L. A. & Flavell, R. A. Recent advances in IL-22 biology. *Int Immunol* **23**, 3, 159-163, (2011).

246 Kotenko, S. V. *et al.* Identification of the functional interleukin-22 (IL-22) receptor complex: the IL-10R2 chain (IL-10Rbeta) is a common chain of both the IL-10 and IL-22 (IL-10-related T cell-derived inducible factor, IL-TIF) receptor complexes. *J Biol Chem* **276**, 4, 2725-2732, (2001).

247 Dumoutier, L., Lejeune, D., Colau, D. & Renauld, J. C. Cloning and characterization of IL-22 binding protein, a natural antagonist of IL-10-related T cell-derived inducible factor/IL-22. *J Immunol* **166**, 12, 7090-7095, (2001).

248 Martin, J. C. *et al.* Interleukin-22 binding protein (IL-22BP) is constitutively expressed by a subset of conventional dendritic cells and is strongly induced by retinoic acid. *Mucosal Immunol* **7**, 1, 101-113, (2014).

249 Velardi, E., Dudakov, J. A. & van den Brink, M. R. Clinical strategies to enhance thymic recovery after allogeneic hematopoietic stem cell transplantation. *Immunol Lett* **155**, 1-2, 31-35, (2013).

250 Uehira, M. *et al.* The development of dermatitis infiltrated by gamma delta T cells in IL-7 transgenic mice. *Int Immunol* **5**, 12, 1619-1627, (1993).

251 Lundmark, F. *et al.* Variation in interleukin 7 receptor alpha chain (IL7R) influences risk of multiple sclerosis. *Nat Genet* **39**, 9, 1108-1113, (2007).

252 Totsuka, T. *et al.* IL-7 is essential for the development and the persistence of chronic colitis. *Journal of Immunology* **178**, 8, 4737-4748, (2007).

253 Al-Shami, A., Spolski, R., Kelly, J., Keane-Myers, A. & Leonard, W. J. A role for TSLP in the development of inflammation in an asthma model. *Journal of Experimental Medicine* **202**, 6, 829-839, (2005).

254 Shikotra, A. *et al.* Increased expression of immunoreactive thymic stromal lymphopoietin in patients with severe asthma. *J Allergy Clin Immun* **129**, 1, 104-U147, (2012).

255 Ying, S. *et al.* Expression and cellular provenance of thymic stromal lymphopoietin and chemokines in patients with severe asthma and chronic obstructive pulmonary disease. *Journal of Immunology* **181**, 4, 2790-2798, (2008).
256 Ying, S. *et al.* Thymic stromal lymphopoietin expression is increased in asthmatic airways and correlates with expression of TH2-attracting chemokines and disease severity. *Journal of Immunology* **174**, 12, 8183-8190, (2005).
257 Camelo, A. *et al.* Blocking IL-25 signalling protects against gut inflammation in a type-2 model of colitis by suppressing nuocyte and NKT derived IL-13. *Journal of Gastroenterology* **47**, 11, 1198-1211, (2012).
258 Halim, T. Y., Krauss, R. H., Sun, A. C. & Takei, F. Lung natural helper cells are a critical source of Th2 cell-type cytokines in protease allergen-induced airway inflammation. *Immunity* **36**, 3, 451-463, (2012).
259 Ikutani, M. *et al.* Identification of Innate IL-5-Producing Cells and Their Role in Lung Eosinophil Regulation and Antitumor Immunity. *Journal of Immunology* **188**, 2, 703-713, (2012).
260 Ito, R., Takahashi, T., Katano, I. & Ito, M. Current advances in humanized mouse models. *Cell Mol Immunol* **9**, 3, 208-214, (2012).

Appendix

Abbreviations and symbols

Ab	antibody
Ag	antigen
Aire	autoimmune regulator
Alum	aluminium potassium
APC	antigen presenting cell
BEC	blood endothelial cell
BM	bone marrow
bp	base pair
CD	cluster of differentiation
CFSE	carboxyfluorescein succinimidyl ester
CK	cytokeratin
CM	central memory
CMJ	corticomedullary junction
CRLF2	cytokine receptor - like factor 2
cTEC	cortical thymic epithelial cell
DC	dendritic cell
dGuo	2'-Deoxyguanosine
DN	double negative
DNSC	double negative stromal cell
DP	double positive
E	embryonic day
EM	effector memory
ELISA	enzyme linked immunosorbent assay
EpCAM	epithelial cell adhesion molecule
Fab	fragment antigen - binding
Fc	fragment crystallizable
FDC	follicular dendritic cell
FGF	fibroblast growth factor
Flt3L	FMS - like tyrosine kinase 3 ligand
FL	fetal liver

fol	follicular
FoxP3	forkhead box protein P3
FTOC	fetal thymus organ culture
γc	common cytokine gamma chain
GM-CSF	granulocyte macrophage colony stimulating factor
GVHD	graft versus host disease
HEV	high endothelial venule
HSC	hematopoietic stemm cell
HSCT	hematopoietic stemm cell transplantation
Id2	inhibitor of DNA binding 2
IFN-γ	Interferon-gamma
Ig	Immunoglobulin
IL	interleukin
ILC	innate lymphoid cell
i.p.	intraperitoneal
i.v.	intravenous
KGF	keratinocyte growth factor
LEC	lymphatic endothelial cell
lin	lineage
LN	lymph node
LP	lamina propria
LT	lymphotoxin
LTi	lymphoid tissue inducer
mLN	mesenteric lymph node
MHC	major histocompatibility complex
mLN	mesenteric lymph node
MΦ	macrophage
mTEC	medullary thymic epithelial cell
MZ	marginal zone
NCR	natural cytotoxicity receptor
NF-κB	nuclear factor kappa-light-chain-enhancer of activated B cells
NK	natural killer
NP-OVA	4-Hydroxy-3-nitrophenylacetyl NP- (18)-Ovalbumin
nTreg	naturally occurring Treg
OD	optical density
OVA	Ovalbumin

o/n	over night
PDGFRα	platelet - derived growth factor receptor α
PP	peyers patch
preFDC	FDC precursor
pTreg	peripheral induced Treg
RAG	recombination activating genes
Rank	receptor activator of NF-κB
RankL	receptor activator of NF-κB ligand
RegIIIβ/γ	regenerating islet - derived protein III beta/ gamma
RORγt	retinoic acid related orphan receptor gamma
RTOC	re - aggregated thymus organ culture
SCF	stem cell factor
SI	small intestine
SP	single positive
TCR	T cell receptor
TEC	thymic epithelial cell
TD	thymus - dependent
Tg	transgenic
Th	T helper
TI	thymus - independent
TLR	Toll - like receptor
TNF	tumor necrosis factor
TRA	tissue restricted antigen
TRC	T zone reticular cell
Treg	regulatory T cell
TSLP	thymic stromal lymphopoietin
TSLPR	thymic stromal lymphopoietin receptor
UCB	umbilical cord blood
UEA-1	Ulex europaeus agglutinin - 1
WT	wild type

%	percent
°C	degree celsius
h	hour
kDA	kilo dalton

min	minutes
mm	milimeter
ng	nanogram
rpm	rounds per minute
µg	microgramm
µm	micromter
µL	microliter
µM	micromol

Curriculum Vitae

Simone Neu
Müssmattstrasse 25, 79618 Rheinfelden, Germany
Phone: +49 7623 3079703
E-mail: simone.neu@unibas.ch

Personal information

Date of birth:	10. December 1984
Place of birth:	Rheinfelden, Germany

Research experience

2011 - present	**PhD student** in the Lab of Prof. Daniela Finke, Developmental Immunology, Department of Biomedicine, Basel, Switzerland
2009 - 2011	**Master student** in the Lab of Prof. Hans Hirsch, Transplantation Virology, Department of Biomedicine, Basel, Switzerland Title of Master Thesis: Prediction and Characterization of Polyomavirus BK Large T specific T-cell response; (Grade: 5.0) Supervisor: Prof. Hans Hirsch, Referee: Dr. Ingrid Felger

Education

2011 - present	**PhD in Immunology and Cell Biology**, Department Biomedicine, University of Basel, Switzerland
2009 - 2011	**Master' course in Infection Biology and Epidemiology**, Swiss Tropical and Public Health Institute, Basel, Switzerland
2005 - 2009	**Bachelor of Science in Biology** with Major in integrative Biology, University of Basel, Switzerland
1995 - 2004	**Gymnasium with Abitur**, Georg-Büchner Gymnasium, Rheinfelden, Germany

Technical skills

Cellular biology and immunology techniques: isolation, cultivation and stimulation of cells from murine organs and human blood; organ culture; ELISA; ELISpot; FACS (up to 12 colours, intra- and extracellular)

In vivo **experiments in mice:** anesthesia, intraperitoneal, intravenous, and subcutaneous injections; oral gavage**;** adoptive transfer of cells; immunization of mice with proteins/peptides

Molecular biology and biochemical techniques: RNA extraction; cDNA synthesis; RT and qRT PCR; cloning

others: immunohistochemistry; microscopy

Computer skills: Microsoft Office, Mac Office, GraphPad Prism, FlowJo, Adobe illustrator, ImageJ

Congress Participations

- **4th International Symposium:** Regulators of Adaptive Immunity (2013, DFG, Erlangen, Germany)
- **3rd Basel Immunology Focus Symposium** – Immune Intervention (2013, Department of Biomedicine, University of Basel, Switzerland
- **Symposium: Development of Innate Cellular Immunity:** Basic and Translational Aspects (2011, University Hospital Freiburg, Germany)
- **Symposium: Gut Microbiota in Health and Disease** (2011, Global Health Institute, School of Life Sciences, EPFL, Lausanne, Switzerland)

Poster presentations

- Research Day of the Children's University Hospital Basel (2014,Basel, Switzerland) „**TSLP improves Thymus development under immunodeficient conditions"**
- Research Day of the Children's University Hospital Basel (2013, Basel, Switzerland) „**Role of TSLP and ILC3s in lymphoid tissue remodeling and homeostasis"**
- PhD winter retreat (2013, University of Basel, Switzerland) **„The role of LTi cells after BM reconstitution"**
- PhD winter retreat (2012, University of Basel, Switzerland) **„A new mouse model to investigate TSLP function in the intestinal immune system**

- Research Day of the Children's University Hospital Basel (2011, Basel, Switzerland) **„A new mouse model to investigate TSLP function in the intestinal immune system**

Awards

2014: Prize for the best Poster in the category of basic research at the Research day of the Children`s Hospital
Title: Role for TSLP in thymus development under immunodeficient conditions

Languages

german (native language), **english** (fluent in speaking and writing), **french** (intermediate knowledge), **danish** (basic knowledge)

Teaching experience

2011 - 2015:	assistance in the annual "Blockkurs" for undergraduate students (Basic Immunology laboratory course, University of Basel, Switzerland)

Voluntary activities

Musikverein Nollingen 1826 e.V.

2010 - present	President of the music club Musikverein Nollingen 1826
2006 - 2010	Vice - cashier of the music club Musikverein Nollingen1826
1991 - present	active member of the music club Musikverein Nollingen1826

References

Prof. Daniela Finke:	Daniela.Finke@unibas.ch; +41 (0) 61 267 16 34
PD Dr. Nina Khanna:	Nina.Khanna@usb.ch; +41 (0) 61 328 73 25